Energy Efficient Core Networks with Clouds

Leonard Nonde

Submitted in accordance with the requirements for the degree

of

Doctor of Philosophy

The University of Leeds

School of Electronic and Electrical Engineering

September 2016

The candidate confirms that the work submitted is his own, except where work which has formed part of jointly-authored publications has been included. The contribution of the candidate and the other authors to this work has been explicitly indicated below. The candidate confirms that appropriate credit has been given within the thesis where reference has been made to the work of others.

Chapter 4 and Chapter 5 are based on the work from:

Leonard Nonde, T.E.H. El-Gorashi, and J.M.H. Elmirghani, "Energy Efficient Virtual Network Embedding for Cloud Networks", IEEE/OSA Journal of Lightwave Technology, 2015. 33(9): p. 1828-1849

This paper has been published jointly with my PhD supervisor Prof. Jaafar Elmirghani and my co-supervisor Dr Taisir Elgorashi

Chapter 6 is based on the work from:

Leonard Nonde, T.E.H. El-Gorashi, and J.M.H. Elmirghani, "Green Virtual Network Embedding in Optical OFDM Cloud Networks," in 16th IEEE Conference on Transparent Optical Networks (ICTON), 2014.

This paper has been published jointly with my PhD supervisor Prof. Jaafar Elmirghani and my co-supervisor Dr Taisir Elgorashi

Chapter 7 is based on the work from:

Jaafar M. H. Elmirghani, T. Klein, K. Hinton, A. Q. Lawey, L. Nonde, T.E.H. El-Gorashi, M. O. I. Musa, X. Dong "GreenTouch GreenMeter Core Network Energy efficiency Improvements ", to be submitted to IEEE/OSA Journal of Lightwave Technology, 2016.

This paper will be published jointly with my PhD supervisor Prof. Jaafar Elmirghani, my co-supervisor Dr Taisir Elgorashi, Thierry Klein from Bell Labs, Kerry Hinton from University of Melbourne, Ahmed Lawey and Mohamed Musa from University of Leeds and Xiaowen Dong from Huawei Shannon Labs.

Chapter 8 is based on the work from:

Leonard Nonde, T.E.H. El-Gorashi, and J.M.H. Elmirghani, "Cloud Virtual Network Embedding: Profit, Power and Acceptance," in proc. IEEE Global Comminications Conference (GLOBECOM), 2015.

This paper has been published jointly with my PhD supervisor Prof. Jaafar Elmirghani and my co-supervisor Dr Taisir Elgorashi

Chapter 9 is based on the work from:

Leonard Nonde, T.E.H. El-Gorashi, and J.M.H. Elmirghani, "Virtual Network Embedding Employing Renewable Energy

Sources," Accepted in proc. IEEE Global Comminications Conference (GLOBECOM), 2016.

This paper has been published jointly with my PhD supervisor Prof. Jaafar Elmirghani and my co-supervisor Dr Taisir Elgorashi.

Theresa and Michael Nonde, this PhD thesis is dedicated to you.

Acknowledgments

First and foremost I would like to give thanks and praise to the almighty God for my life and all the abundant gifts that He has bestowed on me. I wish to acknowledge my supervisor, Professor Jaafar Elmirghani for his astute leadership, guidance and patience throughout my entire PhD journey. His timely advice and constant encouragement is much appreciated.

I would also like to acknowledge my co-supervisor Dr. Taisir Elgorashi for her guidance during my PhD.

I am also highly indebted to the Commonwealth Scholarship Commission for fully funding my PhD studies in Leeds. Many thanks to them.

I wish to thank my spouse Mwansa Changufu Nonde and my children Chengelo and Neema-Christina, for their love and sacrifice during some very challenging times; they always gave me assurance. Thank you Mwansa for letting me pursue my dreams. Love you so much.

I wish to thank my colleagues in the Communication Systems and Networks group in the School of Electronic and Electrical Engineering. I enjoyed working with them and I thank them for the company and fruitful discussions.

A big thank you to my family back home in Zambia. My late parents Theresa and Michael Nonde for making everything I have achieved in life possible. My uncle, Bishop Aaron Chisha for being a parent to me throughout my life and to my brothers George, Richard and Michael for your inspiration. To my sister Lillian for being like a mother to me.

Leonard

Abstract

The popularity of cloud based applications stemming from the high volume of connected mobile devices has led to a huge increase in Internet traffic. In order to enable easy access to cloud applications, infrastructure providers have invested in geographically distributed databases and servers. However, intelligent and energy efficient high capacity transport networks with near ubiquitous connectivity are needed to adequately and sustainably serve these requirements. In this thesis, network virtualisation has been identified as a potential networking paradigm that can contribute to network agility and energy efficiency improvements in core networks with clouds.

The work first introduces a new virtual network embedding core network architecture with clouds and a compute and bandwidth resource provisioning mechanism aimed at reducing power consumption in core networks and data centres. Further, quality of service measures in compute and bandwidth resource provisioning such as delay and customer location have been investigated and their impact on energy efficiency established. Data centre location optimisation for energy efficiency in virtual network embedding infrastructure has been investigated by developing a MILP model that selects optimal data centre locations in the core network. The work also introduces an optical OFDM based physical layer in virtual network embedding to optimise power consumption and optical spectrum

utilization. In addition, virtual network embedding schemes aimed at profit maximization for cloud infrastructure providers as well greenhouse gas emission reduction in cloud infrastructure networks have been investigated. GreenTouch, a consortium of industrial and academic experts on energy efficiency in ICTs, has adopted the work in this thesis as one of the measures of improving energy efficiency in core networks.

Table of Contents

List of Figures

List of Tables

Glossary of Terms

ADM	**Add and Drop Multiplexer**
ALR	**Adaptive Link Rate**
API	**Application Programming Interface**
ATM	**Asynchronous Transfer Mode**
BAU	**Business as Usual**
BPSK	**Binary Phase Shift Keying**
BV-OXC	**Bandwidth Variable Optical Cross Connect**
BVT	**Bandwidth Variable Transponder**
CAPEX	**Capital Expenditure**
CLI	**Command Line Interface**
CMOS	**Complementary Metal-Oxide Semiconductor**
CostVNE	**Cost Virtual Network Embedding**
CostVNE-LD	**Cost Virtual Network Embedding with Location and Delay**
CPU	**Central Processing Unit**
DSP	**Digital Signal Processing**
DVFS	**Dynamic Voltage and Frequency Scaling**
DXC	**Digital Cross Connect**
ECostGVNE	**Electricity Cost Green Virtual Network**

	Embedding
ECostVNE	**Electricity Cost Virtual Network Embedding**
EDFA	**Erbium Doped Fibre Amplifier**
EE	**Energy Efficient**
EEVNE	**Energy Efficient Virtual Network Embedding**
EEVNE-LD	**Energy Efficient Virtual Network with Location and Delay**
EIA	**Energy Information Administration**
EU	**European Union**
FEC	**Forward Error Correction**
Gbps	**Gigabit per second**
GCA	**Green Cloud Architecture**
GHG	**Greenhouse Gas**
GHz	**Giga Hertz**
GMPLS	**Generalized Multiprotocol Label Switching**
GT	**GreenTouch**
GVNE	**Green Virtual Network Embedding**
GVNE-DC	**Green Virtual Network Embedding with Data Centre Optimisation**
IaaS	**Infrastructure as a Service**
ICT	**Information and Communications Technology**
InP	**Infrastructure Provider**

IP	**Internet Protocol**
IPTV	**Internet Protocol Television**
ISI	**Inter-symbol Interference**
ITU	**International Telecommunications Union**
LAN	**Local Area Network**
MILP	**Mixed Integer Linear Programming**
MLR	**Mixed Line Rate**
MSC	**Modular Services Card**
NaaS	**Network as a Service**
NGN	**Next Generation Networks**
NIC	**Network Interface Card**
NSFNET	**National Science Foundation Network**
OADM	**Optical Add and Drop Multiplexer**
OEO	**Optical to Electrical to Optical**
OFDM	**Orthogonal Frequency Division Multiplexing**
OLA	**Optical Line Amplifier**
OLT	**Optical Line Terminal**
ONOS	**Open Network Operating System**
O-OFDM	**Optical Orthogonal Frequency Division Multiplexing**
OOK	**On-Off Keying**
OPEX	**Operational Expenditure**

OSC	**Optical Supervisory Channel**
OSNR	**Optical Signal to Noise Ratio**
OSPF	**Open Shortest Path First**
OTN	**Optical Transport Network**
OXC	**Optical Cross Connect**
PLIM	**Physical Layer Interface Module**
POEM	**Profit Optimised Energy Minimised**
PUE	**Power Usage Effectiveness**
PV	**Photovoltaics**
QAM	**Quadrature Amplitude Modulation**
QoS	**Quality of Service**
QPSK	**Quadrature Phase Shift Keying**
RAM	**Random Access Memory**
REOViNE	**Real-time Energy Optimised Virtual Network Embedding**
ROADM	**Re-configurable Optical Add and Drop Multiplexer**
SDH	**Synchronous Digital Hierarchy**
SDN	**Software Defined Networking**
SLA	**Service Level Agreement**
SLR	**Single Line Rate**
SOA	**Service Oriented Architecture**

SONET	**Synchronous Optical Network**
SP	**Service Provider**
SR	**Short Reach**
TCP	**Transmission Control Protocol**
TDM	**Time Division Multiplexing**
TDS	**Time Driven Switching**
TF	**Time Frame**
ToR	**Top of the Rack**
USNET	**United States Network**
VLAN	**Virtual Local Area Network**
VN	**Virtual Network**
VNE	**Virtual Network Embedding**
VNE-EA	**Virtual Network Embedding Energy Aware**
VNR	**Virtual Network Request**
VPN	**Virtual Private Network**
VSB	**Vestigial Sideband**
W	**Watt**
WDM	**Wavelength Division Multiplexing**
WR	**Wavelength Router**

Chapter 1: Introduction

The Cisco Visual Networking Index of 2016 reports that more than half a billion mobile devices and connections were added in the year 2015 and mobile data traffic grew by 74% in 2015 reaching 3.7 exabytes per month. This amount is expected to grow almost tenfold to 30 exabytes per month by the year 2020. With such a huge amount of traffic being generated, intelligent transport networks with near ubiquitous connectivity are needed. Aside from the capacity problem, the other heavy price to be paid by this rapid growth is the rising energy requirement of these systems.

Applications on all these devices and others need access to geographically distributed databases and servers using public and private clouds requiring flexible traffic management, energy efficiency and bandwidth on demand capabilities. The high capacity transport network architectures of today will therefore need to evolve in order to adequately meet these requirements. The energy use by ICT equipment and services represented about 8% of electrical power in the EU, and about 2% of carbon emissions

in 2008 [1]. Estimates indicate that in the long term, if current trends continue, companies operating data centres will spend more money per year on energy than on equipment [2]. On a world wide scale, based on the 2009 data, ICT consumes about 9% of the world's total electricity output [3].

Most of the energy resources available for use today come from hydrocarbons. In the US for example, 82% of all the primary energy consumption is derived from hydrocarbons [4]. It is however a well-known fact that this type of energy resource is not renewable and it is expected to be used up in a not too distant future and it is also an energy source that is responsible for the release of large amounts of greenhouse gas (GHG) emissions that are very harmful to the environment. Considering this fact as well as the increase in the cost of energy, it is necessary in both academia and industry to focus on energy-efficient paradigms that ultimately lead to a reduction in the amount of energy consumed in ICT networks.

Recently, there have been significant research efforts aimed at reducing energy consumption in ICT networks. Gupta et al [5], introduced the concept of "greening the internet" as a means of reducing the amount of energy consumed in ICT networks. There have also been various efforts from researches on reducing power consumption in data centres. The research carried out in [6] focuses on reducing power consumption inside the data centre by use of low power processors in servers, use of efficient power supplies, use of blade servers and server virtualisation. A group

known as the Green Grid [7] was founded to increase energy efficiency inside data centres.

Energy efficiency in core networks has also received a lot of attention. Bandwidth intensive applications such as IPTV call for increased capacity in core network infrastructure, which leads to an increase in power consumption. In [8], the authors have examined the energy efficient design of IP over WDM networks by implementing lightpath bypass in the optical layer. The goal is to enhance energy efficiency of core network nodes which are usually in few locations but handle intensive amounts of traffic because of traffic aggregation which mainly comes from co-located high capacity data centres and metro networks.

In this thesis, network virtualisation has been identified as a potential networking paradigm that can contribute to energy efficiency improvements in core networks. A networking environment is considered to support network virtualisation if its infrastructure services have been decoupled from the physical assets on which the services operate. Core networks connect geographically distributed public and private cloud data centres. In [9], the authors have stated that the success of future cloud networks where clients are expected to be able to specify the data rate and processing requirements for hosted applications and services will greatly depend on network virtualisation. Software Defined Networking has been identified as the enabler of network virtualisation [10]. Software Defined Networking (SDN) has brought about many possibilities in service

provisioning in cloud networks. The fact that it is now possible to program a network on the fly as well as dictate how it behaves under different conditions provides opportunities for optimisation of the physical resources that make up the network. A centralized control plane that is isolated from the data plane allows custom designed algorithms to dynamically route application specific flows or wavelengths in a network in order to fulfil a specific goal. As an example, an algorithm, which automatically uses minimum hop routing for a live video stream at a particular time of the day and then tears it down when circumstances change could be implemented in the controller. In the absence of SDN, this process would have to be statically implemented and resources assigned even when they may not be used all the time.

Network virtualisation has been proposed as an enabler for energy savings by means of resource consolidation [11] - [15]. In all these proposals, the models and/or algorithms do not address the link embedding problem as a multi-layer problem spanning from the virtualisation layer through the IP layer and all the way to the optical layer. Except for the authors in [14], the others do not consider the power consumption of network ports/links as being related to the actual traffic passing through them. In contrast, in this study, a very detailed and accurate approach towards energy efficient virtual network embedding is developed. Granular power consumption of various network elements that form the network engine in backbone networks as well as the power consumption in data centres is considered.

Mixed Integer Linear Programming models and real-time heuristics have been developed to model the problems with the goals of reducing the power consumption in core networks and data centres, improve the profitability of infrastructure providers and to mitigate the release of greenhouse gas emissions into the environment.

1.1 Research Objectives

All the research so far that has considered the use of resource consolidation in network virtualisation as a means of reducing energy consumption in networks has not specifically considered the practical implementation of virtual network embedding across all the multiple layers in core networks. It is important to note that virtualisation is done for many reasons such as sharing the infrastructure dynamically. The hypothesis in this thesis is that virtualisation can improve energy efficiency in core networks with clouds. In this research therefore, the fundamental objectives are as follows:

1. Propose an energy efficient virtual network embedding approach in IP over WDM networks with data centres to reduce the overall power consumption in both the core network and in data centres. In addition, explore the effects of considering both non-energy efficient data centres and energy efficient data centres on the proposed design.

2. Investigate the energy efficiency benefits of data centre location optimisation in virtual network embedding infrastructures and the

impact on the power consumption of considering quality of service measures such as delay and client location.

3. Investigate the energy and spectral efficiency gains of virtual network embedding brought about by the use Optical OFDM as an underlying physical layer technology in core networks with data centres.

4. Propose a virtual network embedding solution in core networks with data centres that jointly maximises the profit for infrastructure providers and minimises the power consumption while keeping the acceptance ratio of requests at acceptable levels.

5. Propose a hybrid power virtual network embedding architecture in core networks with data centres employing renewable energy sources and then develop a MILP model that optimises the use of non-renewable power to reduce the overall greenhouse gas emissions of infrastructure providers and the overall electricity cost in a geographically price discriminated environment.

1.2 Original Contributions

1. A novel virtual network embedding model has been developed based on mixed integer linear programming (MILP) in an IP over WDM network with data centres. The model incorporates the optical layer in the link embedding stage. A real-time energy optimised virtual

network embedding (REOViNE) algorithm has been developed as a real time implementation of the proposed MILP model.

2. Development of virtual network embedding MILP formulations that incorporate data centre location optimisation for energy consumption minimisation and taking delay and customer location requirements into consideration.

3. A MILP model has been proposed for optimising power consumption and optical spectrum utilization in virtual network embedding infrastructures that uses optical OFDM as the underlying physical layer.

4. Novel realistic router port power consumption estimates have been produced and the GreenTouch Consortium has used these results in the GreenMeter study. The work on energy efficient virtualisation was also adopted by the GreenTouch Consortium as one of the solutions for energy minimisation in core networks. The GreenMeter study has been awarded the Edison Prize for 2016. The work on energy efficient virtual network embedding has been awarded the University of Leeds 2015 Carter Prize for the Best Published paper.

5. A virtual network embedding approach that jointly maximises the profit and minimises the power consumption of an infrastructure provider in core networks with clouds has been developed. The approach also guarantees acceptable request rejection ratios to

minimise customer churn. The profit optimised and energy minimised heuristic algorithm ensures real time implementation.

6. An approach to virtual network embedding in core networks with clouds that jointly reduces the overall greenhouse gas emissions and the OPEX accrued from electricity costs of an infrastructure provider has been developed.

1.3 Related Publications

The work in this thesis resulted in the following journals and conference papers:

1. Leonard Nonde, T.E.H. El-Gorashi, and J.M.H. Elmirghani, "Energy Efficient Virtual Network Embedding for Cloud Networks", IEEE/OSA Journal of Lightwave Technology, 2015. 33(9): p. 1828-1849

2. Jaafar M. H. Elmirghani, T. Klein, K. Hinton, A. Q. Lawey, L. Nonde, T.E.H. El-Gorashi, M. O. I. Musa, X. Dong "GreenTouch GreenMeter Core Network Energy efficiency Improvements ", to be submitted to IEEE/OSA Journal of Lightwave Technology, 2016.

3. Leonard Nonde, T.E.H. El-Gorashi, and J.M.H. Elmirghani, "Cloud Virtual Network Embedding: Profit, Power and Acceptance," in proc. IEEE Global Comminications Conference (GLOBECOM), San Diego CA. 2015.

4. Leonard Nonde, T.E.H. El-Gorashi, and J.M.H. Elmirghani, "Virtual Network Embedding Employing Renewable Energy Sources," Accepted in IEEE Global Comminications Conference (GLOBECOM), 2016.

5. Leonard Nonde, T.E.H. El-Gorashi, and J.M.H. Elmirghani, "Green Virtual Network Embedding in Optical OFDM Cloud Networks," in 16th IEEE Conference on Transparent Optical Networks (ICTON), Graz, Austria. 2014.

6. "GreenTouch Final Results from Green Meter Research Study: Reducing the Net Power Consumption in Communication Networks by upto 98% by 2020," A GreenTouch White Paper, Version 2.0, August 15, 2015.

1.4 Thesis Organisation

This thesis is organised as follows: Chapter 2 reviews Optical Networks and the various energy efficient approaches that have been introduced in Information and Communication Technology (ICT) networks. Most of the attention has been given to energy efficient approaches in core networks so as to enable a clear understanding of the proposed designs in the subsequent chapters.

Chapter 3 is a detailed review of network virtualisation and virtual network embedding. Network virtualisation has been defined in this

chapter and its use has been contextualised. Virtual network embedding is also introduced and its link to network virtualisation explained. Various approaches to virtual network embedding have also been described.

Chapter 4 introduces the novel network architecture and mixed integer linear programming (MILP) model for energy efficient virtual network embedding (EEVNE) in IP over WDM networks with data centres. The MILP model and real-time heuristic to represent the EEVNE approach for clouds in IP over WDM networks are developed. The model is tested with two different power consumption profiles for servers in data centers to determine the energy efficiency; an energy inefficient power profile and an energy efficient power profile.

Chapter 5 investigates the introduction of delay and client location constraints to the energy efficient virtual network embedding problem. It also investigates the power consumption benefits of data centre location optimisation in virtual network embedding infrastructures.

Chapter 6 investigates the spectral and power consumption benefits of introducing optical OFDM as the underlying physical layer in virtual network embedding infrastructures.

Chapter 7 is a study on the development of port power consumption values for core network routers at various lines rates. The study uses the modular design of the Cisco CRS chassis to estimate more accurately the power consumption of router ports, which have been used in later chapters.

The chapter also details the contributions that have been made to the GreenTouch GreenMeter study for energy efficiency improvements in core networks.

Chapter 8 is an investigation into the virtual network embedding design that jointly maximises profits for infrastructure providers and minimises the power consumption in the network. The design is such that request rejection is minimised to acceptable levels that do not encourage customer churn. A profit optimised and energy minimised (POEM) heuristic algorithm is developed for real time implementation.

Chapter 9 investigates virtual network embedding design in core networks with clouds that are connected to hybrid power sources. The virtual network embedding goal is to reduce the amount of greenhouse gas emissions of infrastructure providers while at the same time minimizing the OPEX due to electricity costs in the network.

The thesis is finally concluded in Chapter 10 where the major contributions of this work are presented and the future directions are discussed.

Chapter 2: Optical Networks and Energy Efficiency

2.1 Introduction

In this chapter, a review of optical networks and energy efficiency is presented. Optical networks have played a very crucial role in the development of the Internet ecosystem without which, there would be serious capacity limitations in service provisioning of Internet based applications. Detailed descriptions of generations of optical network designs and how they have interfaced with IP systems are presented. The chapter also makes an important review of the efforts that have so far been made to improve energy efficiency in Information and Communications Technology (ICT) systems over the years.

2.2 Optical Networks

2.2.1 SONET/SDH Networks

In the first generation of optical networks, optical fibres were mainly used to provide high capacity transmission for point to point links as they offered very low bit error rates. The switching functions and all the necessary control functions were all done by electronic components. The technology associated with the first generation of optical networks is Synchronous Digital Hierarchy (SDH) or Synchronous Optical Network (SONET) [16] the latter being the term used in North America and the former in Europe.

SDH/SONET technology offered an optical transport layer on which other technologies would ride. Time Division Multiplexing (TDM) is used to aggregate IP traffic with several other types of traffic for transport over SDH/SONET as shown in Fig. 2-1. A single wavelength is used to optically transport multiplexed SDH/SONET services over optical fibre links.

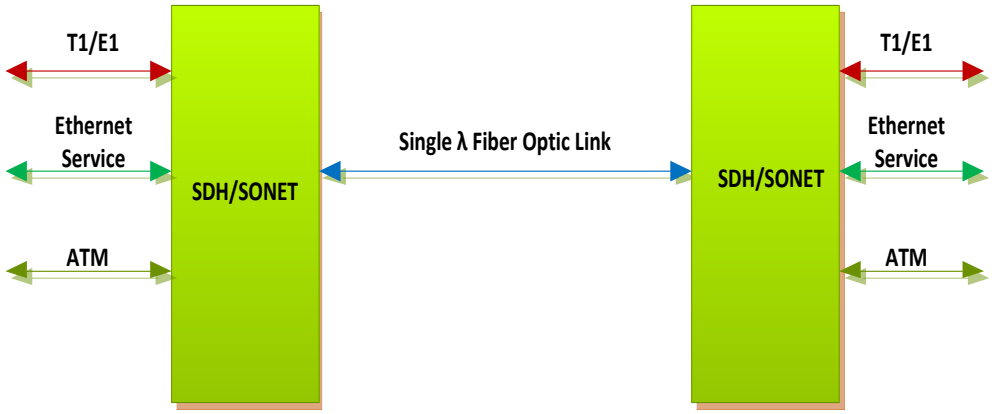

Figure 2-1: SDH/SONET Traffic Aggregation

Currently, SDH/SONET networks can support link transmission rates of tens of gigabits per second. The STM-64/OC-192 un-channelised system has transmission rates of 10 Gbps. Most of the traffic that is now carried by most networks is IP traffic, as a result, the present day SDH/SONET networks are mostly carrying IP over SDH/SONET traffic.

2.2.2 WDM Networks

As the Internet transport infrastructure grows rapidly towards a model of high speed routers connected by highly intelligent optical networks and widely geographically spaced data centres, SDH/SONET technologies have failed to fully meet the bandwidth requirements. The only present day technology that can effectively meet this demand for bandwidth is Wavelength Division Multiplexing (WDM). In the early years, WDM was a point to point deployment with SDH/SONET used as a standard layer for interfacing to the higher layers of the protocol stack [17]. Fig. 2-2

illustrates the interactions of WDM and IP with SDH/SONET as an interfacing layer.

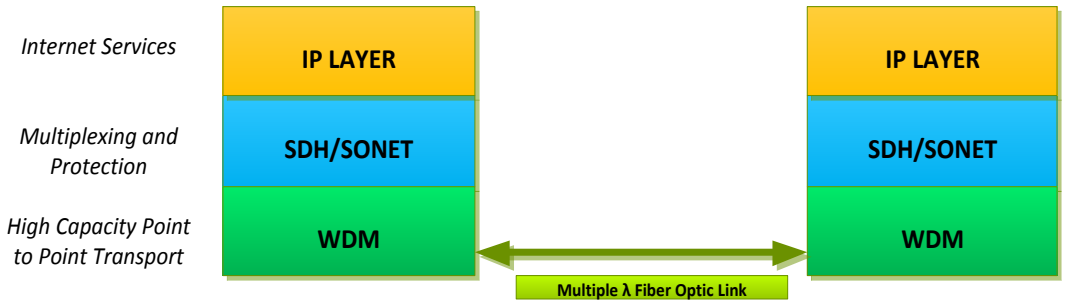

Figure 2-2: IP Over WDM with SDH/SONET as the Interfacing Layer

WDM networks provide circuit switched end to end optical channels or lightpaths between network nodes and their users. A lightpath is simply an optical channel or wavelength between two network nodes traversing through multiple nodes in the network. Intermediate nodes may switch and convert wavelengths. These networks are also referred to as wavelength-routing networks [18].

The major network components in the WDM network architecture are Optical Line Terminals (OLTs), Optical Add/Drop Multiplexers (OADMs), Optical Cross Connects (OXCs) and Optical Line Amplifiers (OLAs) [18]. These components work together to form a network that is protocol independent (Transparent Network) capable of carrying high capacity traffic. OLTs multiplex several wavelengths into a single fibre and de-multiplex a WDM signal into individual wavelengths. OADMs are used for grooming at stations where fractional wavelength traffic is added or

dropped from the WDM network. OXCs perform large scale routing of wavelengths in high capacity meshed networks.

Signals that come from the client equipment, such as IP Routers, cannot be readily presented and routed over the WDM network. OLTs therefore transponders, which adapt signals presented to them into a form that can be used in the WDM network. This is done by optical to electrical to optical (OEO) conversion within these devices. An interface between the client equipment and the long distance transponder is used and is often referred to as a short reach (SR) interface. In some cases, the transponder also adds overheads for purposes of network management and forward error correction (FEC). The outgoing signals of different wavelengths from the transponder are then multiplexed and transmitted over a single fibre. OLTs also terminate an optical supervisory channel (OSC) carried on a separate wavelength which is used for performance monitoring and other management and control functions.

The signal in the optical fibre undergoes attenuation as it travels from one node to the other. This is mainly due to absorption and scattering of photons by the glass along the length of the optical fibre [18]. Therefore, optical line amplifiers are used in between nodes at periodic intervals typically every 80km to 120km. Erbium Doped Fibre Amplifiers (EDFAs) are used as line amplifiers. EDFAs are capable of amplifying signals at many wavelengths simultaneously.

OADMs as mentioned earlier perform traffic grooming in WDM networks. These devices can have a static configuration or they could be implemented in a reconfigurable manner. Reconfigurable Optical Add and Drop Multiplexers (ROADMs) are very desirable in WDM networks. This is because they allow wavelengths to be dropped and added as and when they are required as opposed to having a fixed add/drop plan during equipment deployment, which can only be changed with interruptions to service. In today's ROADM architectures, there is transparent interconnectivity among nodes, flexible add/drop configurations and support for multiple service rates, including 2.5Gbps, 10Gbps and 40Gbps [19].

Optical cross connects are used to handle wavelength switching and routing in large meshed topologies where huge numbers of wavelengths are used. These devices are capable of providing lightpaths in large WDM networks in a fully automated manner. OXCs also perform wavelength conversion in addition to multiplexing and grooming.

2.2.3 IP Over WDM Networks

In today's world, almost all forms of end user communications make use of the ubiquitous TCP/IP protocol. This coupled with the high bandwidth capabilities of WDM networks makes IP over WDM the ideal choice for high capacity transport supporting today's Internet services. Fig 2-3 shows the interaction of the IP and Optical layers in an IP over WDM network.

IP over WDM can be implemented in two different ways; the Overlay Model and the Peer Model [20]

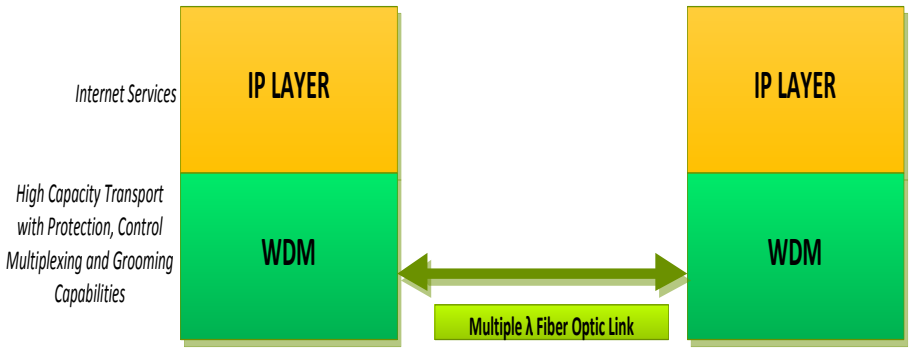

Figure 2-3: IP over WDM Network

2.2.3.1 Overlay Model

As shown in Fig. 2-4, in the overlay model, the optical transport network (OTN) is completely opaque to the IP network and as a result, two separate control planes exist. One control plane operates within the optical network and the other control plane between the core optical network and the IP Routers.

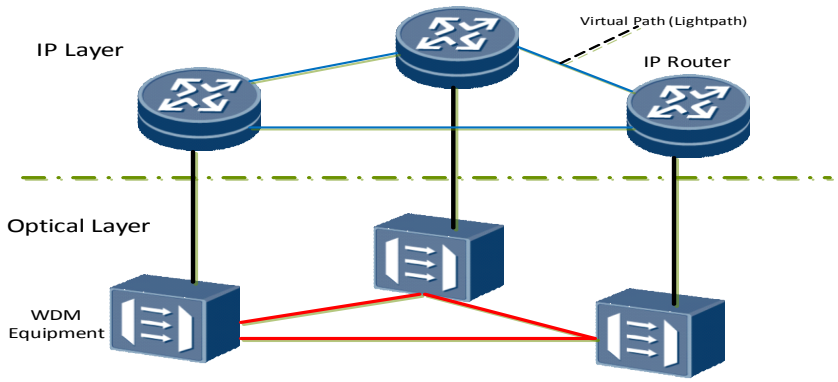

Figure 2-4: IP over WDM Overlay Model

This model also has two separate routing protocols; IP routing in the IP layer and wavelength routing in the optical layer. In the IP layer, routes are determined from the IP addresses by the IP routing protocol. In the optical layer, the lightpath could be statically provisioned or maybe dynamically determined. In the dynamic overlay model, lightpaths are dynamically established by the wavelength routers (WR). In this model, the OXC (WR) must have the ability to do neighbour discovery, obtain link state updates, do route computations and path establishment, traffic engineering and bandwidth provisioning. The Multiprotocol Label Switching (MPLS) protocol with modifications has been identified as the suitable control plane for optical switching [21].

2.2.3.2 Peer Model

In the peer model (Fig. 2.5), only one control plane exists. This means that both IP routing and wavelength routing are performed by the same control plane. Cisco has pioneered most of this work to meet the demand for converged packet infrastructure moving towards what they term the IP NGN-based architecture [5]. A modified generalised multiprotocol label switching (GMPLS) protocol has been adopted for the unified control plane.

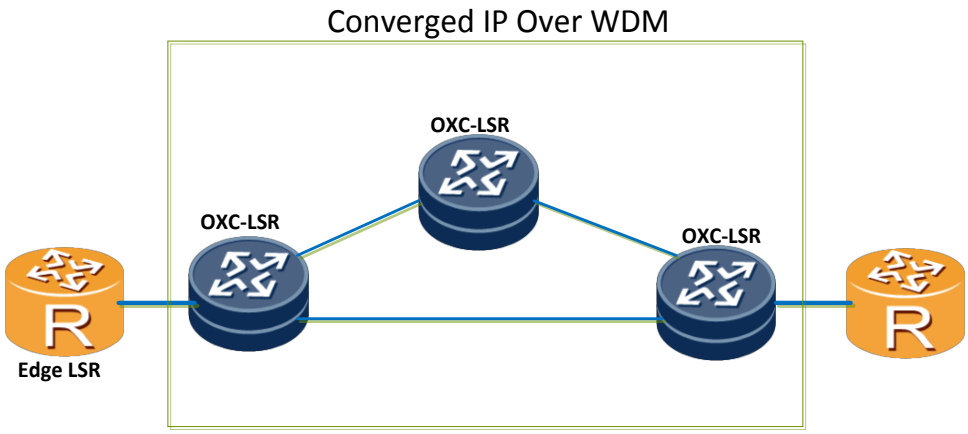

Figure 2-5: Converged IP over WDM Network - Peer Model

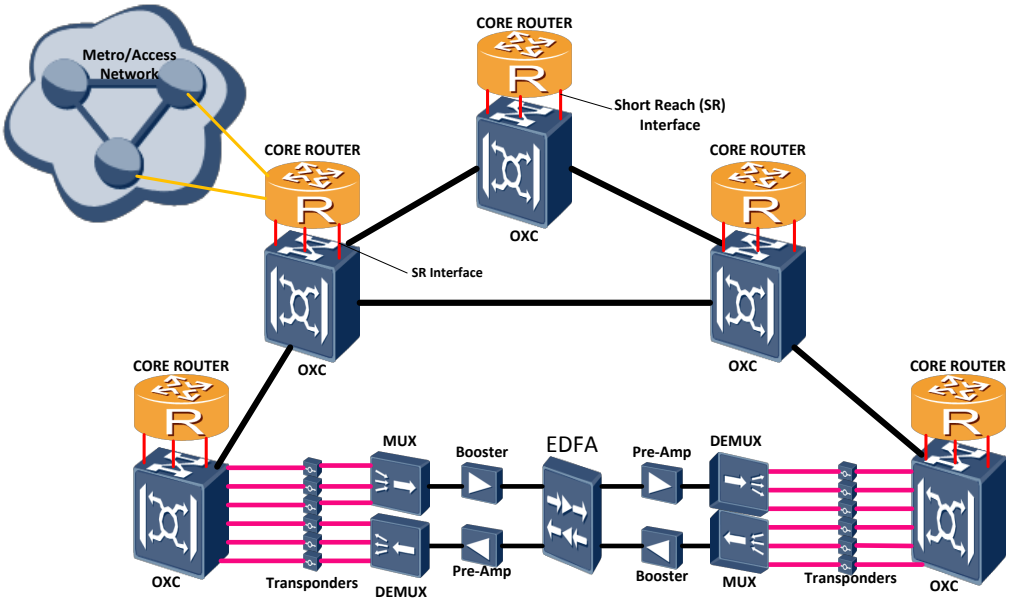

Figure 2-6: IP over WDM Core Network Architecture

Fig. 2.6 shows the IP over WDM network architecture with all the layers and components described earlier included.

2.3 Energy Efficient Approaches in ICT Networks

2.3.1 Introduction

There has never been a sector that has seen so much rapid growth in this generation as the Information and Communications Technology (ICT) sector. The Cisco Visual Networking Index of 2016 [22] reports that more than half a billion mobile devices and connections were added in the year 2015 and mobile data traffic grew by 74% in 2015 reaching 3.7 exabytes per month. This amount is expected to grow almost tenfold to 30 exabytes per month by the year 2020 as shown in Fig. 2-7. Applications on all these devices and others will need to access geographically distributed databases and servers using public and private clouds requiring flexible traffic management and bandwidth on demand capabilities. The high capacity network transport architectures of today will therefore need to evolve in order to adequately meet these requirements. This growth has put so much pressure on service providers to increase their Capital Expenditure (CAPEX) to meet the demand for the required high capacity equipment. The other price that has been paid by this growth is that ICT equipment is now consuming more and more energy and contributing an annual volume of greenhouse gas emissions just as much as the airline industry. [23]

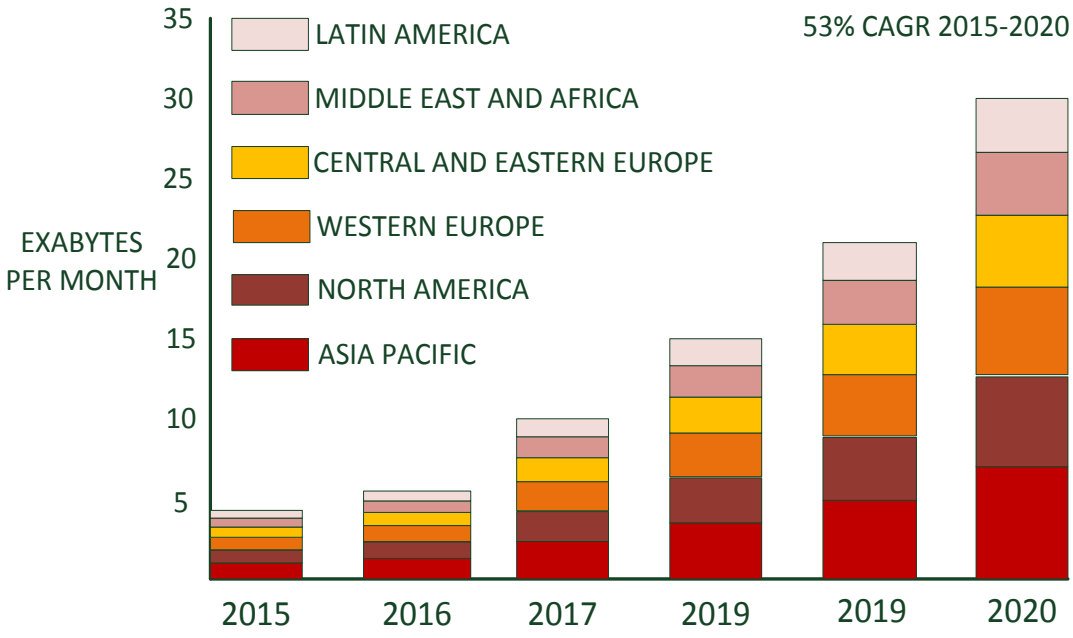

Figure 2-7: Global Mobile Data Traffic Forecast By Region [22]

This therefore calls for both academia and industry to come up with ways of minimising energy consumption in ICTs and in turn reduce the overall carbon footprint contribution from the ICT Industry. Earlier research work has examined energy efficiency in the ICT industry from different layers of the Internet ecosystem. The Internet ecosystem can be divided into three major network domains: The Core Network, Metro Network and Access Network. This study is however restricted only to the Core Network.

The term core network refers to the backbone network infrastructure in telecommunication networks that interconnects major cities, countries and even continents. These networks are usually topologically meshed to ensure survivability. Since core networks are high capacity networks, their

physical infrastructure is mainly supported by optical technologies discussed earlier. Several optical network architectures exist in core networks and these include; IP over SONET/SDH, IP over SONET/SDH over WDM and IP over WDM. These architectures have all been reviewed in the earlier sections and it can be seen that they are all multi-layered structures. This therefore entails that any meaningful efforts to bring about energy efficiency in core networks should include both the IP and optical transport layers as well as the data centres.

2.3.2 Energy Efficient Approaches in Core Networks

Recent research efforts have adopted several approaches to reducing energy consumption in core networks. These approaches can be divided into five categories: (i) Selective On-Off switching (ii) Improved Network Architectures (iii) Improved Routing Protocols and (iv) Improved Hardware Design.

2.3.2.1 Selective On-Off Switching

One of the approaches to saving energy in Core Networks is to selectively switch off the nodes in the network which are not carrying traffic during low traffic periods while still maintaining the important nodes in the network to support the remaining traffic. This entails that a core network node, which in this case could be an optical node or an electronic router, is switched off when it is completely idle and not carrying any traffic or when

it is carrying traffic below a certain threshold which could be routed to other nodes in the network.

One of the pioneering papers using this approach [5] discusses the impact on network protocols of saving energy by putting network interfaces and other router and switch components to sleep. Current Internet protocols would need some changes to achieve the objective of lowering the energy consumption by putting network interfaces and some other components to sleep when the equipment is idle.

The Authors in [24] consider the possibility of switching off routers and links in a wide area network under connectivity and quality of service (QoS) constraints. A physical topology comprising routers and links of known capacities is considered. There is also knowledge of the average traffic between the source and destination pairs in the network, the maximum supported link utilisation and the power utilisation of links and nodes. A problem of finding a set of routers and links that must be powered on so that the total power consumption is minimised is formulated. Since the problem is a capacitated multi-commodity flow problem, and thus NP-Complete, heuristics have been proposed to solve the problem. The results show that it is possible to reduce the percentage of powered nodes and links in the network as well as guaranteeing the quality of service at a given resource utilisation threshold. The problem with this approach is that it is not practical to switch off an entire node in a backbone network and expect it to recover instantly when required. The

approach also needs a separate control plane with links that would ensure that a node gets the knowledge of the status of the network even when it is asleep. The authors in [25] have proposed a technique that would help mitigate the control challenges of selective on-off switching. The work investigated the reduction of energy consumption in networked computers that operate in a clustered environment. Using traffic characterisation of university computers, it was shown that there is significant idle time that can be exploited for power management and subsequently energy consumption reduction. A proxying Ethernet adapter that handles routine network tasks for a desktop computer when it is in a low-power sleep mode was introduced. Such an addition to the hardware considered by the authors in [24] would resolve the control problem.

The other issue with the approach by the authors in [24] is that a real network with a real traffic profile has not been considered and as such the model may yield different results in a real network. This concern is addressed in [26] where a real IP backbone network and a real traffic profile have been considered. In this case however, protection nodes whose capacity is not required to transport off-peak traffic are selectively turned off. The results show that energy savings of more than 23% per year could be achieved through this approach, though at the expense of system reliability. Since only protection nodes have been considered, there is no need for the proxying adapter solution for the control plane as the active nodes can easily wake up the idle protection nodes provided that the

master active node itself does not fail first. The authors of [27] have also adopted a similar strategy except it has been applied in WDM networks and an enhancement to the manner in which the nodes are put to sleep has been made. A sleep mode operation of optical devices (Amplifiers and Optical Switches) that are installed for protection purposes only has been proposed. The sleep mode definition in this case is a low-power, inactive state in which devices can be suddenly waken up upon occurrence of a triggering event. An energy-efficient network planning problem for resilient WDM networks where optical devices can be configured in sleep mode was proposed and results of an Integer Linear Programming (ILP) model show savings of up to 25% in overall power consumption.

Since most traffic profiles are not constant throughout the day, some researchers have explored the opportunities of saving energy during low traffic periods. The authors in [28] evaluated the potential energy savings in IP over WDM Networks that could be achieved by switching off router line cards in low traffic demand periods. The authors propose dynamically adapting the network topology and the number of active components to the traffic patterns as a means of reducing energy consumption in IP over WDM backbone networks. An estimate and comparison of potential energy savings of three different approaches; Fixed Upper Fixed Lower, Dynamic Upper Fixed Lower, and Dynamic Upper Dynamic Lower is investigated. Line cards are put in idle state through routing reconfiguration at the IP and/or WDM layer. The results indicate that re-routing demands in the IP

layer (Using the Dynamic Upper Fixed Lower Approach) and subsequently switching off line cards that become redundant as a result, contributes the most to the energy savings. The authors also conclude that vendors should endeavour to design line cards that have in built fast on and off switching functionalities. The authors of [29] have also adopted this method of shutting down line cards in off-peak traffic periods but the approach has been extended further to include switching off the router chassis as well. When equipment is being shut-down or turned on, traffic interruptions may occur since new routes are needed. To mitigate this scenario, the authors in [30] have introduced a novel approach which focuses on the minimisation of the amount of re-configurations so that potential traffic interruptions can be minimised.

The approaches considered so far could be categorised as switch-off schemes aimed at reducing the energy consumption of already existing networks by switching off IP ports, links and even nodes during low traffic periods. Caria et al. [31] addresses the fact that, although it has been shown that these schemes can notably reduce the network's energy consumption, they are prone to instabilities in the IP routing service and decreased resilience due to reduced connectivity, and they may induce monitoring reconfigurations. In order to address these challenges, a switch-on scheme in an IP over WDM network has been proposed, where the network is designed so that the essential IP connectivity is maintained during low traffic periods while dynamic circuits are switched on in the

optical layer to boost network capacity during periods of high traffic demand.

2.3.2.2 Energy Efficient Network Architectures

The architectural design of the core network is another area that can be exploited to bring about energy efficiency in ICT networks. This is usually done through the incorporation of energy efficiency at the network design stage.

As a way of saving energy, some researchers have proposed the use of mixed line rates (MLR) in core networks. In [32] the authors evaluate the energy efficiency of an MLR network. A transparent optical network with no wavelength conversion and different reach for different line rates is considered. Considering the fact that currently there are vendors on the market who have manufactured line cards carrying 100Gbps on a single wavelength [33] and even as high as 400Gbps as seen on Cisco's CRS-X core router [34], the authors' proposal of mixed line rate networks is feasible. In this case, as opposed to a network providing a single line rate (SLR) of 2.5Gbps or 10Gbps or 40Gbps or 100Gbps as the demands for bandwidth grow, multiple line rates could be offered by the same network. The results from the work shows that MLR networks consume much lower energy than SLR networks.

The advent of bandwidth intensive user applications such as high definition IPTV has significantly increased the energy consumption in

backbone networks and is expected to continue increasing because of the high popularity of such applications. The authors in [8] have proposed energy minimisation of the IP over WDM backbone network as an important research problem. An investigation to reduce energy consumption in IP over WDM networks by applying lightpath bypass in the optical layer has been proposed. The study is based on the goal of reducing the number of required IP router ports as a way of increasing energy efficiency. Based on the lightpath bypass concept, a mixed integer linear programming optimisation model and two simple but efficient heuristics to minimise energy consumption have been developed. This has been achieved by considering all the physical layer issues concerning power consumption of all the components in both the IP and optical layers of the IP over WDM network. The results show that the energy-minimised IP over WDM design with lightpath bypass can significantly reduce energy consumption compared to the non-bypass design with energy savings ranging from 25% to 45%. It was also shown that energy consumption in IP over WDM networks follows an approximately linear relationship with the network traffic demand and that the lightpath bypass strategy can equalise the geographic distribution of power consumption which is important for some situations that are subject to maximal electricity supply at a network node location. IP routers were found to be the major consumers of power in IP over WDM networks accounting for over 90% of the total power consumed. The authors assumed a linear and proportional relationship between the traffic in the network and the power consumption

of the router ports. This may not necessarily be the case however as the use of 8 ports on a 10 port line card could consume just as much power as using all the 10 ports.

The authors in [35] have developed further the bypass model introduced by the authors in [8] to incorporate router line cards instead of only considering router ports. This is because in reality, router ports are organised by line cards or modules. In most cases, if not all for the case of the 40Gbps ports on the CISCO CRS1 Router [36], the addition or subtraction of a router port means the addition or removal of a line card. It was established that for modularized router ports, the strategy of optical bypass can significantly outperform the strategy of non-bypass in terms of energy consumption.

Increased network and equipment efficiency may lead to increased consumption of ICT services in accordance with the Khazzoom-Brooks postulate [37] and thus still increase the carbon footprint contribution. Therefore, researchers have investigated network architectures that incorporate the use of renewable energy sources by means of taking ICT infrastructure to renewable energy source sites [38]. In a bid to reduce the CO_2 emissions from IP over WDM networks, the authors in [39] have proposed an approach for energy minimisation in IP over WDM networks employing renewable energy sources. A linear programming model and heuristic for energy minimisation in the network when renewable energy is used has been proposed for improving renewable energy utilisation. The

results show that compared with routing in the electronic layer, routing in the optical layer coupled with renewable energy sources significantly reduces CO_2 emissions in the IP over WDM network by 47% to 52%. It was also shown that the nodes at the centre of the network have more impact than other nodes if they used renewable energy sources. Further investigations of additional energy savings resulting from the use of adaptive link rate (ALR) techniques under different load dependent energy profiles achieved even higher energy savings.

There has been significant research on energy consumption in data centres. This research has however mainly focussed on how to minimise energy inside the data centre by looking at cooling and other environmental concerns inside the data centres [40, 41]. However, the authors in [42] have investigated the power consumption associated with transporting data between data centres and end users. Based on the developed linear programming models and simulations, the results show that the selection of optimal locations of data centres in an IP over WDM network leads to a reduction in the network's power consumption. The authors also investigated replication of content with varying popularity to minimise power consumption. They have also addressed the question of whether to locate data centres next to renewable energy sources or to transfer renewable energy to data centres in a given network topology considering the power losses of 15% per 1000km of power transmission lines. The results from the work have shown that by identifying the optimum data

centre locations, combining the multi-hop bypass heuristic with renewable energy and employing the content replication scheme, power consumption savings of up to 73% can be achieved.

The authors in [43] investigate the power savings obtained by optimising the physical topology of an IP over WDM network. A mixed integer linear programming model is developed to optimise the physical topology of IP over WDM networks with the objective of minimizing the total network power consumption. An investigation of the physical topology optimisation under a symmetric full-mesh connectivity traffic matrix and an asymmetric traffic demand where data centres create a hot node scenario in the network is carried out. Simulation results show that the full-mesh and star topologies result in significant power savings of 95% and 92% respectively. Upon inclusion of renewable energy sources in the design, it was shown that optimising the physical topology increases the utilization of renewable energy sources. The authors in [44] have also evaluated at the role of network topology in energy efficient architectural designs of IP over WDM Networks. A large set of randomly-generated topologies, characterised by different values of the network connectivity index is considered. The connectivity index is defined as the measure of the average number of links per node within the network. A study is then carried out on how the connectivity index influences energy consumption of different IP over WDM network architectures. The different architectures are named; Basic, Transparent and Opaque IP Over WDM. A quantification of how the

energy consumption of these different architectures depends on network connectivity, geographical dimension and offered traffic is then established.

So far, several optical core network architectures aimed at energy minimisation in core networks have been reviewed. However, none of them has addressed the effect of physical layer impairments in their design and implementation. Musumeci et al.[45] have considered the fact that optical signals are subject to relevant physical layer impairments when traversing core network devices. Therefore, signal regeneration is often required, which has to be accomplished either at the electronic layer by routers or digital cross connects or directly at the optical layer through 3R-regenerators. In the study, a comprehensive comparison is done on four core network architectures namely: (i) Basic IP Over WDM without Optical Switching (ii) IP over SDH over WDM and (iii) IP over WDM with transparent or translucent switching, by performing energy assessment of the devices used at the transport layer. An ILP formulation is then developed for an energy minimised and impairment-aware design of each of the four architectures. The physical impairment-aware evaluation of the power consumption demonstrated that optical technology can provide benefits if, as happens in the translucent IP over WDM architecture, 3R-regenerators are used to increase end to end signal quality directly at the WDM layer. Power savings of up to 60% can be reached with translucent architectures.

2.3.2.3 Energy Efficient Routing Protocols

Optimisation of routing protocols in the IP layer and the optical layer has also been extensively researched as a way of minimizing energy consumption in core networks. Energy optimisation of routing and wavelength assignment (RWA) and the use of energy-aware routing have been identified as potential ways of reducing energy consumption at the optical and IP layers respectively in core networks.

The traditional open shortest path first (OSPF) protocol falls short of addressing the need to save energy in core networks. As highlighted by the authors in [8] router line cards and interfaces are the biggest consumers of energy in core networks compared to their optical counterparts. It is therefore necessary to design energy-aware routing schemes that would minimise energy consumption in IP core router networks. The authors in [46] have shown that significant energy savings can be achieved by incorporating power-awareness in the design of routers and routing networks. Routes in power aware routing networks would have to be calculated subject to power consumption constraints. In this case, the shortest route may not necessarily be 'short' as it would be very inefficient energy-wise for traffic to be routed over a particular path. Quality of service constraints could be added to the routing calculations to ensure that service levels are met all the time.

In a bid to make the OSPF protocol greener than what it is currently, the authors in [47] examine the modification of current link-state routing protocols such as OSPF to achieve energy efficiency. The modification would allow IP routers to power off some network links during low traffic periods. An algorithm that undergoes three phases in its operation has been proposed. The first phase involves the selection of routers in the network to be used as exporters of their own shortest path trees; and in the second phase, one of the neighbouring routers to these routers performs a task to detect the links to power off and in the final phase, new network paths in a modified topology are then computed. The study showed that 60% of the links could be turned off during low traffic periods. Further research has been proposed here by devising an optimum criterion for the choice of the set of exporter routers and a criterion for the choice of the number of exporter routers so that a given load threshold cannot be exceeded on the active links and the evaluation of such a design in a real network.

Fig. 2.8 shows the fractional energy consumption of a high-end electronic router in different functional blocks obtained from Tucker et al. [48]

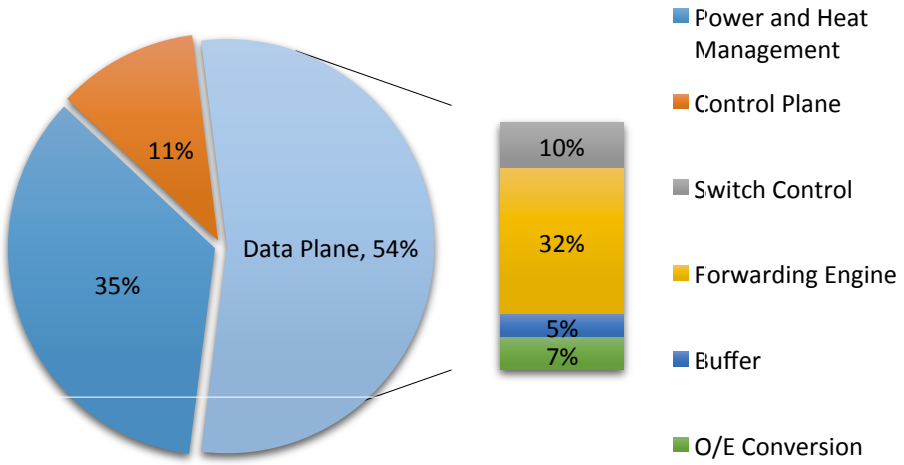

Figure 2-8: Fractional Energy Consumption of an Electronic High End IP Router [48]

It is evident from Fig. 2-8 that the data plane consumes the largest portion of energy in the router accounting for 54% while the control plane and the cooling fans and power supply account for 11% and 35% respectively. Breaking down further the energy consumption within the data plane, it can be observed that the forwarding engine (responsible for IP look up on packets) consumes 60% of the data plane's energy while the switching control plane, the buffer and the interfaces consume 18.5%, 9.2% and 13% respectively.

Therefore, efforts to minimise energy consumption of high end electronic routers should focus on the IP forwarding engine. Conventional routers that are in operation today, process each and every IP packet that they

receive and then consult the routing table to determine the destination of a particular packet. This method of packet routing is the major reason for the high energy consumption of the forwarding engine in IP routers because even in high traffic instants the router has to process each and every packet for onward transmission. In instances where the router gets overwhelmed, it randomly drops packets and then informs the source routers to reduce the rate of packet transmission. This can have very drastic effects on time sensitive applications such as video and voice which are slowly becoming the largest consumers of internet bandwidth. Consumers have not yet felt the full implications of this because service providers have over provisioned transmission resources whose design is based on the consideration of peak traffic. This has led to transport networks on average operating much below their full installed capacity and therefore current networks are characterised by significant power wastage due to overprovisioning.

There has been significant research in the area of packet forwarding and the author in [49] has proposed a method of treating packets as flows as one method of making the router forwarding engine efficient. The key concept is that each packet contains a full identification of the flow it belongs to. This identification, encapsulated by the packet's header according to the IP Protocol version 4, or version 6 consists of five values namely source address, source port, destination address, destination port and protocol. It therefore means that all packets that are part of the same

flow will carry the same five-value identification. Therefore, in flow management, you only need to process or route the first packet. You would then take the routing parameters that apply to the first packet and store them in what the author calls a hash table which is a data structure that allows for fast look up. When a new packet comes in, its identity is checked in the hash table, and if it is found to be present, it is then switched straight to an output port and thus saving time and power. The flow manager is shown in Fig. 2-9.

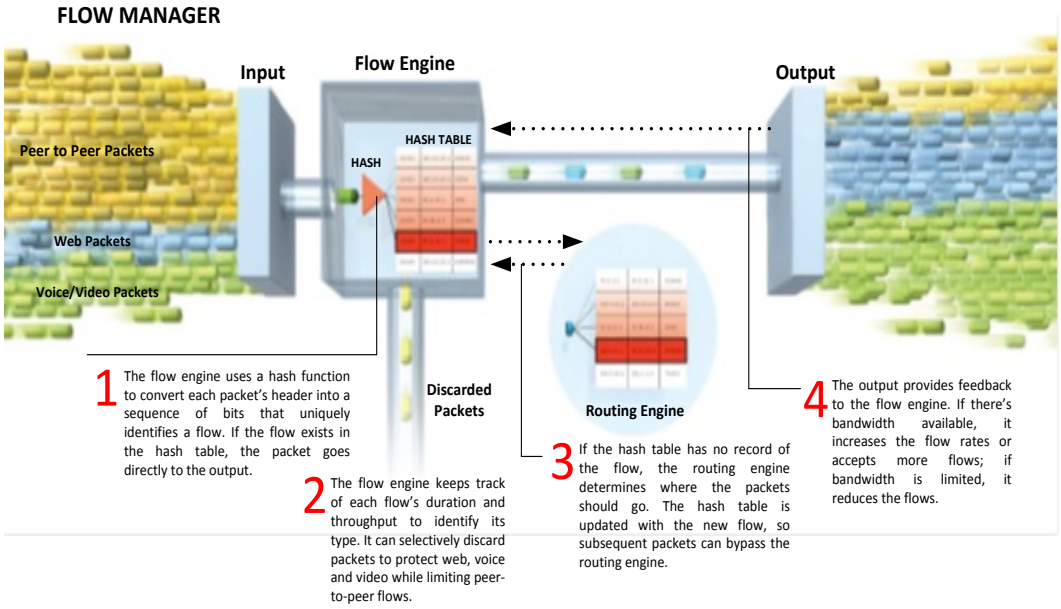

Figure 2-9: Flow Manager [49]

The other method under consideration for achieving more energy-efficient packet forwarding is the synchronous time-based IP switching approach. The authors in [50] have proposed synchronizing the operation of routers and scheduling traffic in advance. This is based on pipeline forwarding

concepts incorporating time-driven switching and sub-lambda switching. This will significantly reduce the complexity of most routing equipment because there would be no need for header processing, buffer size limitations, switching speed etc. The key to this concept is the availability of one clock source for all the routers on earth which are part of this network. The good side to this is that there are already existing sources of such synchronous time sources through satellites which are accessible everywhere on earth. This concept when extended to the optical domain would also enable all optical operation which has been made very difficult by the current nature of IP packet forwarding.

The aggregation of multiple traffic streams on one channel or wavelength (traffic grooming) has often been used in the context of reducing blocking and improving capacity utilization in optical networks [51]. Traffic grooming has, however, been also advocated in the context of energy-aware routing. The authors in [52] have modelled the total power consumption of an optical WDM network in terms of the power consumed by individual lightpaths. This approach leads to a useful representation of the total power consumption as a function of the number of lightpaths and total amount of electronically switched traffic. An ILP formulation which effectively combines and generalizes the two existing approaches to the traffic grooming problem namely the minimisation of the number of lightpaths and the minimisation of electronically routed traffic is developed. The results show that significant energy savings can be achieved with

power efficient grooming. The authors in [53] have also addressed the issue of power awareness and energy efficiency in WDM networks through traffic grooming. According to the authors in [54] the energy-efficient traffic grooming approaches reviewed thus far do not address the very important factor in energy saving – time. An argument has been advanced that minimising power consumption may not necessarily minimise the energy consumption. Therefore, the authors proposed both the static (all connection requests with their setup and tear-down times are known in advance) and dynamic traffic grooming problem with the additional consideration of time information. The additional time parameters in consideration are holding times of the lightpaths and the connection time requests.

The concept of traffic grooming with the goal of reducing energy consumption in optical WDM systems has been identified to have its own pros and cons. The authors in [55] have shown that traffic grooming is more advantageous to keep power proportional to traffic volume, while on the other hand, optical bypass reduces operational power by avoiding energy intensive electronic-domain processing. In order to find the optimum strategy which combines both, a power-aware provisioning scheme has been proposed. The results from the proposed scheme show that it uses less power than both the direct-lightpath approach and the traffic grooming approach. It has also been suggested that traffic grooming should be performed only at the end nodes and not intermediate nodes in order to

achieve energy efficiency. The authors in [56] have also appreciated the contributions of traffic grooming to energy efficiency, but contend that sometimes it does pay off not to groom. The research looks at energy-efficient path selection under the scheduled traffic model in IP over WDM optical networks. An energy-aware routing algorithm that is based on traffic grooming has been developed, but has the flexibility to deviate from it where needed. The results show that the energy-aware routing algorithm brings both significant energy savings as well as a lower blocking probability in comparison to a shortest paths based routing algorithm and traffic grooming algorithm.

The authors in [57] have considered the impact on the number of ports consumed in optical cross connects (OXCs) due to the use of traffic grooming and optical bypasses for purposes of power savings. An argument has been presented that it is necessary to achieve joint power efficiency and port savings in live IP over WDM networks where the traffic between each network node pair and resource assignment of each fibre link are not known in advance.

Time driven switching (TDS) is a slotted technique based on the availability of global time, retrievable from a variety of sources, such as GPS and Galileo. The authors in [58] contend that this technique could be used to switch fractions of wavelengths directly in the optical domain by the exploitation of time-coordination of all network components. A basic time period, called a Time Frame (TF), is identified and switched

independently by reconfiguring the optical switches at the end of the TF based on the global time synchronisation. Traffic Grooming, as discussed in the preceding paragraphs, can be used to achieve efficient link capacity utilisation and energy efficiency. However, since it is usually performed in the electronic domain, expensive routers and/or digital cross connects (DXCs) are needed and a lot of power is consumed while performing OEO conversions and the related amount of processing. TDS effectively addresses this issue according to the authors in [58] by sub- dividing the wavelength capacity in smaller portions of bandwidth (sub-λ granularity), enabling grooming directly in the optical domain. The results have shown that power savings of over 40% compared to the existing architectures are possible.

2.3.2.4 Energy Efficient Hardware Design

Hardware design of electronic routers is one area that has been assessed with the aim of increasing their energy efficiency. Line cards and chassis of core routers in core networks consume considerably a very high amount of energy as highlighted earlier. Chassis and router line cards can be realised in different hardware design configurations to yield different results in energy consumption. The authors in [59] have suggested that a routing system with different purpose-built components residing in a single chassis system, allowing for a better mix-and-match of features would have a better power budget. This is because even an empty chassis without line cards and other associated components does consume a considerable

amount of energy. It therefore makes sense to say that a chassis with a much higher fill level has lower energy consumption per processed bit than the ones with lower fill levels.

However, the author in [60] brings out the fact that there is difficulty in packaging large-scale routers in a single rack or a single room of equipment. Most of the routers on the market including the Cisco high performance CRS1 router are multi-rack systems. These systems suffer from poor scalability since the internal interconnections are critical when increasing the number of switching fabrics, line cards and racks. State of the art electronic routers like the Cisco CRS1 have already reached capacities of 1.2 Tbps per rack with a rack power consumption of 9.63kW [61] and the most recent CRS-X has reached a switching capacity of 922Tbps and rack power consumption of 18kW. Under these circumstances, the scaling of these electronic routers to support significantly more than hundreds of terabits per second would be very difficult indeed. According to Slaviša Aleksić [62] future petabit routers would probably consume more than 10MW of electricity when realised using current technologies and approaches. Using a hybrid approach, in which data processing on line cards as well as switch control and scheduling are performed electronically while interconnects and switching fabrics are implemented in optics, large capacities of hundreds of terabits per second are currently possible. The author, however, contends that optical switches cannot easily reach the

features of current high performance electronic switches, but they can potentially provide high switching speed and low power consumption.

The other hardware design paradigm that has been looked at in mitigating high power consumption in electronic routing devices is dynamic voltage and frequency scaling. The authors in [63] have brought out the importance of considering power efficiency in the design of interconnects instead of just focussing on performance. A motivation on the use of dynamic voltage and frequency scaling (DVFS) for links, where the frequency and voltage of links are dynamically adjusted to minimise power consumption is advanced. The basic idea is to use a high supply voltage, needed to deliver high bit rates and bandwidth, when data traffic is high and use a low supply voltage and lower clock frequencies when traffic is light. A history based DVFS policy that judiciously adjusts link frequencies and voltages based on past utilization has been proposed. The approach realizes up to 6.3x power savings and 4.6x on average. This reduction in power consumption is accompanied by 15.2% increase in latency before network saturation and 2.5% reduction in throughput. The authors in [64] have gone further to design and implement an opto-electronic transceiver front-end block where supply voltage can scale from 1.2V to 0.6V with almost linearly scalable bandwidth from 8Gbps to 4Gbps, and power consumption from 36mW to 5mW in a 130nm CMOS process. The design demonstrates the feasibility of dynamic voltage scalable optical I/Os which

could be incorporated in core electronic routers as well as optical equipment.

2.4 Summary

This chapter has given a detailed review of optical networks and how they have evolved over the years. A description of optical technologies that have been used for optical transport has been provided. A detailed review of the IP over WDM network has also been carried out so has to provide a clear understanding of the network architectures that will be presented in the coming chapters. A review of the current research efforts undertaken to enhance energy efficiency in ICT networks has also been presented. The focus has been narrowed down to core networks because it is the segment of the Internet ecosystem on which the following chapters are based.

Chapter 3: Network Virtualisation and Virtual Network Embedding

3.1 Introduction

Network virtualisation has been identified as the solution to the gradual ossification problem faced by the existing Internet architecture. By allowing multiple heterogeneous network architectures to coexist on a shared physical platform, network virtualisation provides scalability, customised and on demand allocation of resources as well as increased manageability of the network infrastructure [65]. A networking environment is considered to support network virtualisation if its infrastructure services have been decoupled from the physical assets on which the services operate. For many years now, server virtualisation has matured and enabled remarkable compute functions such as mobility, instant service on demand, push button disaster recovery among others, but the network side has not seen such kind of improvements. It is expected that network virtualisation will bring all these benefits enjoyed on the compute side into the networking

environment. In order for network virtualisation to work, there must exist a framework that efficiently allocates physical network resources to the virtual network instances. Resource allocation in network virtualisation relies on algorithms developed to embed virtualized networks onto the shared physical platform known as the substrate network. This class of algorithms are commonly referred to as "Virtual Network Embedding (VNE)" algorithms.

3.2 Network Virtualisation

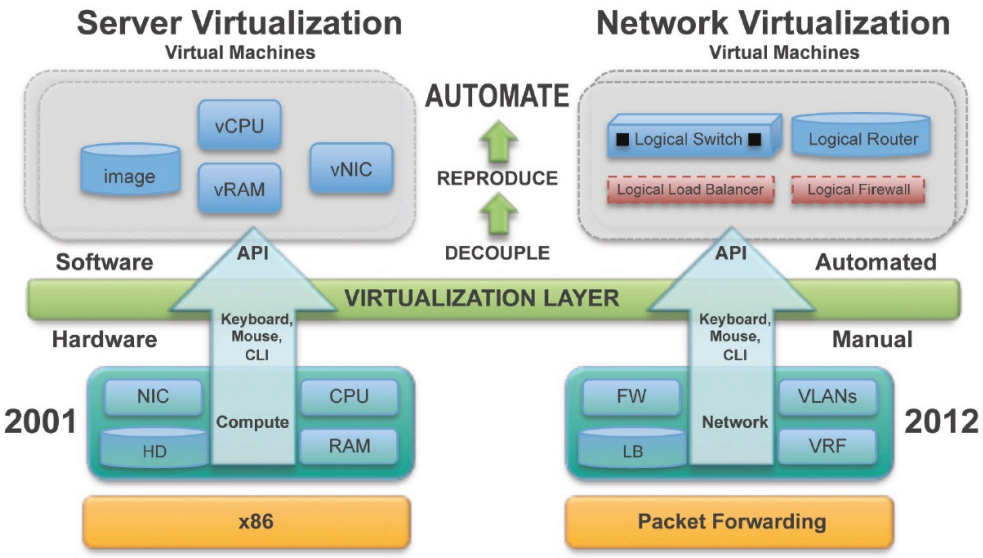

Figure 3-1: Server and Network Virtualisation [66]

The network provides traffic forwarding and routing functions to enable access to services in the cloud. The traditional way of service provisioning for networks is to dimension the network for, maximum expected traffic

and individually configure a multitude of physical proprietary hardware through various command line interfaces (CLIs) to bring up the service. Fig. 3-1 shows server and network virtualisation implementation. In the same way as CPU, RAM and NIC hardware resources are visualized on the server side, the firewall, LAN switch and router hardware resources are virtualized on the network side in a network virtualized environment. All the virtualized resources are implemented in software which means that they can easily be provisioned and withdrawn in an instant. The virtualisation layer shown in Fig. 3-1 is where the intelligence resides responsible for controlling traffic flows as well as service provisioning. In this implementation, there is no CLI configuration per physical device. Application program interfaces (APIs) are used at the virtualisation layer to configure all the necessary features needed to provision the virtual networks. The physical network now only performs the traffic forwarding functions and all the control and configuration functions move to the virtualisation layer.

In the research community, various predispositions toward network virtualisation have been taken. The authors in [67] argue that network virtualisation may bring nothing new in terms of technical capabilities and theoretical performance, but it provides a way of organizing networks in such a way that it can help the current practical problems facing the Internet. The authors identify the benefits of machine virtualisation and the similarities in functionality between an operating system and a network

and then derive potential benefits that network virtualisation would bring. Their conclusion is that the first widespread use case of network virtualisation would only be related to increased network flexibility of network management and deployment. On the other hand, the work done by the authors in [68] brings in Software Defined Networking as the practical enabler of network virtualisation in data centre infrastructure networks. The authors present the FlowN scalable architecture which supports numerous tenants having heterogeneous topologies. By doing so, a cloud computing infrastructure in which tenants can exercise greater control over their own virtual networks is created.

Aside from the benefits of enhanced network management and multi-tenancy, from the perspective of the network operator, network virtualisation is seen as an enabling tool in several perspectives including; ability to resell infrastructure, diversification of infrastructure for private purposes, provisioning of network infrastructure as a service and minimisation of the cost of ownership. However, the authors in [69] have pointed out that there will be many challenges in implementation despite the obvious business case. Some of the challenges lie in finding the optimal solutions to map a specific virtual network in a physical substrate. They also point out the existence of several crucial, but rather conflicting goals for infrastructure providers in scalability, flexibility and strict virtual network isolation.

The huge benefits that server virtualisation has brought to cloud computing are usually not exploited to the full because the networking side in its current traditional sense is just not robust enough. The fact that the two, compute and networking, cannot work in isolation means that the other must also evolve to provide the much needed balance. In suggesting that computing and networking resources should have a combined control, management and optimisation framework in a cloud environment, the authors in [70] have proposed that network virtualisation is a credible enabler of such an architecture. A Service-Oriented Architecture (SOA) in network virtualisation has been proposed and thus enabling a network-as-a-Service (NaaS) paradigm which would facilitate convergence of networking and cloud computing.

There are also opportunities for introduction of energy efficiency in networks through the use of network virtualisation. As it has already been learned from server virtualisation, the ability to host multiple distinct virtual machines onto a single server brings about efficiencies in energy consumption. Taking the same concept to the network, as opposed to having only one routing instance in a single physical router, a physical router could have several virtual routers with all the routing capabilities. The authors in [71] have proposed a network architecture where router virtualisation is used to optimise power consumption in the network. The developed Green Cloud Architecture (GCA) has the ability to either shutdown or put a router into a sleeping mode or migrate virtual routers to

another physical router depending on the energy minimisation requirements.

Opportunities for network virtualisation do not only lie in servers and networking components such as IP routers and LAN switches. Cloud networks are comprised of data centres which are geographically dispersed and are usually connected to each other by high capacity optical networks described in chapter two. Effective and efficient functioning of cloud networks in service provisioning is very highly dependent on these networks that interconnect the data centres. Virtualisation has also been proposed as a means to enhance network management scalability in high capacity optical networks. The authors in [72] have proposed an optical network virtualisation architecture and have evaluated how optical switching technologies can be used for virtualisation. The challenges that optical network virtualisation presents are also highlighted. Unlike layer 3 (VPN) and layer 2 (VLAN) virtualisation implementations where digitization is readily available, optical network resources are differentiated by their analogue properties. In a situation where an optical network resource is virtualized, due to physical layer impairments, different virtual instances would interfere with each other. Therefore, virtualisation solutions should always take into account the physical characteristics of the optical network resources.

3.3 Virtual Network Embedding

It is expected that future Internet architectures will be based on the Infrastructure as a Service (IaaS) [73] business model which will give rise to a two tier service provider structure comprising of: Infrastructure Providers (InPs) who own and are responsible for the physical network and Service Providers (SPs) who are responsible for providing services to the end users. There is therefore a need for a resource allocation framework that defines exactly how infrastructure resources can be efficiently shared and provisioned for a specific goal. A Virtual Network (VN) is the primary entity in network virtualisation. It comprises of virtual nodes interconnected with virtual links both with their own resource requirements. Node resources could represent processing power, memory or storage while link resources could represent bandwidth requirements or minimum delay requirements or both. Each VN is totally independent of the other and can thus have different protocols and services configured without impacting on the other.

The resource allocation challenge in network virtualisation leads to a problem commonly known as the Virtual Network Embedding (VNE) problem. As clearly outlined by the authors in [74], the VNE problem is a very challenging problem because the mapping of virtual nodes and links onto the physical network comes with very specific constraints on both nodes and links which must be satisfied. The other problem in VNE is that the physical network, usually referred to as the substrate network, has

limited resources which means that some of the requested virtual networks would have to be rejected or buffered to avoid disturbing existing virtual networks. There are two cases to virtual network embedding. The first case is where the requirements of all the virtual network requests (VNRs) are known in advance and therefore the mapping could be done in what is often referred to as the offline mode. The second case, known as the online mode is where the VNRs are not known in advance and may arrive dynamically and stay in the network for an indiscriminate period of time. It has been proven that the process of mapping virtual nodes onto a substrate network without violating bandwidth constraints in both online and offline cases is NP-hard and similar to a multiway separator problem [74], [75]. For this reason, most of the developed solutions involve the use of heuristic algorithms.

Solving the VNE problem should have a specific resource allocation objective. This objective ensures that the desired benefit of network virtualisation is realised by either the infrastructure provider or the end user or both. Some of the desired goals in the VNE include: Revenue maximization, network resilience and survivability, load balancing, efficient network management and energy efficiency.

3.3.1 Revenue Maximization

Revenue maximization is one of the major goals of every infrastructure provider. If there is an opportunity that would allow an InP to obtain more

revenue from the existing infrastructure by simply changing the way resources are provisioned, then there are possibilities of higher profits. Various authors have proposed different virtual network embedding approaches focused on revenue enhancements in infrastructure networks. The authors in [76] have developed a revenue driven virtual network embedding algorithm that maximises revenue by making use of the global resource information in the network. When embedding nodes in the network, substrate nodes are ranked according to their global resources. The substrate nodes which offer the best opportunities for revenue are ranked higher and selected for node mapping and then the links are connected using the shortest path algorithm. Similar work involving node ranking has been done in [77] using the Markov random walk model based on the resource and topological attributes of a node. Instead of treating the node and link embedding stages of VNE separately, the work in [78] introduces better coordination between the node and link embedding stages which significantly increases the solution space and thus produces better results in the number of accepted requests, revenue generated and the cost of resource provisioning. The authors in [79] have developed a profit maximization VNE approach based also on the use of global resource capacity to quantify the embedding potential of each node in the substrate network. A virtual network embedding design with an admission control policy that selectively accepts virtual network requests that have high revenue-to-cost ratios has been developed.

3.3.2 Network Resilience and Survivability

The current extensive use of cloud based services demand that both the network infrastructure and data centres that support them are always available to avoid any disruptions. Resiliency and survivability then become very important subjects to consider in order to guarantee service reliability. Survivability can also be introduced into network virtualisation to enhance the availability of embedded virtual networks. The authors in [80] have formulated a survivable virtual network embedding problem that incorporates single substrate link failures. Survivable mechanisms have been incorporated at the link mapping stage using efficient restoration and protection policies. Service level assurance has been added to the mapping process in order to prioritise the restoration of failed virtual links. The resilience problem is also addressed through provisioning of dedicated backup links for all embedded virtual links. However, the authors in [81] argue that this method is not efficient in terms of resource utilization for the InP and would lead to higher request rejections depriving the InP of the much needed revenue. Therefore, a mechanism that allows for the sharing of backup resources for protection of several virtual networks and thereby providing room to accommodate more requests is proposed.

Virtual node migration and virtual link re-mapping have also been proposed as measures to improve network resilience in network virtualisation. The process involves incorporating virtual node migration into virtual network embedding algorithms such that if there is a substrate

node failure, virtual nodes embedded at that node are migrated to other locations in the substrate network and then their links re-mapped accordingly. The work in [82] uses this approach by using the artificial bee colony algorithm to obtain the optimal virtual network embedding solution. In the same context, the authors in [83] have developed an integer programming algorithm that dynamically recovers the failures on substrate resources without an advance provision of backup resources. The recovery process is only activated once a failure occurs in the network.

3.3.3 Energy Efficiency

Energy efficiency continues to be a major concern among infrastructure providers given the huge demand for cloud applications by the ever increasing number of users. The fact that network virtualisation consolidates the use of cloud resources, provides opportunities for efficient energy utilization in cloud infrastructure networks. Over provisioning, which results from designing systems for peak demand, leads to high energy inefficiencies because energy resources are still used to the same level during periods of low demand. The on demand allocation of resources brought about by network virtualisation breaks this trend since energy resource utilization can now scale together with resource provisioning. The authors in [12] and [13] have developed an energy aware virtual network embedding approach that concentrates the embedding of virtual network requests in a reduced subset of already active links and nodes to avoid

turning on new ones. The approach saves energy resources in the network through resource consolidation.

Other approaches to power consumption minimisation through virtual network embedding have gone beyond just considering turning on and off of nodes and links. The assumption that the power saved by turning off a physical node is equal to the power saved by turning off a physical link was argued to be an inaccurate assumption by the authors in [11]. Therefore a generalised power consumption model is devised for both active nodes and active links as comprising of both idle power consumption and the CPU utilization dependent variable power consumption. Using the developed power consumption model, a two stage power efficient virtual network embedding model with better coordination between the node and link mapping phases has been developed.

The flexibility offered by network virtualisation to move virtualized compute and networking instances from one physical location to another seamlessly is exploited by the authors in [14] to enhance energy efficiency. The energy-aware reconfiguration heuristic which takes a set of already embedded virtual network requests as an input and then re-allocate them in the substrate network in an energy efficient manner without violating the virtual network acceptance ratio is introduced. The work in [84] introduces a virtual network embedding technique that incorporates energy costs of operation and migration of virtual nodes. The energy savings are achieved through predicting future networking and computing demands of

virtual networks and then intelligently migrating virtual networks at those times in order to put other nodes and links into a sleep mode. In line with reducing energy costs, infrastructure providers would also benefit from energy efficient approaches that focus on electricity cost reductions in infrastructure networks. The authors in [85] have formulated an electricity cost model and designed an efficient cost-aware virtual network embedding algorithm that exploits the geographical and time varying diversity in electricity pricing to optimise the energy consumption.

Concerns for the environment and possible penalties that might be introduced by regulatory bodies to limit the amount of greenhouse gas (GHG) emissions into the environment have led to consideration for virtual network embedding research approaches that focus on reduction in GHG emissions. The work in [86] focusses on the design of a virtual network embedding solution in which virtual networks are embedded in nodes with the cleanest sources of energy. The authors use the concept of emission factors where each node in a particular city is assigned a metric that defines how "clean" or how "dirty" its energy sources are.

3.4 Summary

The future Internet architectures will be based on the infrastructure as a service (IaaS) business model that decouples the role of the current Internet Service Providers into two roles: The infrastructure provider who deploys and maintains the network equipment and the service provider in

charge of deploying network protocols and offering end to end services. This model will be made possible by network virtualisation because the substrate network will be deployed and maintained by the Infrastructure Service Provider while the Service Providers, who will be dealing with end to end users, are the ones who will own the virtual networks. Network virtualisation relies on virtual network embedding algorithms which dictate how physical resources are utilised and shared among various users. Virtual network embedding algorithms can be implemented to achieve various goals which may include revenue maximization, network survivability and resilience, network infrastructure management and energy efficiency.

Chapter 4: Energy Efficient Virtual Network Embedding

4.1 Introduction

The energy consumption in both high capacity core networks and in data centres is continuously increasing due to the growth in demand for computing and networking resources that heavily depend on them. As discussed in Chapter 3, network virtualisation has been proposed as an enabler of energy savings by means of resource consolidation in both the network and data centres. In all these proposals, the virtual network embedding (VNE) models and/or algorithms do not address the link embedding problem as a multi-layer problem spanning from the virtualisation layer through the IP layer and all the way to the optical layer. On the contrary, in this chapter, a very detailed and accurate approach towards energy efficient VNE (EEVNE) where the model determines the optimum approach to minimise the total network and data centre server power consumption is considered.

In this chapter the granular power consumption of various network elements that form the network engine in backbone networks is considered as well as the power consumption in data centres. A mixed integer linear programming (MILP) model and a real-time heuristic to represent the EEVNE approach for clouds in IP over WDM networks are developed. The MILP model is tested with two different power consumption profiles for servers in data centres to determine the energy efficiency; an energy inefficient power profile and an energy efficient power profile. A comparison in performance of the model under different load conditions has also been carried out. Two randomly generated physical network topologies and three real physical network topologies have been used for MILP modeling and heuristics to provide a wide scope of substrate networks. The real topologies used are the National Science Foundation Network (NSFNET), the United States NETwork (USNET) and the Italian Network.

4.2 Virtual Network Embedding in IP over WDM Network Architecture

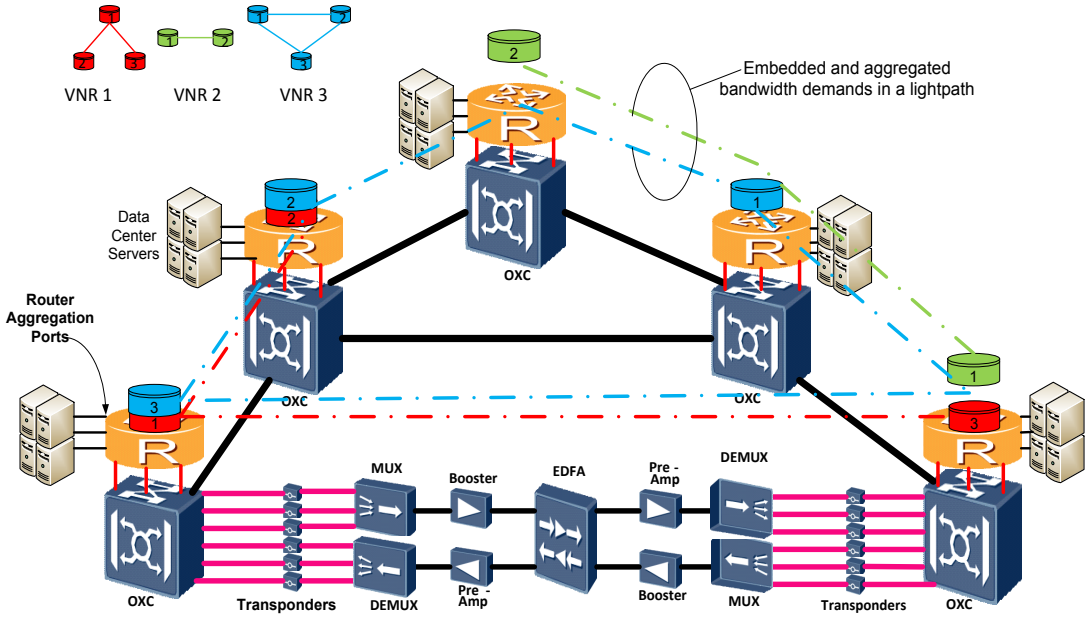

Figure 4-1: Architecture of Virtual Network Embedding In IP over WDM Network with Data Centres

The VNE problem defines how virtualized resources should be realized onto the substrate network. As described in Chapter 3, virtual network requests (VNRs) are annotated with node and link demands and in the same way, the substrate network is annotated with node and link resources. Demands and resources have to be matched in order to achieve complete embeddings. In Fig. 4-1, the VNRs 1, 2 and 3 with node and link demands are to be embedded onto the substrate network, which is an IP over WDM network with data centres. Each substrate node is considered to host a data centre in addition to the IP and optical equipment. When a virtual node is embedded in the substrate network, its CPU demands instantiate

virtual nodes in the data centre and its bandwidth demands instantiate a virtual router in the core router such that the requester of the service is granted control of both the virtual node and virtual router and has the ability to configure any protocols and run any applications. The transport network supporting the flow of traffic due to the embedded VNRs is the IP over WDM network. As shown in Fig. 4-2, it is composed of two layers, the IP layer and the optical layer. Successful embedding of VNRs' link demands will therefore need resources both in the IP layer and the optical layer. IP routers aggregate traffic from VNRs and in each substrate node IP routers are connected to optical switches which are connected by optical fibre links. The optical layer provides the large bandwidth required for communication between IP routers. On each fibre, a pair of multiplexers/demultiplexers is used to multiplex/demultiplex wavelengths. The transponders provide OEO processing for full wavelength conversion at each switching node. In addition, for long-distance transmission, erbium-doped fibre amplifiers (EDFAs) are used to amplify the optical signal in each fibre. Based on this architecture, a MILP formulation has been developed with the overall aim of minimizing power consumption.

4.3 MILP Model for Energy Efficient Virtual Network Embedding

The substrate network is modeled as a weighted undirected graph $G = (N, L)$ where N is the set of substrate nodes and L is the set of

substrate links. Each node or link in the substrate network is associated with its own resource attributes. The VNR v is represented by the graph $G^v = (R^v, L^v)$ where R^v is the set of virtual nodes and L^v is the set of virtual links. In Fig. 4-2, an illustration of how demands in a VNR are mapped onto the substrate network across multiple layers is clearly shown. The locations of some of the variables and parameters used in the model across the layers are also shown.

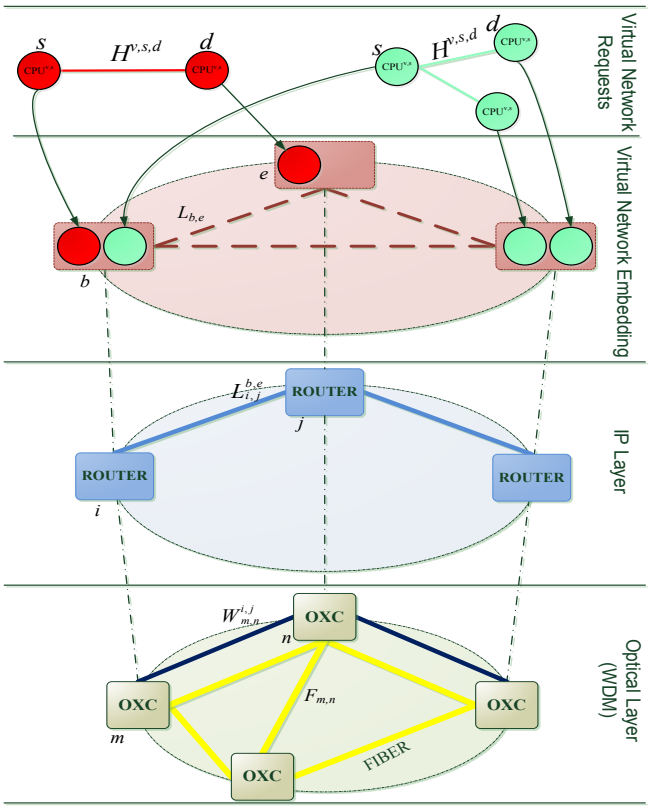

Figure 4-2: Illustration of VNE across Multiple Layers in IP/WDM

As discussed in [87], CPU utilization is the main contributor to the power consumption variations in a server. Therefore, the CPU utilization of servers in

a data centre is also the main contributor to the variation in the power consumption of a data centre. Only the servers' power consumption is considered when calculating the power consumption of data centres since the largest proportion of data centre power is drawn by servers. According to the authors in [88], 59% of the power delivered in the data centre goes to IT equipment. It also states that decreasing the power draw of servers clearly has the largest impact on the power cost in data centres. While the efforts made by other researchers and institutions like Google and Microsoft in improving the energy consumption due to cooling and the use of efficient power supplies are appreciated, the efforts in this work are restricted to the power consumed in servers and high capacity network equipment in data centres. It is worth noting here that large data centres have now achieved power usage effectiveness (PUE) approaching 1, where PUE is the ratio of the total amount of power used in a data centre to the power consumed by IT equipment. For example [89] and [90] report PUE values of 1.12 and 1.125 respectively, where it is clear that, in large data centres, server and communication equipment power consumption now dominates cooling, lighting and power supply units' losses. The power consumption due to the local area network (LAN) inside the data centre also contributes to the power consumption in the data centre. However, as it will be shown later, the LAN power consumption is very low compared to the power consumption due to servers. Therefore the energy inefficient data centre power profile shown in Fig. 4-3 is considered which accounts only for the power consumption due to servers. The power profile in Fig. 4-3 is constructed

from a data centre containing 500 Dell Power Edge R720 Servers [91] each with idle power rated at 112W and 365W at full load.

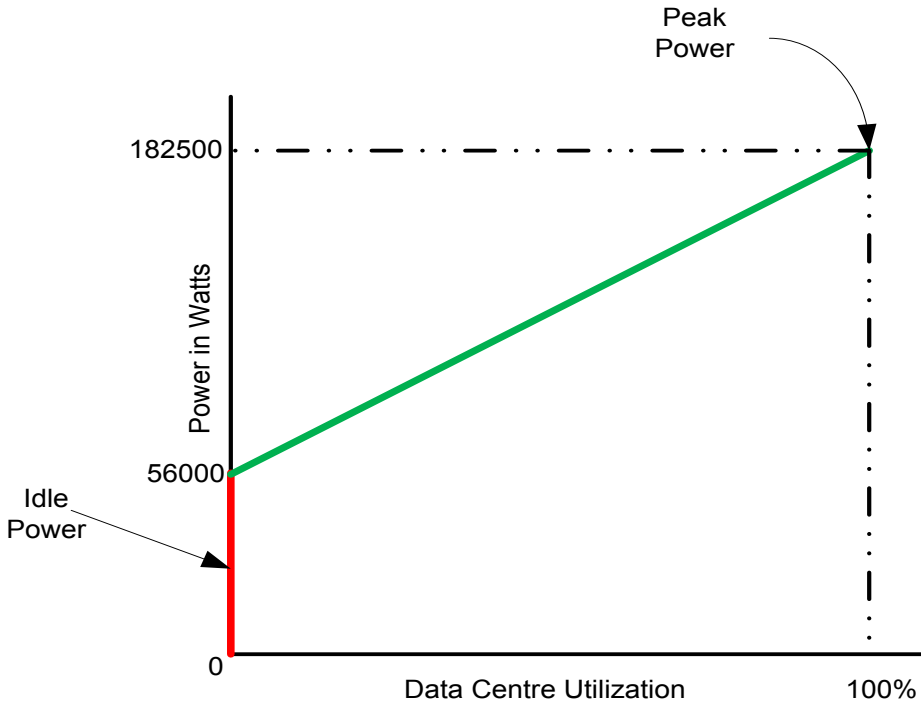

Figure 4-3: Data Centre Servers Power Profile with 500 Dell R720 Servers

Before the introduction of the MILP model, the sets, parameters and variables used are defined.

Sets:

V	Set of VNRs
R	Set of nodes in a VNR
N	Set of nodes in the substrate network
N_m	Set of neighbor nodes of node m in the optical layer

Parameters:

$s\ and\ d$	Index the source and destination nodes in the topology of a VNR
$b\ and\ e$	Index source and destination substrate nodes of an end to end traffic demand aggregated from all VNRs
$i\ and\ j$	Index the nodes in the virtual lightpath topology (IP layer) of the substrate network
$m\ and\ n$	Index the nodes in the physical topology (optical layer) of the substrate network
CPU_b	Available CPU resources at substrate node (data centre) b
N_b	Number of servers at substrate node b
$NCPU^{v,s}$	Number of the servers required by VNR v in node s
$CPU_b^{v,s}$	$CPU_b^{v,s} = \frac{NCPU^{v,s}}{N_b}$, is the percentage CPU utilization of virtual node s of VNR v when embedded in node b
$H^{v,s,d}$	Bandwidth requested by VNR v on virtual link (s,d)
B	Wavelength rate
W	Number of wavelengths per fibre
$D_{m,n}$	Length of the physical link (m,n)
DO_b	$DO_b = 1$ if the data centre at node b has been activated by previous embeddings

$F_{m,n}$	Number of fibres in physical link (m,n)
$EA_{m,n}$	Number of EDFAs in physical link (m,n). Typically $EA_{m,n} = \left\lvert\left(\frac{D_{m,n}}{S}\right) - 1\right\rvert + 2$, where S is the distance between two neighboring EDFAs
PR	Power consumption of a router Port
PT	Power consumption of a transponder
PE	Power consumption of an EDFA
PO_m	Power consumption of an optical switch at node m
PMD	Power consumption of a multi/demultiplexer
DM_m	Number of multi/demultiplexers at node m
P_{idle}	Idle server power consumption of a data centre
μ	Data centre server power consumption per 1% CPU load

Variables:

$\delta_b^{v,s}$	$\delta_b^{v,s} = 1$, if node s of VNR v is embedded in a substrate node b, otherwise $\delta_b^{v,s} = 0$.
Ψ^v	$\Psi^v = 1$, if all the nodes of a VNR v are fully embedded in the substrate network, otherwise $\Psi^v = 0$
$\rho_{b,e}^{v,s,d}$	$\rho_{b,e}^{v,s,d} = 1$, if the embedding of virtual nodes s and d of virtual request v in substrate nodes b and e, respectively

	is successful and a link b, e is established if a virtual link s, d of VNR v exists.
$\omega_{b,e}^{v,s,d}$	$\omega_{b,e}^{v,s,d}$ is the XOR of $\delta_b^{v,s}$ and $\delta_e^{v,d}$, i.e. $\omega_{b,e}^{v,s,d} = \delta_b^{v,s} \oplus \delta_e^{v,d}$
$L_{b,e}$	Traffic demand between the substrate node pair (b, e) aggregated from all embedded VNRs
Φ^v	$\Phi^v = 1$, if all the links of VNR v are fully embedded in the substrate network, otherwise $\Phi^v = 0$
$L_{i,j}^{b,e}$	Amount of traffic demand between node pair (b, e) passing through the lightpath (i, j) in the substrate network
$C_{i,j}$	Number of wavelengths in lightpath (i, j) in the substrate network
Q_b	Number of aggregation router ports at node b
$W_{m,n}^{i,j}$	The number of wavelengths of lightpath (i, j) passing through a physical link (m, n)
$W_{m,n}$	Number of wavelengths in physical link (m, n)
$\lambda_{m,n}$	$\lambda_{m,n} = 1$, if the physical link $(m, n)$is activated otherwise $\lambda_{m,n} = 0$

K_b	$K_b = 1$ if the data centre in node b is activated, otherwise $K_b = 0$

The power consumption in a data centre due to the embedding of node s of VNR v is given as:

$$PD_b^{v,s} = \begin{cases} P_{idle} + \mu \cdot CPU_b^{v,s} & if\ the\ data\ centre\ at\ b\ is\ ON \\ 0, & otherwise \end{cases}$$

The power consumption of data centres due to servers is given as:

$$PD = \sum_{b \in N} \sum_{v \in V} \sum_{s \in R} CPU_b^{v,s} \cdot \delta_b^{v,s} \cdot \mu + K_b \cdot P_{idle}$$

The network power consumption under non-bypass where lightpaths passing through an intermediate node are terminated and forwarded to the IP router [8] is composed of:

Power consumption of router ports:

$$\sum_{m \in N} PR \cdot \left(Q_m + \sum_{n \in N_m} W_{m,n} \right)$$

Power Consumption of transponders:

$$\sum_{m \in N} \sum_{n \in N_m} PT \cdot W_{m,n}$$

Power Consumption of EDFAs:

$$\sum_{m \in N} \sum_{n \in N_m} PE \cdot EA_{m,n} \cdot F_{m,n} \cdot \lambda_{m,n}$$

Power Consumption of Optical Switches:

$$\sum_{m \in N} PO_m$$

Power Consumption of multi/demultiplexers:

$$\sum_{m \in N} PMD \cdot DM_m$$

The model is defined as follows:

Objective:

Minimise the overall power consumption in the network and data centres given as:

$$\begin{aligned} \sum_{m \in N} PR \cdot \left(Q_m + \sum_{n \in N_m} W_{m,n} \right) + \sum_{m \in N} \sum_{n \in N_m} PT \cdot W_{m,n} \\ + \sum_{m \in N} \sum_{n \in N_m} PE \cdot EA_{m,n} \cdot F_{m,n} \cdot \lambda_{m,n} + \sum_{m \in N} PO_m \\ + \sum_{m \in N} PMD \cdot DM_m + \sum_{b \in N : DO_b = 0} \sum_{v \in V} \sum_{s \in R} CPU_b^{v,s} \cdot \delta_b^{v,s} \cdot \mu \\ + K_b P_{idle} \end{aligned} \quad (4\text{-}1)$$

Subject to:

VNRs constraints:

$$\sum_{v \in V} \sum_{s \in R} CPU_b^{v,s} \cdot \delta_b^{v,s} \leq CPU_b \qquad b \in N \tag{4-2}$$

Constraint (4-2) ensures that the CPU demands allocated to a substrate node do not exceed the capacity of its data centre.

$$\sum_{b \in N} \delta_b^{v,s} = 1 \quad \forall v \in V, \quad \forall s \in R \tag{4-3}$$

Constraint (4-3) ensures that each node in a VNR is embedded only once in the substrate network.

$$\begin{gathered} \delta_b^{v,s} + \delta_e^{v,d} = \omega_{e,b}^{v,d,s} + 2 \cdot \rho_{b,e}^{v,s,d} \\ \forall\, v \in V, \qquad \forall b, e \in N : b \neq e, \qquad \forall s, d \in R : s \neq d \end{gathered} \tag{4-4}$$

Constraint (4-4) ensures that virtual nodes connected in the VNR are also connected in the substrate network. This is achieved by introducing a binary variable $\omega_{e,b}^{v,d,s}$ which is only equal to 1 if $\delta_b^{v,s}$and $\delta_e^{v,d}$ are exclusively equal to 1 otherwise it is equal to zero.

$$\begin{gathered} \rho_{b,e}^{v,s,d} = \rho_{b,e}^{v,d,s} \\ \forall\, v \in V, \qquad \forall b, e \in N : b \neq e \;\; \forall s, d \in R : s \neq d \end{gathered} \tag{4-5}$$

Constraint (4-5) ensures that the bidirectional traffic flows are maintained after embedding the virtual links.

$$\sum_{v\in V}\sum_{s\in N}\sum_{d\in N:s\neq d} H^{v,s,d}\cdot \rho_{b,e}^{v,s,d} = L_{b,e}\ \forall b,e\in N: b\neq e \tag{4-6}$$

Constraint (4-6) generates the traffic demand matrix resulting from embedding the VNRs in the substrate network and ensures that no connected nodes from the same VNR are embedded in the same substrate node.

$$\sum_{b\epsilon N}\sum_{s\in R} CPU_b^{v,s}\cdot \delta_b^{v,s} = \Psi^v \sum_{b\epsilon N}\sum_{s\in R} CPU_b^{v,s} \quad \forall v\in V \tag{4-7}$$

Constraint (4-7) ensures that nodes of a VNR are completely embedded meeting their CPU demands.

$$\sum_{b\in N}\sum_{e\in N:b\neq e}\sum_{s\in R}\sum_{d\in R:s\neq d} H^{v,s,d}\cdot \rho_{b,e}^{v,s,d} = \Phi^v \sum_{s\in R}\sum_{d\in R:s\neq d} H^{v,s,d} \quad \forall v\in V \tag{4-8}$$

Constraint (4-8) ensures the bandwidth demands of a request are completely embedded.

$$\Phi^v = \Psi^v \quad \forall v\in V \tag{4-9}$$

Constraint (4-9) ensures that both nodes and links of a VNR are embedded. Constraints (4-7), (4-8) and (4-9) collectively ensure that a request is not partially embedded.

Flow conservation in the IP Layer:

$$\sum_{j \in N: i \neq j} L_{i,j}^{b,e} - \sum_{j \in N: i \neq j} L_{j,i}^{b,e} = \begin{cases} L_{b,e} & if \quad i = b \\ -L_{b,e} & if \quad i = e \\ 0 & otherwise \end{cases} \qquad \forall b, e \in N: b \neq e \tag{4-10}$$

Constraint (4-10) represents the flow conservation constraint for the traffic flows in the IP Layer.

Lightpath capacity constraint:

$$\sum_{b \in N} \sum_{e \in N: b \neq e} L_{i,j}^{b,e} \leq C_{i,j} \cdot B \qquad \forall i, j \in N: i \neq j \tag{4-11}$$

Constraint (4-11) ensures that the sum of all traffic flows through a virtual link does not exceed its capacity.

Flow conservation in the optical layer:

$$\sum_{n \in N_m} W_{m,n}^{i,j} - \sum_{n \in N_m} W_{n,m}^{i,j} = \begin{cases} C_{i,j} & if \; m = i \\ -C_{i,j} & if \; m = j \\ 0 & otherwise \end{cases} \qquad \forall i, j \in N: i \neq j \tag{4-12}$$

Constraint (12) ensures the conservation of flows in the optical layer.

Physical Link capacity constraints:

$$\sum_{i \in N} \sum_{j \in N: i \neq j} W_{m,n}^{i,j} \leq W \cdot F_{m,n} \quad \forall m \in N, n \in N_m \tag{4-13}$$

$$\sum_{i \in N} \sum_{j \in N: i \neq j} W_{m,n}^{i,j} = W_{m,n} \quad \forall m \in N, n \in N_m \tag{4-14}$$

Constraints (4-13) and (4-14) represent the physical link capacity constraints. Constraint (4-13) ensures that the number of wavelengths in a physical link does not exceed the capacity of fibres in the physical links. Constraint (4-14) gives the total number of wavelength channels used in a physical link.

Aggregation ports constraint:

$$Q_b = \sum_{e \in N: e \neq b} {}^{L_{b,e}}/_{B} \quad \forall b \in N \tag{4-15}$$

Constraint (4-15) gives the number of aggregation router ports at each node in the substrate network.

4.4 The Real-Time Energy Optimised Virtual Network Embedding (REOViNE) Heuristic

The REOViNE (Real-time Energy Optimised Virtual Network Embedding) heuristic provides real-time implementation of the EEVNE approach. The flow chart of the heuristic is shown in Fig. 4-4. The heuristic obtains the graph $G^v = (R^v, L^v)$ of VNR v. The nodes of v are grouped such that those that are not connected to each other in the VNR topology graph

G^v are put into one group. Separate groups are created for all the other nodes that are connected to each other to avoid embedding nodes that are connected in the VNR into the same substrate node. The heuristic determines the number of candidate substrate nodes required to embed a full VNR based on the number of node groups created. Fig. 4-5 shows examples of node groupings of a VNR with four nodes and three links. In Fig. 4-5(a), Nodes 1 and 3 are not connected and therefore, they are grouped together to form a group. Similarly nodes 2 and 4 are grouped together to form another group. With this grouping, the VNR requires a minimum of two substrate nodes for the node embedding to be successful. Fig. 4-5(b) shows another grouping option where the unconnected nodes 1 and 4 are placed in one group. In this case, node 3 has to be in a group of its own as it cannot be in the same group as it is connected to node 2 and cannot be in the same group as nodes 1 and 4, as it is connected to node 4. Similarly node 2 has to be in a group of its own. The grouping in Fig. 4-5(b) results in the use of 3 substrate nodes, whereas Fig. 4-5(a) grouping needs only 2 substrate nodes to embed the VNR. The grouping is done to achieve maximum compaction, i.e. minimum number of substrate nodes. Therefore the grouping in Fig. 4-5(a) will be selected as the optimal grouping. From this example, the node grouping rules can be summarized as follows:

(i) Nodes that are not connected in the virtual network request can be put in one group and embedded in the same substrate node

(ii) Nodes that are connected to each other must belong to different groups

(iii) The grouping process is only finished when all nodes in the virtual network request have been placed in a group

(iv) There may be more than one grouping option. The grouping option that leads to the minimum number of substrate nodes is selected.

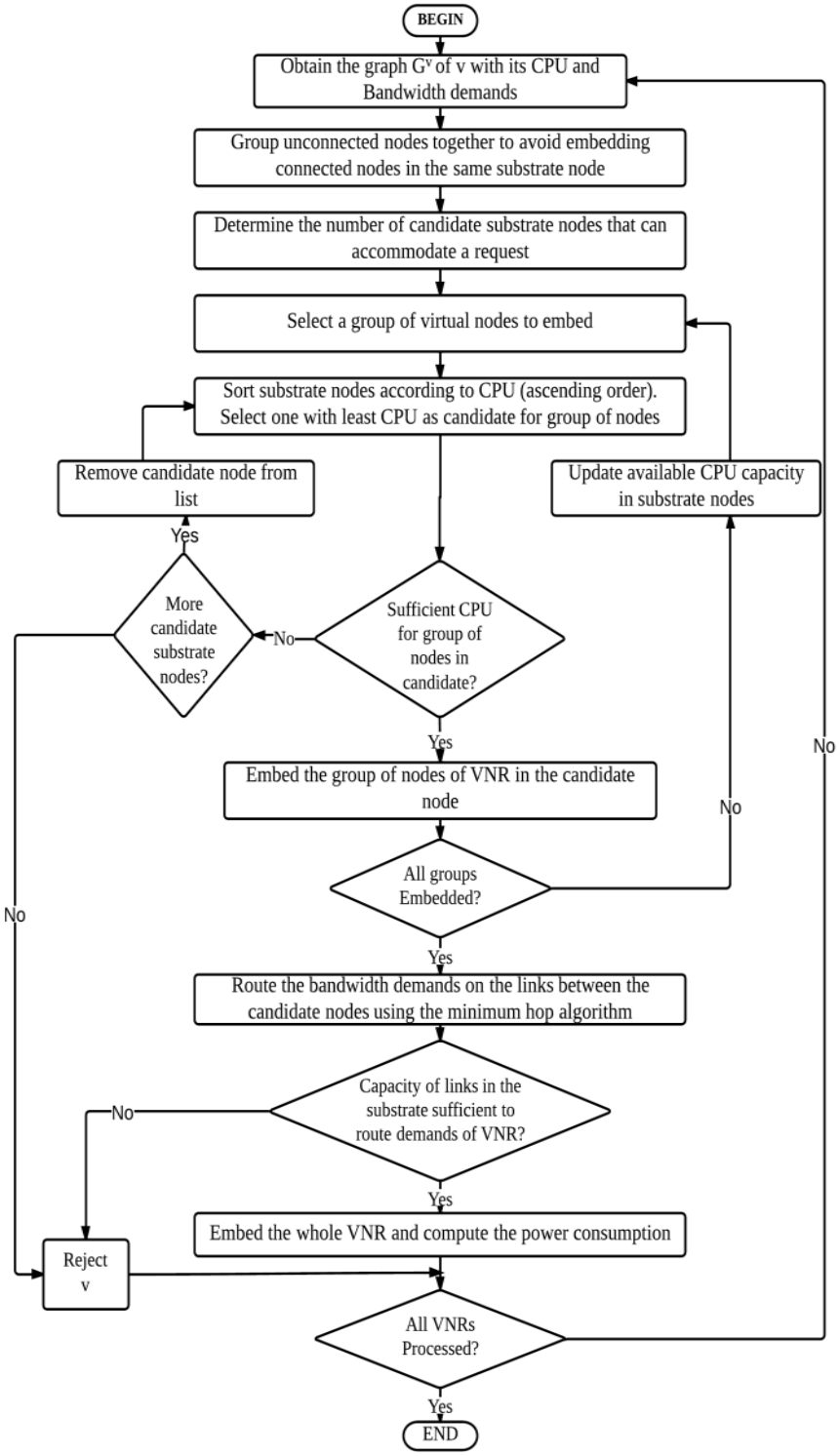

Figure 4-4: REOViNE Heuristic Flow Chart

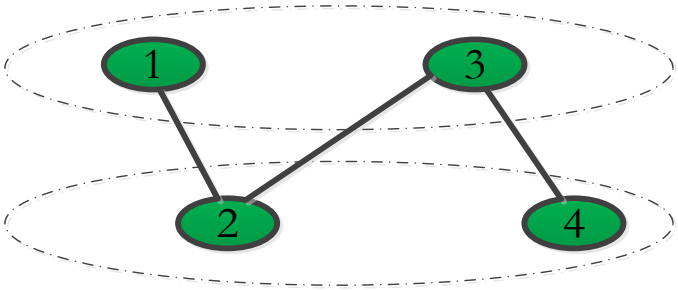

(a) A VNR requiring a minimum of two substrate nodes

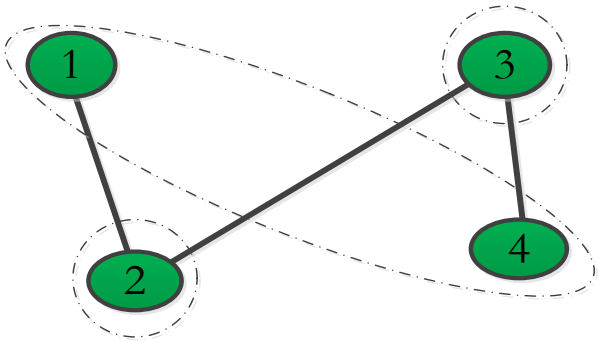

(b) A VNR requiring a minimum of three substrate nodes

Figure 4-5: Grouping of Nodes of a VNR

The substrate nodes are sorted according to the available CPU capacity in ascending order. Because of the energy inefficient power profile of the data centres (large idle power), the heuristic tries to consolidate the embeddings in data centres by filling the ones with least residual capacity before switching on others. The substrate node with the least available CPU capacity is selected as the candidate to embed the first group of nodes. The order in which the groups are selected is not important because it does not affect the success or failure of the embedding of nodes. However, the selected grouping option is one that requires the minimum number of substrate nodes. If the candidate substrate node has sufficient capacity, the virtual nodes will be embedded in that substrate node; otherwise the

heuristic will try to embed the virtual nodes in another substrate node. If, however, all the candidate substrate nodes have been exhausted, the request will be rejected and the heuristic will proceed to embed another request. After embedding all the nodes of the VNR, the heuristic proceeds to route the bandwidth demands on the links between the candidate substrate nodes using the minimum hop algorithm to minimise the network power consumption. The request will be blocked if any of the links does not have sufficient capacity to accommodate the traffic. If the traffic is successfully routed, the request is accepted. The heuristic calculates the power consumption of the accepted request and continues to embed other VNRs.

4.5 Performance Evaluation of the EEVNE Model and the REOViNE Heuristic

In order to evaluate the performance of the proposed model and heuristic, the NSFNET network is used as the primary substrate network. However, evaluation of both the model and heuristic has also been done in other substrate network topologies for results verification. The NSFNET comprises 14 nodes and 21 links as shown in Fig. 4-6. A scenario in which each node in the NSFNET network hosts a small data centre of 500 servers to offer cloud services has been considered. Table 4-1 shows the parameters used. The power consumption of the network devices that have been used are based on the work done by the authors in [42] which are derived from

datasheets in [92] - [96]. The IP router ports are the most energy consuming devices in the network.

The Dell Power Edge R720 [91] server power specifications have been used to evaluate the data centre server power consumption. The Cost Virtual Network Embedding (CostVNE) model developed by the authors in [97] and the Virtual Network Embedding Energy Aware (VNE-EA) model developed by the authors in [12] have been adapted to incorporate the IP over WDM network architecture with data centres. Their performance has been used as a benchmark to evaluate the performance of the EEVNE model and the REOViNE heuristic in terms of power consumption and the number of accepted virtual network requests. The detailed description and objective functions of the two models are as follows:

4.5.1 CostVNE Model

The CostVNE model minimises the use of substrate resources allocated to a VNR. Since the amount of CPU resources allocated to a request cannot be reduced through consolidation, the model only optimises the use of bandwidth on the links by consolidating wavelengths. The objective of the CostVNE model is given as:

$$minimize \sum_{m \in N} \sum_{n \in N_m} W_{m,n} \tag{4-16}$$

Table 4-1: Evaluation Scenario Parameters

Distance between two neighboring EDFAs	80 (km)
Number of wavelengths in a fibre (W)	32
Number of Fibres per link ($F_{m,n}$)	1
Power consumption of a transponder (PT)	73 (W)
Power consumption of a single router port (PR)	1000(W)
Power consumption of an EDFA (PE)	8 (W)
Power consumption of an optical switch (PO)	85(W)
Power consumption of a multi/demultiplexer (PMD)	16(W)
Dell Server full load power consumption	365(W)
Dell Server idle power consumption	112(W)
Data Centre idle power consumption (500 servers)	56000(W)

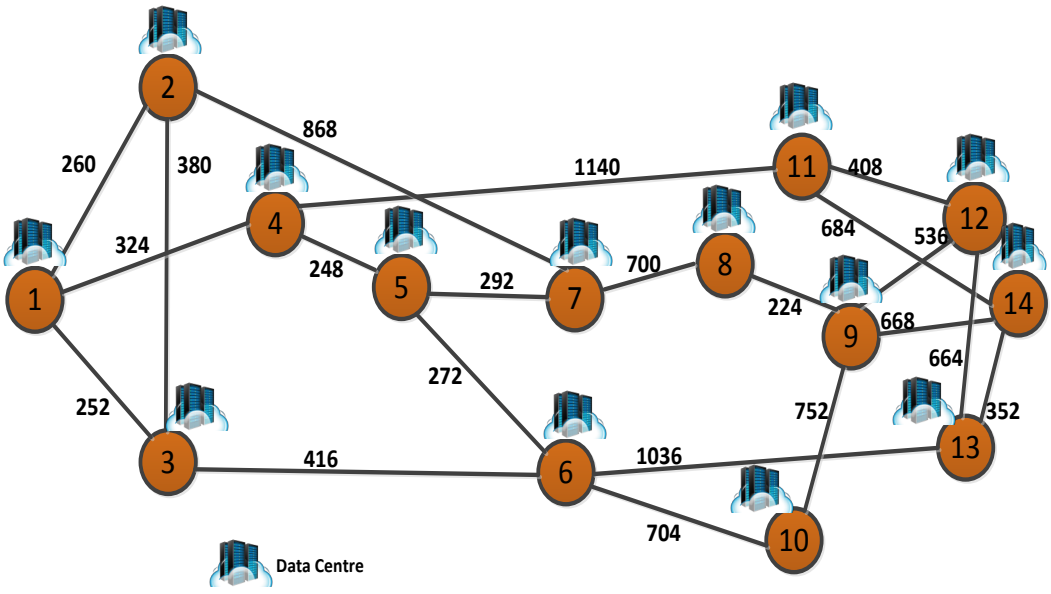

Figure 4-6: The NSFNET Network with Data Centres

4.5.2 VNE-EA Model

The VNE-EA model minimises the energy consumption by minimizing the number of substrate links and nodes that are activated when embedding VNRs. The objective function of this model is given as:

$$minimize \sum_{m \in N: NO_m = 0} \sigma_m + \sum_{m \in N} \sum_{n \in N_m: LO_{m,n} = 0} \beta_{m,n} \quad (4\text{-}17)$$

where σ_m and $\beta_{m,n}$ are binary variables that indicate the active nodes and links in the substrate network, respectively. Note that NO_m and $LO_{m,n}$ are binary parameters indicating the already activated substrate nodes and links, respectively before the embedding of requests.

4.5.3 Embedding of VNRs of Uniform Load Distribution

The complexity of the MILP model grows exponentially with the number of nodes in the VNR. Therefore, virtual nodes in a VNR uniformly distributed between 2 and 6 have been considered. The CPU demand of each node in a VNR is uniformly distributed between 2% and 10% of the total CPU resources of a data centre. The bandwidth on links connecting virtual nodes in a VNR is also uniformly distributed between 10Gb/s and 130Gb/s. The model attempts to embed a total of 50 VNRs onto the 14 node NSFNET substrate network. AMPL software with the CPLEX 12.5 solver is used as the platform for solving the MILP models and the REOViNE heuristic is implemented in Matlab. All the Models and REOViNE were executed on a PC with an Intel® Core™ i5-2500 CPU, running at 3.30 GHz, with 8 GB RAM.

The results in Fig. 4-7 show the network power consumption, the power consumption in data centres and the overall power consumption versus the number of VNRs. The requests arrive two at an instance and the existing requests are not reconfigured when embedding arriving requests. The CostVNE model has resulted in the minimum network power consumption as it optimises the use of bandwidth of the substrate network by consolidating wavelengths regardless of the number of data centres activated (Fig. 4-7(a)). Compared to the EEVNE model, the CostVNE model saves a maximum of 5% (average 3%) of the network power consumption.

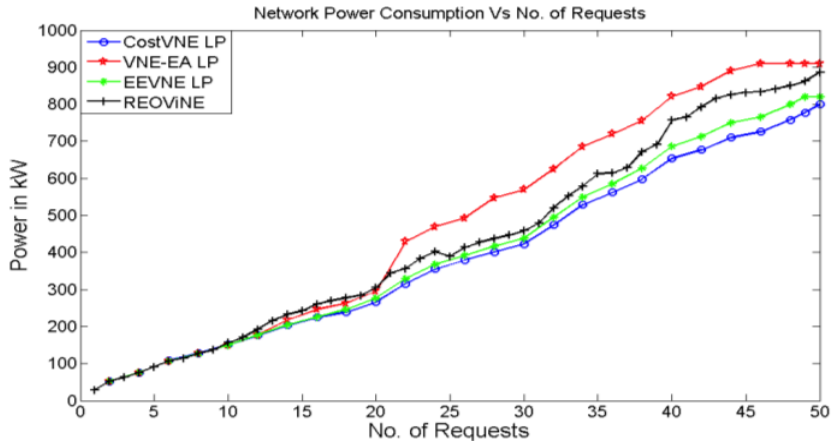

Fig. 4-7(a)

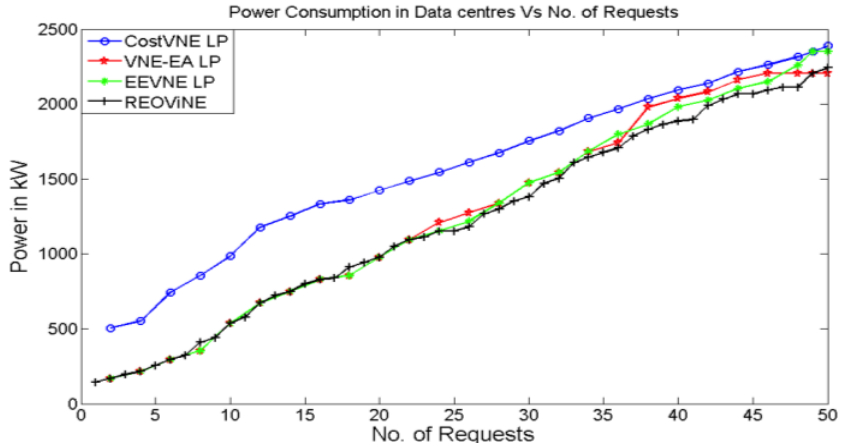

Fig. 4-7(b)

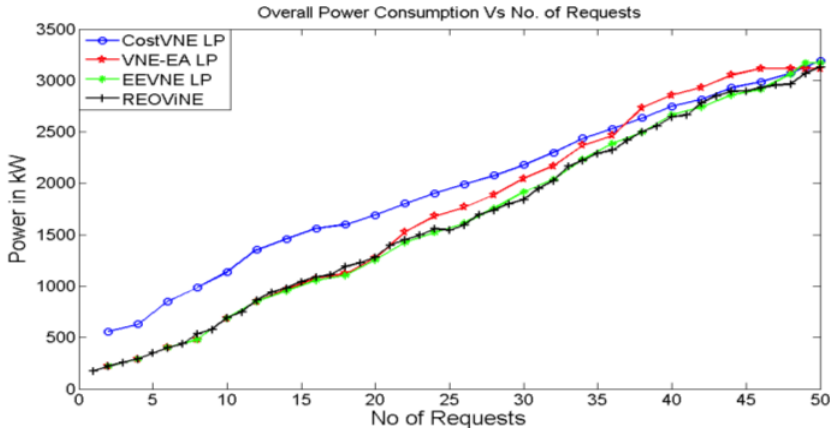

Fig. 4-7(c)

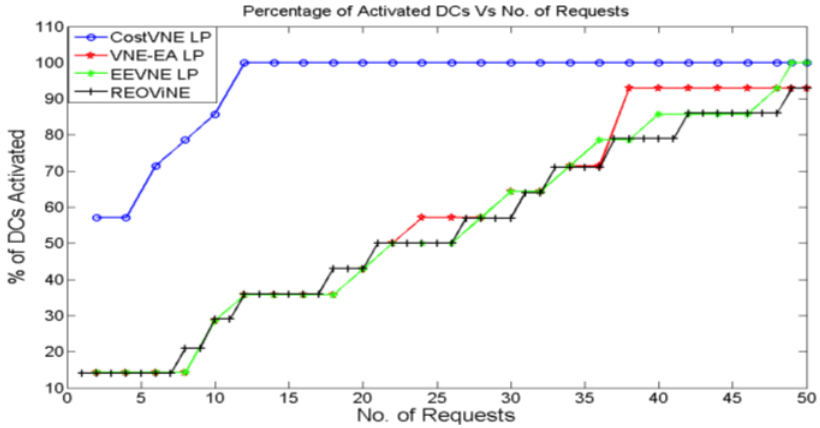

Fig. 4-7(d)

Figure 4-7: (a) Network Power Consumption of the Different Approaches, (b) DCs Power Consumption of the Different Approaches, (c) Overall Power Consumption of the Different Approaches, (d) Data Centre Activation of the Different Approaches

The EEVNE model, where the energy consumption is minimised by jointly optimising the use of network resources and consolidating resources in data centres, has better power savings compared to the VNE-EA model where the power consumption is minimised by switching off substrate links and nodes. This is because the network power consumption is mainly a function of the number of wavelengths rather than the number of active links as the number of wavelengths used determines the power consumption of router ports and transponders, the most power consuming devices in the network (Table 4-1). The REOViNE heuristic approaches the EEVNE model in terms of the network power consumption performance.

Fig. 4-7(b) shows the power consumption of data centres under the different models and heuristic. As mentioned above, the CostVNE model does not take into account the number of activated data centres, therefore it performs very poorly as far as the power consumption in data centres is concerned. However, as the network gets fully loaded and all the data centres are activated, the EEVNE model loses its merit over the CostVNE model. For a limited number of requests, the VNE-EA model performs just as good as the EEVNE model. However as the number of requests increases, the VNE-EA model tends to route the virtual links through multiple hops to minimise the number of activated links and data centres and therefore consumes more power. The REOViNE heuristic also approaches the EEVNE performance in terms of the power consumption in data centres.

Since the power consumption of the data centres is the main contributor to the total power consumption (given the power consumption of servers and network devices (Table 4-1)), the total power consumption, shown in Fig. 4-7(c), follows similar trends to that of the data centres. In the best case over a span of 50 VNRs, the EEVNE model saves 60% of the overall power consumption compared to the CostVNE model with an average saving of 21%. Compared to the VNE-EA model, the EEVNE model achieves maximum combined data centre and network power savings of 9% (3% on average).

Fig. 4-7(d) shows the activation rate of data centres as the mapping of VNRs increases in the network. The CostVNE model readily activates all the data centres while the other models activate them gradually. This ability to consolidate resources in the already active data centres is what leads to low power consumption in both the EEVNE and VNE-EA models.

The revenue of a virtual network service provider can be greatly affected by its inability to accept new requests. Fig. 4-8 shows the number of accepted requests for the different models and the REOViNE heuristic. In an evaluation scenario with sufficient CPU resources to embed all virtual nodes, the CostVNE model has accepted all the 50 requests as it efficiently utilizes the network bandwidth. The improved energy efficiency achieved by the EEVNE model has a limited effect on its ability to accept VNRs. The EEVNE model has however rejected one request. The REOViNE heuristic has rejected three requests. The VNE-EA model is the worst

performer in terms of accepted requests with four rejected. This is because the VNE-EA model tries to fully use activated links before turning on more links therefore depleting the capacity on links to certain destinations. It therefore fails to map VNRs despite the substrate network having sufficient CPU resources.

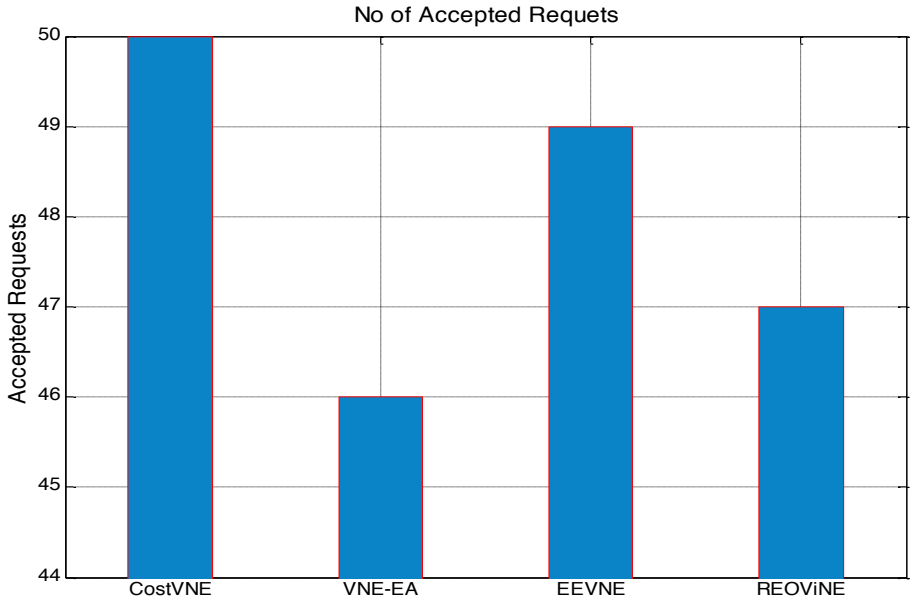

Figure 4-8: Number of Accepted Requests

4.5.4 LAN Power Consumption Consideration inside the Data Centre

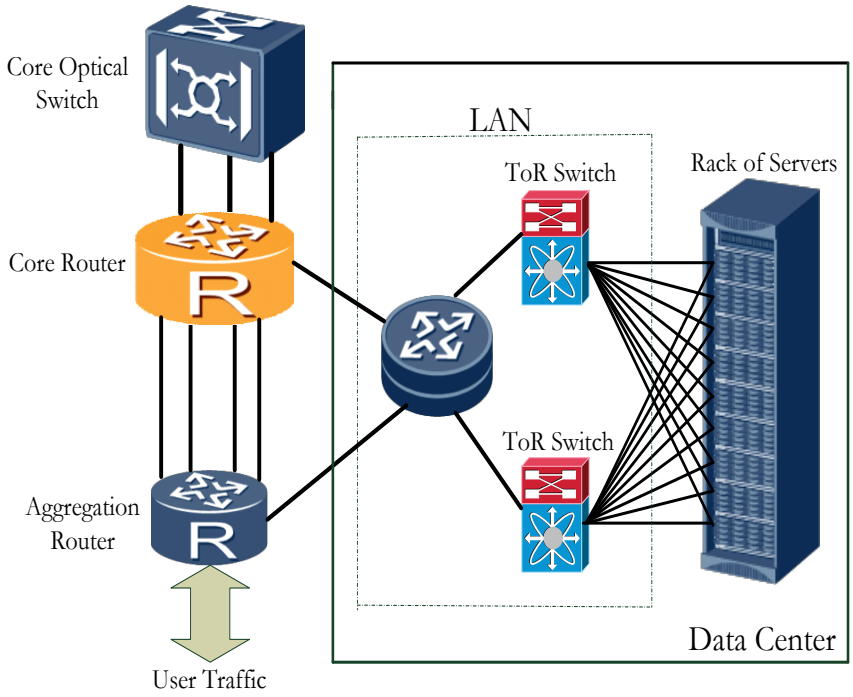

Figure 4-9: Cloud Data Centre Architecture

As mentioned earlier in Section 4.3, the power consumption of the LAN inside the data centre contributes to the overall power consumption of the data centre. Fig. 4-9 shows a typical architecture of the cloud data centre and how it is connected to the core network. Typically, data centres are built very close to the core network nodes to benefit from the large bandwidth capacities available from such nodes. If the data centre is serving users located at this node, the traffic flows from the servers onto the top of the rack (ToR) switches, then to the LAN router located inside the data centre and eventually to the aggregation router. The traffic

serving users located at other core nodes flows to the core router and is then switched by the high capacity optical switch to the desired destination. The server power consumption is proportional to the amount of processing required by the embedded virtual network requests while the network power consumption inside the data centre is proportional to the traffic generated by the requests. For example a low bandwidth and processing intensive virtual network request such as gaming will present low traffic and thus low power consumption in the network inside a data centre but very high server power consumption. On the other hand, the network inside the data centre will consume high power when embedding virtual network requests demanding high bandwidth and low processing like video streaming.

The EEVNE model has been extended to take into account the power consumption due to the LAN inside the data centre. The following are the additional variables and parameters included in the model:

ToR_PC	LAN ToR switch power consumption
ToR_C	LAN ToR switch switching capacity
ToR_PPB	LAN ToR switch energy per bit, ToR_PPB = ToR_PC/ToR_C
R_PC	LAN Router power consumption
R_C	LAN Router routing capacity

R_PPB LAN Router energy per bit, R_PPB = R_PC/R_C

The power consumption of both the LAN ToR switches and routers inside the data centre (LANPC_DC) is proportional to the traffic inside the data centre [98] and can be given as:

$$LANPC\_DC = \sum_{b \in N} \sum_{e \in N: e \neq b} L_{b,e} \cdot (ToR\_PPB + R\_PPB) \tag{4-18}$$

Therefore, the data centre power consumption, which includes both servers and the LAN (PDC), becomes:

$$PDC = \sum_{b \in N} \sum_{v \in V} \sum_{s \in R} CPU_b^{v,s} \cdot \delta_b^{v,s} \cdot \mu + K_b \cdot P_{idle} + \sum_{b \in N} \sum_{e \in N: e \neq b} L_{b,e} \cdot (ToR\_PPB + R\_PPB) \tag{4-19}$$

The Cisco Catalyst 4900M switch [99] with a capacity of 320Gb/s and power rating of 1kW was considered as the ToR switch. The Cisco 7613 Router [100] rated at 720Gb/s and 4kW was considered as the data centre LAN router.

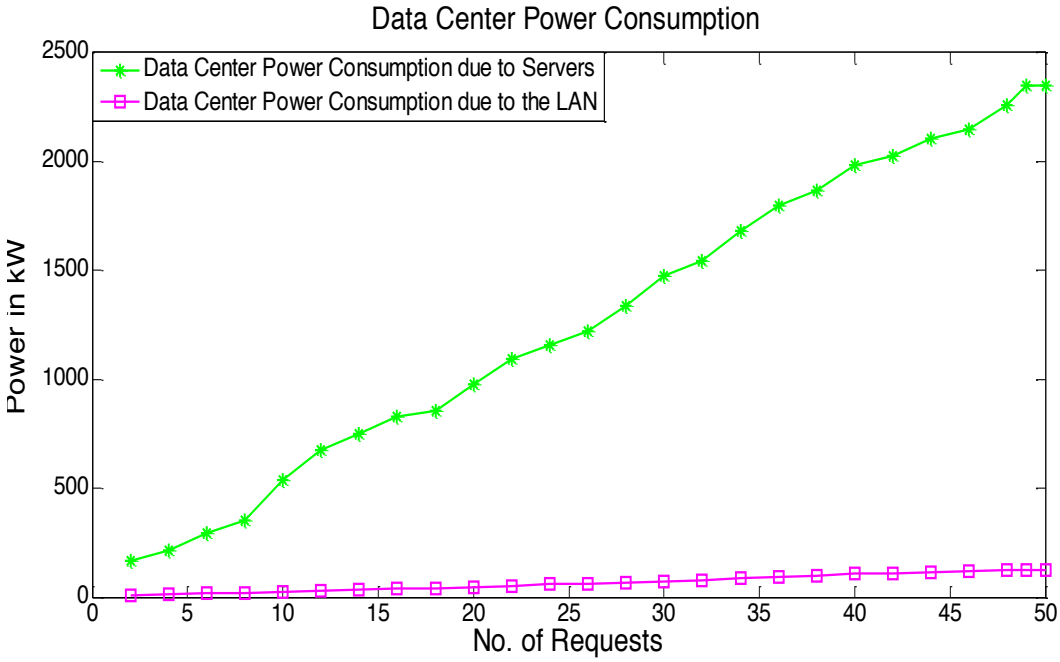

Figure 4-10: Power Consumption in DC due to Servers and the LAN

Fig. 4-10 shows the power consumption in data centres due to servers and due to the LAN. It can be seen that the power consumption due to servers dominates the power consumption due to the LAN. The LAN power consumption only accounts for 4% of the total power inside the data centre. The inclusion of the LAN power consumption has also had no effect on the way the nodes and links are embedded across the network.

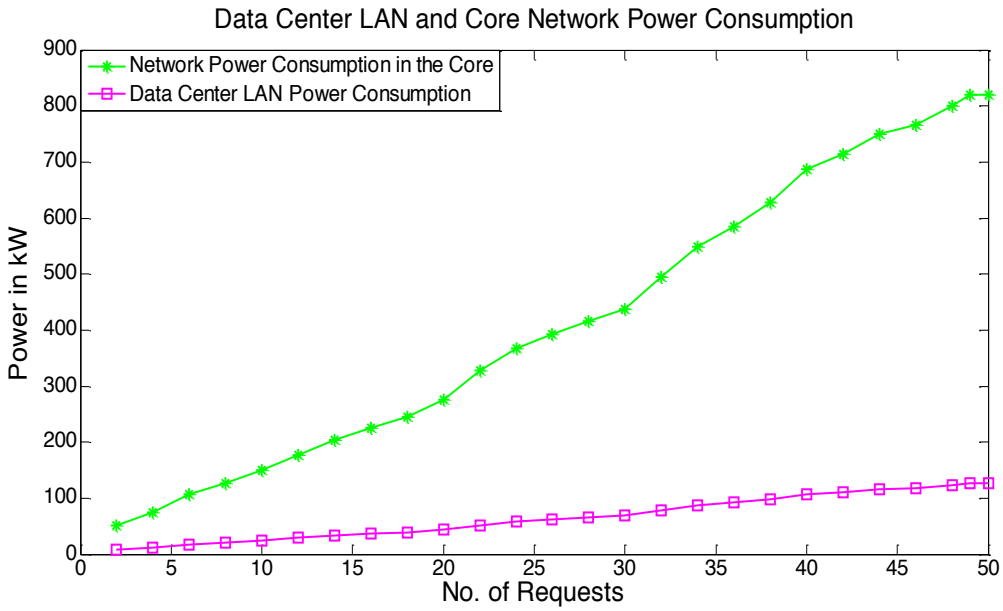

Figure 4-11: Network Power Consumption in the Core and the DC LAN

In Fig. 4-11, the power consumption in the core network is much higher than the LAN power consumption inside the data centres. The LAN power consumption is only 15% of the power consumption in the core when handling the same amount of traffic because the core network comprises more equipment and routes traffic over much longer distances.

4.5.5 EEVNE Model and REOViNE Heuristic Performance Considering Different Physical Topologies

In order to investigate the scalability of the energy efficient VNE approach, the model (EEVNE) is evaluated in small randomly generated topologies and the heuristic (REOViNE) in large network topologies since testing complex MILP models like EEVNE on large networks often leads to huge complexities and unaffordable execution times. The topology matrices

and associated distances of the randomly generated networks were produced in Matlab with link distances randomly distributed between 100km and 1500km. For the large networks the 24-node 43-link USNET [8] substrate network and the 21-node 36-link Italian network [101] were used. Table 4-2 shows the acceptance ratio and the running times for the different topologies under the same load.

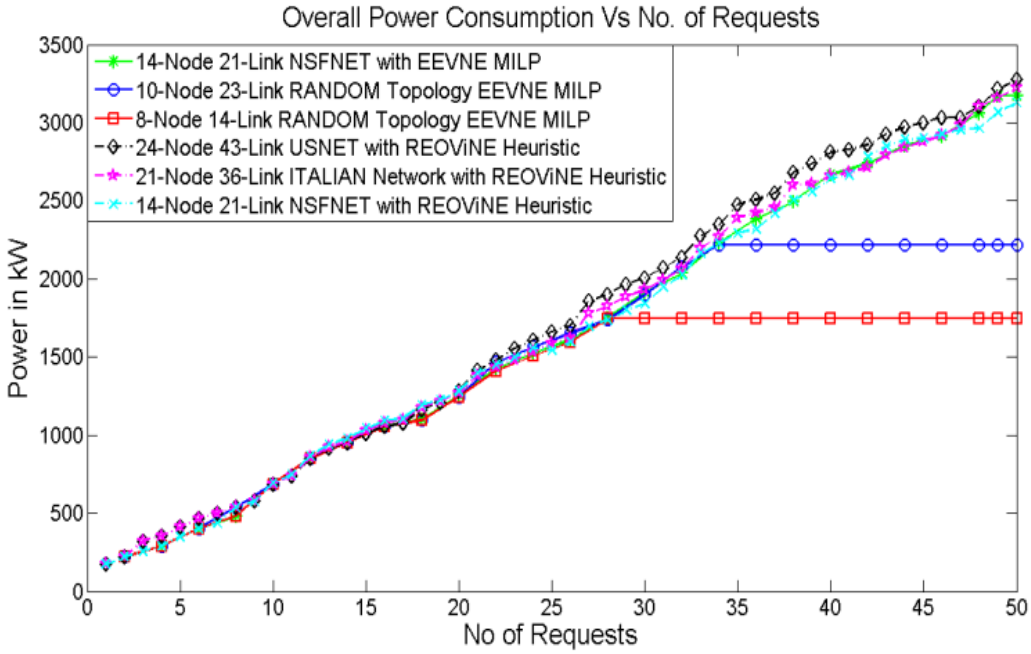

Figure 4-12: REOViNE and EEVNE Model Overall Power Consumption in Different Networks

Fig. 4-12 shows the overall power consumption of the EEVNE model in the small random topologies and the REOViNE heuristic in the large network topologies. The power consumption in the USNET and Italian networks is slightly higher than the power consumption in the NSFNET

network. This is due to the fact that both the USNET and the Italian networks have accepted more requests than the NSFNET network as seen in Table 4-2 since they have more network and data centre resources. The distance between links in a particular network also has a bearing on the power consumption since longer distances call for the deployment of more EDFAs. The power curves for the small randomly generated topologies saturate after reaching the maximum number of requests that they can accommodate given their resources. This is because resources in both the network and data centres get depleted much more quickly under the same load compared to the larger networks. For all the substrate networks, however, the general power consumption performance of both the EEVNE model and REOViNE heuristic is very consistent regardless of the substrate network used.

Table 4-2: Performance of REOViNE and EEVNE in Different Networks

Substrate Network	Method	Request Acceptance	Running Time
NSFNET	EEVNE	49/50, 98%	85000s
Random Topology 10 Nodes 23 Links	EEVNE	34/50, 68%	64800s
Random Topology 8 Nodes 14 Links	EEVNE	28/50, 56%	39600s
NSFNET	REOViNE	47/50, 94%	7s
USNET	REOViNE	49/50, 98%	40s
ITALIAN Network	REOViNE	49/50, 98%	28s

4.5.6 Embedding of VNRs of Non Uniform Load Distribution

In addition to the uniform bandwidth and CPU load distribution considered above, the performance of the different models is investigated under different load conditions. A study of the performance of the model under different combinations of high and low bandwidth and CPU demands is carried out. Table 4-3 shows the characteristics of the different loads studied. Similar to Section 4.5.3, the number of nodes in a VNR is uniformly distributed between 2 and 6.

Table 4-3: Load Distributions

Load	Distribution
High bandwidth and high CPU demands (Load 1)	CPU (9% to 10% of data centre capacity) Bandwidth demand (100Gb/s to 130Gb/s)
High bandwidth and low CPU demands (Load 2)	CPU (2% to 3% of data centre capacity) Bandwidth demand (100Gb/s to 130Gb/s)
Low bandwidth and low CPU demands (Load 3)	CPU (2% to 3% of data centre capacity) Bandwidth demand (10Gb/s to 15Gb/s)
Low bandwidth high CPU demands (Load 4)	CPU (9% to 10% of data centre capacity) Bandwidth demand (10Gb/s to 15Gb/s)

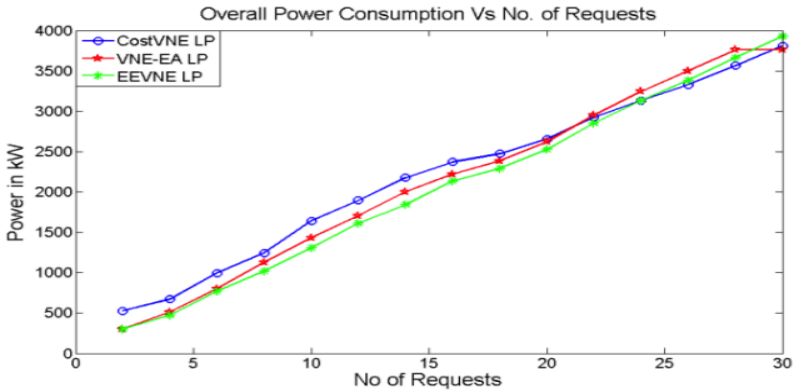

Fig. 4-13(a)

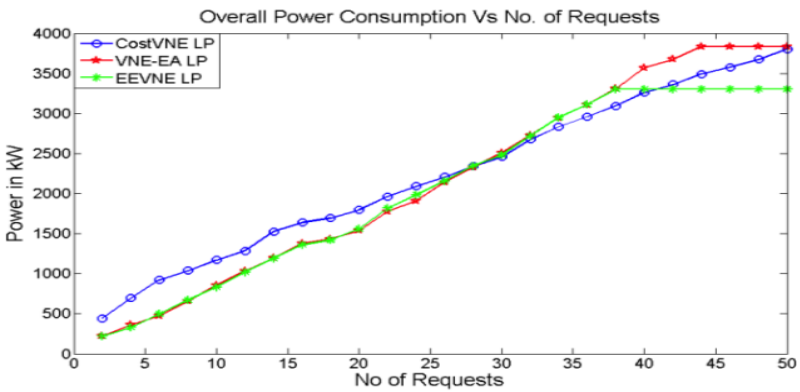

Fig. 4-13(b)

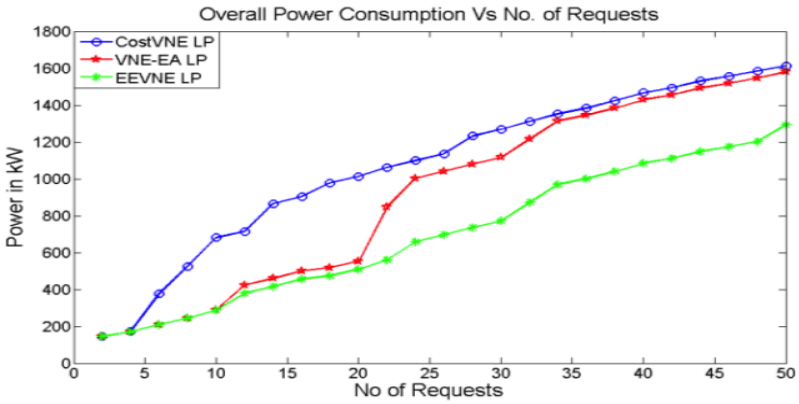

Fig. 4-13(c)

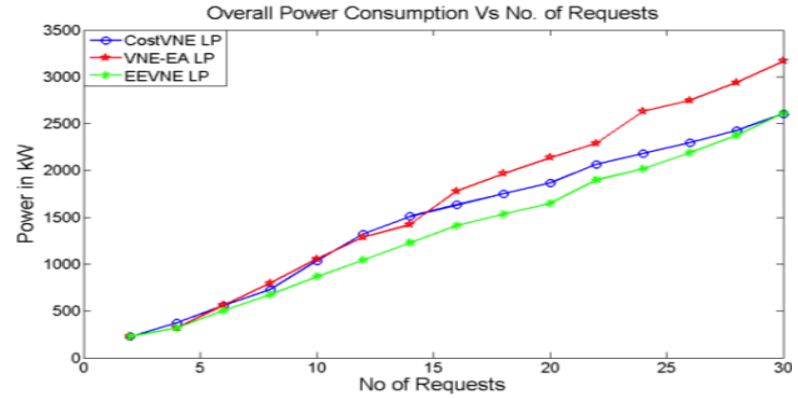

Fig. 4-13(d)

Figure 4-13: (a) Power Consumption under a Load of High Bandwidth and High CPU Demands (Load 1), (b) Power Consumption under a Load of High Bandwidth and Low CPU Demands (Load 2), (c) Power Consumption under a Load of Low Bandwidth and Low CPU Demands (Load 3), (d) Power Consumption under a Load of Low Bandwidth and High CPU Demands (Load 4)

Fig. 4-13 shows the overall power consumption of the different models under the different load conditions shown in Table 4-3. Fig. 4-13(a) shows the performance of the different models under Load 1 (high bandwidth and high CPU demands). At this load, the high CPU demands overwhelm the CPU resources of the data centres allowing the substrate network to only accommodate a maximum 30 VNRs out of 50 as will be seen in Fig. 4-14. The EEVNE model outperforms the other models up to a load of 22 VNRs. However, as the load on data centres approaches their full capacity, the CostVNE model starts to perform better as no further savings can be acquired by consolidating resources in data centres and the model with higher savings in the network, in this case the CostVNE model, will have the minimum power consumption.

Fig. 4-13(b) shows the performance under high bandwidth and low CPU demands. As the links are readily used up to support the high bandwidth demands, the EEVNE model loses its advantage over the VNE-EA model as the bandwidth demands will be routed through paths of multiple hops. The CostVNE model eventually starts to perform better than both the VNE-EA and EEVNE models. The higher propensity of the VNE-EA and EEVNE models to consolidate resources in data centres for minimal power consumption depletes network resources resulting in future requests being embedded further apart and thus increasing network power consumption. Notice that this happens as requests are served sequentially and the new requests are accommodated in the spare capacity. If the network is re-

optimised following each new request, the EEVNE model will always be better (or equal to) the CostVNE model. Note that the EEVNE model starts rejecting VNRs earlier than the VNE-EA as it has higher propensity to consolidate resources in data centres.

For the virtual network requests with low bandwidth and low CPU demands, (Fig. 4-13(c)), the substrate network can successfully accommodate all of them as will be seen in Fig. 4-14. The superior performance of the EEVNE model over both the CostVNE and the VNE-EA model is very clear with average power savings of 35% and 23%, respectively as the EEVNE model is able to consolidate resources in data centres and minimise the network power consumption without being restricted by the depletion of the data centres or network resources. When the low bandwidth and high CPU demands load is presented to the model, only 30 VNRs are successfully mapped onto the substrate network as seen in Fig. 4-14. There is still however superior performance in power savings from the EEVNE model over the other two models as shown in Fig. 4-13(d).

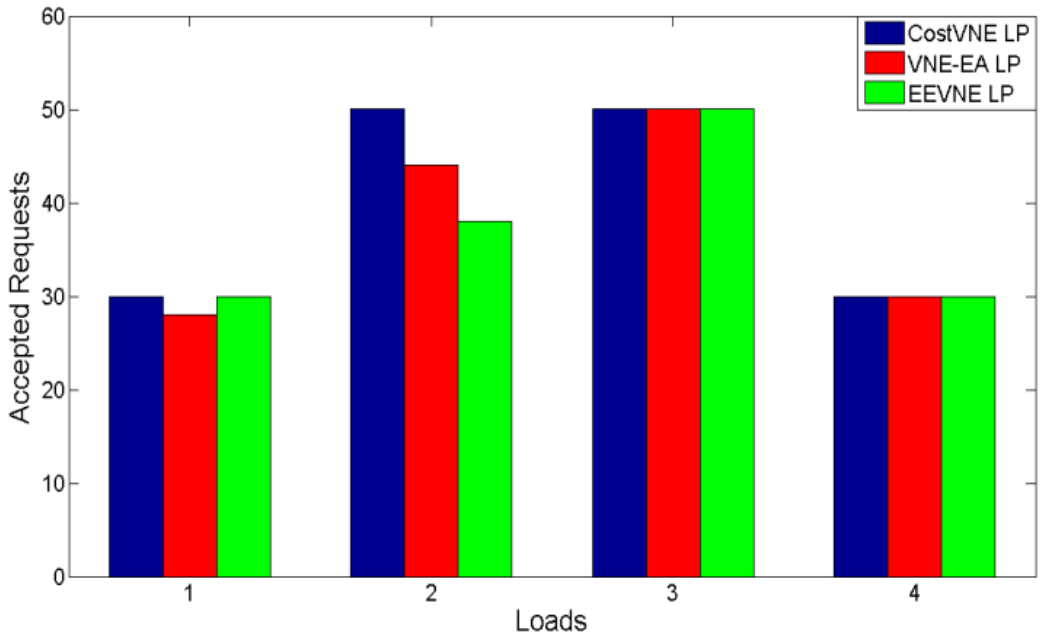

Figure 4-14: Number of Accepted Requests at Various Loads. The Loads refer to those in Table 4-3

Fig. 4-14 shows the number of accepted requests for each model at different loads. At the load representing high CPU and high bandwidth demands (Load 1), both the CostVNE and EEVNE models accept a total of 30 VNRs. Here 20 VNRs have been rejected due to the depletion of CPU resources in data centres. The VNE-EA model has however only successfully mapped 28 VNRs. This is as a result of the model depleting bandwidth resources in the network before depleting CPU resources in data centres. For Load 2, the load of high bandwidth and low CPU demands, the CostVNE model has successfully mapped all the VNRs but both the VNE-EA and the EEVNE models have fallen short as they have depleted the network resources in order to consolidate resources in data centres. For

the load representing low bandwidth and low CPU demands (Load 3), all the three models have successfully mapped all the VNRs because the substrate network has sufficient resources to accommodate them. Finally for Load 4, the load of low bandwidth and high CPU demands, all the three models only successfully map 30 VNRs as they have run out of CPU resources in the data centres.

4.6 Energy Efficient Virtual Network Embedding with Energy Efficient Data Centres

In the previous section the power consumption of VNE in IP over WDM networks was evaluated considering energy inefficient data centres where unused servers are set to idle state. In this section, data centres with an energy efficient (EE) power profile where only servers needed to serve a given workload are activated, i.e. unused servers are switched off, are adopted. The EE power profile is given as a staircase curve as shown in Fig. 4-15. Considering a large number of data centres as shown by the authors in [102] the relationship between the power consumption and the workload reduces to a linear profile given as:

$$PD_b^{v,s} = \begin{cases} \mu \cdot CPU_b^{v,s} & if\ the\ data\ centre\ is\ ON \\ 0, & otherwise \end{cases} \tag{4-19}$$

The server power consumption in the data centres is given as:

$$PD = \sum_{b \in N} \sum_{v \in V} \sum_{s \in R} CPU_b^{v,s} \cdot \delta_b^{v,s} \cdot \mu$$

(4-20)

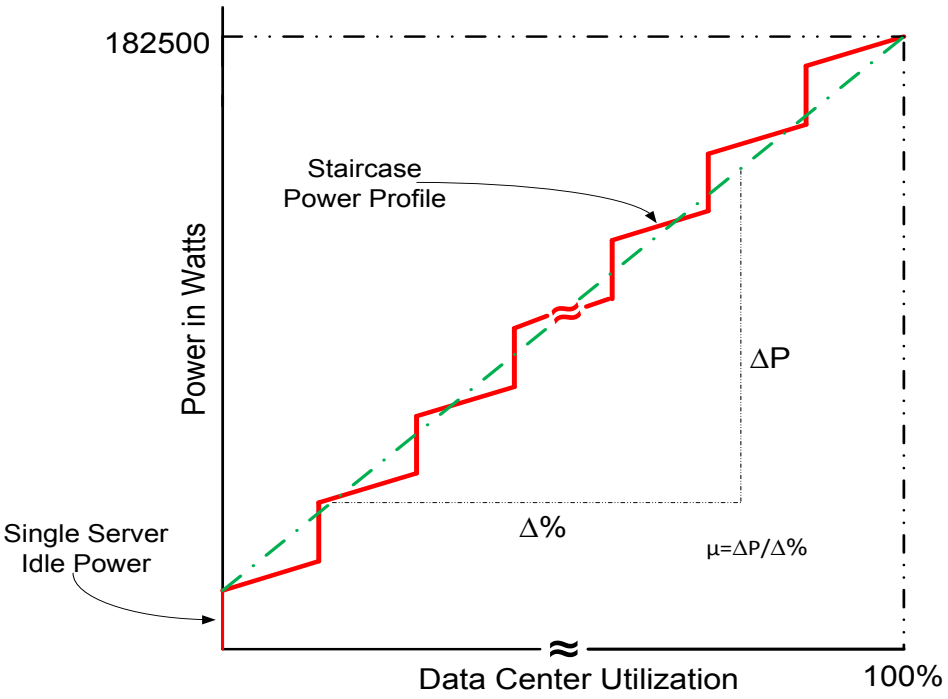

Figure 4-15: Energy Efficient Data Centre Servers Power Profile

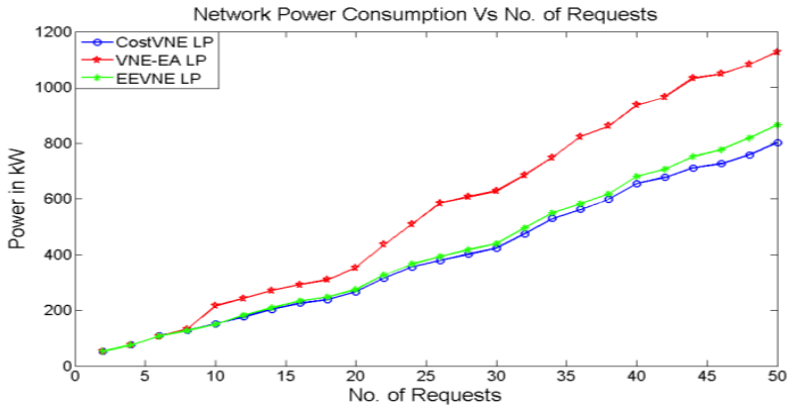

Fig. 4-16(a)

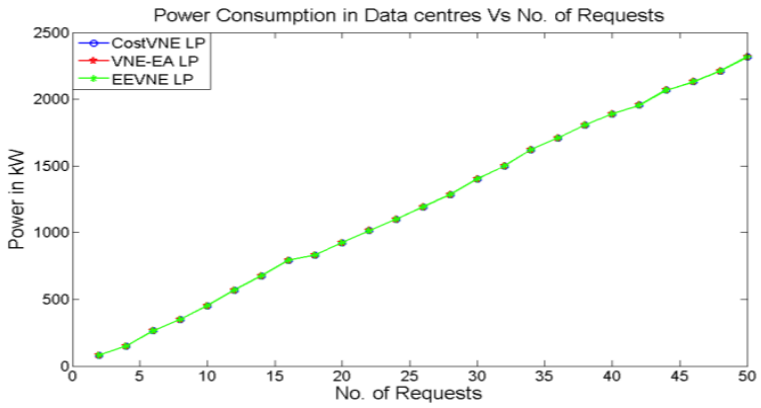

Fig. 4-16(b)

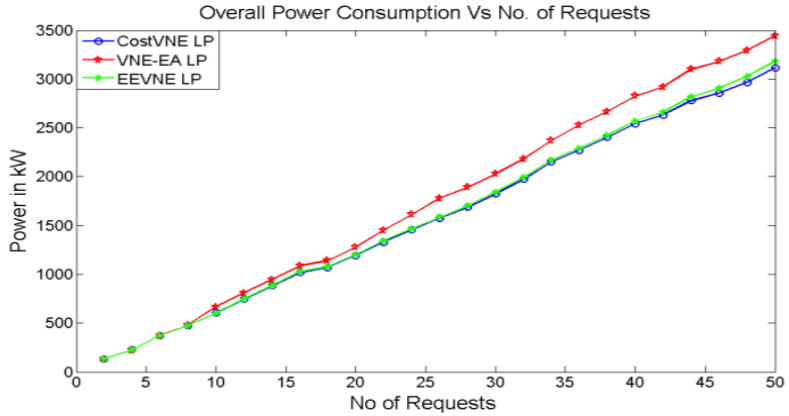

Fig. 4-16(c)

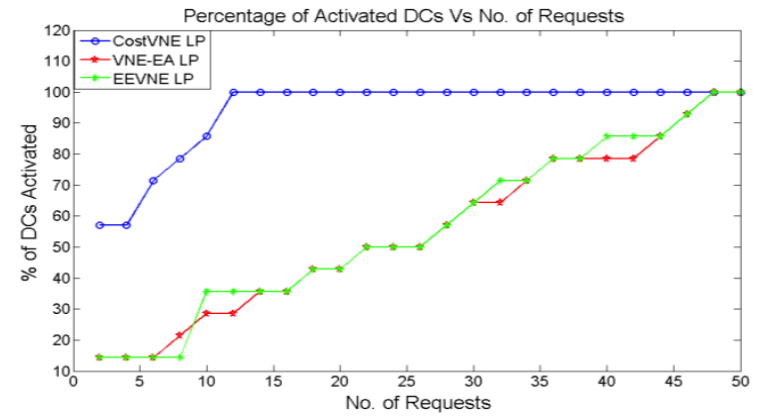

Fig. 4-16(d)

Figure 4-16: (a) Network Power Consumption under the EE Data Centre Power Profile, (b) Data Centre Servers Power Consumption under EE Data Centre Servers Power Profile, (c) Overall Power Consumption under EE Data Centre Servers Power Profile, (d) Data Centre Activation under EE Data Centre Power Profile

Under the EE data centre power profile, the EEVNE model no longer seeks the consolidation of data centres as the power consumption of data centres is a function of the workload only not the number of activated data centres. Replacing the data centre power consumption in the objective function (equation 4-1) of the model in Section 4.3 by equation (4-20) and considering the evaluation scenario in Section 4.5.3, the power consumption of the three VNE models under the energy efficient data centre power profile is evaluated.

Fig. 4-16(a) shows the network power consumption of the different approaches under the EE data centre power profile. The performance of the CostVNE model will not gain any benefit in terms of network power consumption from adopting the energy efficient data centre power profile. This is because the CostVNE model does not take data centre consolidation into account, i.e. the network resource utilization is not restricted by consolidation of resources in data centres. The EEVNE model marginally outperforms the CostVNE model at low loads. This is because in addition to minimizing the hop count between nodes chosen for embedding, the EEVNE model tries to minimise the distance between nodes to reduce number of EDFAs. This results in the EEVNE model clustering embedded nodes close to each other and running out of capacity. As a result, future requests are embedded further apart thus increasing network power consumption. As such, ignoring distance and concentrating on hop count (number of transponders and routers but not EDFAs) has given the

CostVNE model an advantage. As mentioned above, this happens as requests are served sequentially and the new requests are accommodated in the spare capacity. The CostVNE model has maximum power savings of 2% and an average saving of 1% over the EEVNE model, similar to the energy inefficient data centre power profile results in Fig. 4-7(a). The EEVNE model however performs better than the VNE-EA model with a maximum saving of 30% and average of 22%.

Fig. 4-16(b) shows that all the three models have similar power consumption trends in the data centres because the power consumption of energy efficient data centres is a function of the workload and not the number of activated data centres as there is no idle power associated with the activation of data centres. The total power consumption of all the models therefore follows the trends of the network power consumption as seen in Fig. 4-16(c). This leads to the conclusion that with the energy efficient data centre power profile, the optimal VNE approach with the minimum power consumption is the one that only minimises the number of hops, in this case, the CostVNE model. As mentioned earlier, this is only useful if requests are served sequentially and the new requests are accommodated in the spare capacity.

Fig. 4-16(d) shows the rate at which all the three models activate data centres with increasing number of VNRs. The CostVNE model has activated all the data centres after embedding the 12^{th} VNR. The EEVNE

and VNE-EA models however have a much more gradual activation of data centres which only reaches its peak after embedding the 46^{th} VNR.

4.7 Summary

This chapter has investigated the energy efficiency of virtual network embedding in IP over WDM networks considering various network scenarios. A MILP model (EEVNE) and a heuristic (REOViNE) to optimise the use of wavelengths in the network in addition to consolidating the use of resources in data centres were developed. The results show that the EEVNE model achieves a maximum power savings of 60% (average 20%) compared to the CostVNE model which minimises the bandwidth cost of embedding a virtual network request (VNR). The EEVNE model also has higher power savings compared to the Virtual Network Embedding Energy Aware (VNE-EA) model developed by other authors. It has been demonstrated that when it comes to energy savings in the network, it is not sufficient to develop models that just turn off links and nodes in the network but it is important to consider all the power consuming devices in the network and then minimise their power consumption as a whole. The REOViNE heuristic's power savings and number of accepted requests approaches those of the MILP model. The performance of the models under non uniform load distributions was also investigated which showed that the EEVNE model has superior power savings in most load conditions. The investigation went further to consider the energy efficiency of VNE in a network with energy efficient data centres. The results show that the

optimal VNE approach with the minimum power consumption is the one that only minimises the use of network bandwidth, in this case, the CostVNE model. This however only applies when it is assumed that the network is not reconfigured when embedding new requests.

Chapter 5: Energy Efficient Virtual Network Embedding with Location and Delay Constraints

5.1 Introduction

In the previous chapter, node embedding was not subject to any location constraints, i.e. nodes could be embedded anywhere in the cloud as long as connected nodes of a VNR were not embedded in the same substrate node. In this chapter, scenarios where node embedding is subjected to location and delay constraints are evaluated. These scenarios represent, for example, an enterprise solution for a service that requires running applications on a virtual machine(s) in a given fixed location (e.g. company headquarter or branch) with one or more redundant virtual machines for protection or load balancing. The virtual machine(s) with a fixed location is referred to as the master node and the redundant virtual machines are referred to as the slave nodes. Such VNRs typically form star topologies with the master

node at the centre. The slave nodes can be located anywhere in the cloud subject to delay constraints between them and the master node in addition to the bandwidth capacity constraints. Depending on the service level agreement (SLA), the redundant virtual machine can be located in the same data centre but in different racks or full geographical redundancy can be supported by locating each virtual machine in a different substrate node. Locating all the nodes of a VNR in one substrate node eliminates the need for network connections and therefore reduces the network power consumption and allows the service provider to charge the clients less. On the other hand, the cost increases with the provisioning of full geographical redundancy. An investigation on the impact of different redundancy schemes on the power consumption has been done by defining the node consolidation factor (α) as a measure of how many nodes of a VNR can be embedded in the same substrate node. For $\alpha = 1$, the model only allows one virtual node from the same request to be embedded in the same substrate node while for $\alpha = 5$, the model allows 5 virtual nodes from the same request to be embedded in the same substrate node.

In all the scenarios considered so far, each node in the network hosts a small data centre that can be activated on demand. However, practical considerations such as infrastructure cost and security may limit the number of data centres in a network. The work done by the authors in [42], investigated the optimisation of data centre locations in IP over WDM networks. In this chapter, the impact of virtual network embedding on the

design problem of optimally locating data centres for minimal power consumption in cloud networks is also investigated. Scenarios with a single data centre and multiple data centres have all been investigated.

5.2 Mathematical Model for Energy Efficient Virtual Network Embedding with Location and Delay Constraints

The mixed integer linear programming model presented in Chapter 4 has been extended to introduce location and delay constraints. In addition to the sets, parameters and variables defined in Section 4.3 of Chapter 4, the following parameters and variables are defined:

Parameters:

LOC_b^v	$LOC_b^v = 1$ if the master node of VNR v must be located at substrate node b, otherwise $LOC_b^v = 0$
DEL^v	The threshold propagation delay on the links of request v
α	Node consolidation factor.
$\nabla^{m,n}$	Propagation delay on the physical link m,n, given as: $\nabla^{m,n} = \frac{3D_{m,n}}{2C}$, where C is the speed of light.

Variables:

$Z_{m,n}^{v,b,e}$ $Z_{m,n}^{v,b,e} = 1$ if the IP over WDM virtual link (b,e) of VNR v traverses the physical link (m,n), otherwise $Z_{m,n}^{v,b,e} = 0$

In addition to constraints (4-2) to (4-15) presented in the Section 4.3 of Chapter 4, the following new constraints are introduced:

$$\delta_b^{v,1} = LOC_b^v \quad \forall v \in V, b \in N \tag{5-1}$$

$$\sum_{s \in R} \delta_b^{v,s} \leq \alpha \quad \forall v \in V, b \in N \tag{5-2}$$

$$\sum_{n \in N_m} Z_{m,n}^{v,b,e} \leq 1$$
$$\forall v \in V, b \in N, e \in N, m \in N: b \neq e \tag{5-3}$$

Constraint (5-1) fixes the location of the master node of request v at node b in the substrate network. Node number 1, of all the virtual network requests is considered to be the master node. Constraint (5-2) defines the format of node consolidation which determines how many virtual nodes belonging to the same virtual network request can be embedded in the same substrate node. Constraint (5-3) ensures that virtual network link demands are not bifurcated when mapped in the IP layer. This is important because a demand of a virtual network link that is bifurcated would create several paths in the physical layer which would make it

difficult to associate a single calculated delay value to all the paths, therefore, traffic bifurcation is not allowed to facilitate the calculation of propagation delay. Constraint (5-4) ensures that the propagation delay of the embedded virtual links does not exceed the delay threshold.

5.2.1 Model Results and Analysis for Energy Efficient Virtual Network Embedding with Location and Delay Constraints

The NSFNET network, Fig. 5-1, with a population heat map for the cities where the nodes are located is considered as the substrate network to evaluate the energy efficient VNE with delay and location constraints. A scenario where 15 VNRs for the service discussed in Section 5.1 are embedded in the substrate network is considered. The number of nodes in the request range between 2 and 5. The propagation delay threshold of the 15 requests is uniformly distributed between 7.5ms and 75ms. This range adequately covers the tolerable propagation delay for most applications [103].

The five most populated cities (nodes) in the NSFNET network are selected to be the locations of the master nodes of the VNRs. The concentration of virtual network requests on a substrate master node is proportional to its population. The master nodes in a set of 15 requests are distributed as follows: Houston Texas (Node 6) can host a maximum of 5 virtual network requests each with a master node, San Diego (Node 3) can

host 4, and Pittsburg (Node 9), Seattle (Node 2) and Atlanta (Node 10) can host 2.

The power consumption of embedding the 15 VNRs is evaluated versus an increasing CPU and bandwidth load. The range of loads considered is shown in Table 5-1 represented by the numbers (1, 2, 3, 4, 5, 6, 7 and 8).

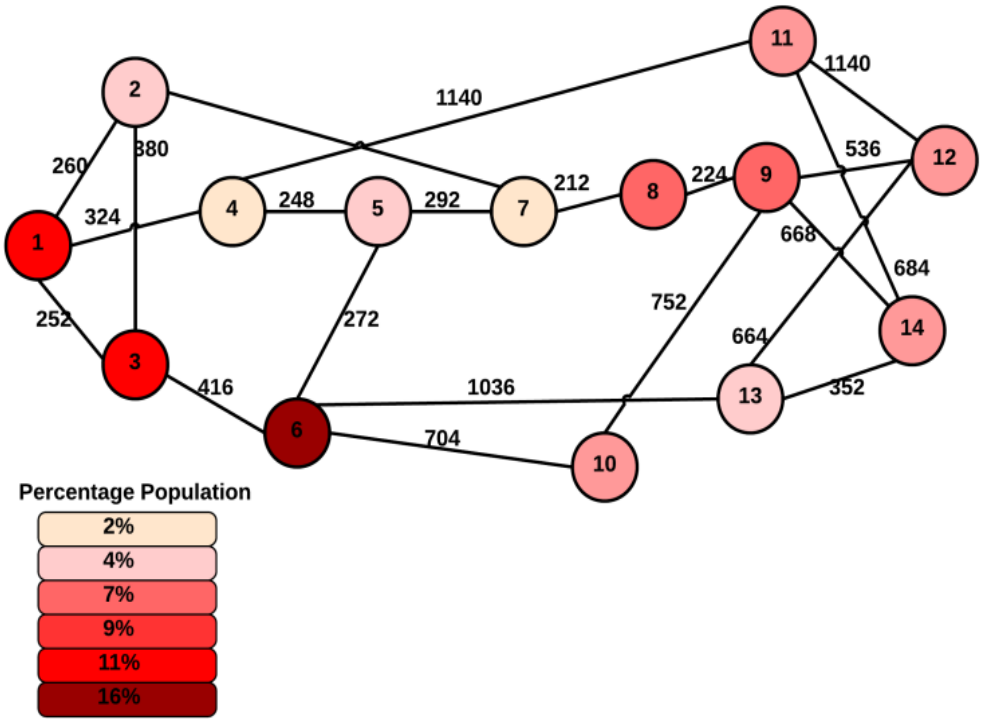

Figure 5-1: NSFNET Network with Population Heat Map

Table 5-1: Load Distribution of Virtual Network Requests

Load	CPU Percentage Workload Distribution	Link Bandwidth Distribution
1	1% - 5%	10Gb/s – 40Gb/s
2	3% - 7%	20Gb/s – 50Gb/s

3	5% - 9%	30Gb/s – 60Gb/s
4	7% - 11%	40Gb/s – 70Gb/s
5	9% - 13%	50Gb/s – 80Gb/s
6	11% - 15%	60Gb/s – 90Gb/s
7	13% - 17%	70Gb/s – 100Gb/s
8	14% - 19%	80Gb/s – 110Gb/s

The CPU load is related to the bandwidth requirement according to the assumption that a server working at its maximum CPU utilizes 1Gbps of its network resources. Therefore a data centre of 500 servers with a 2% workload will generate 10Gbps of traffic. This scenario depicts applications whose networking requirements vary proportionally to CPU processing requirements. Examples include online video gaming and augmented reality applications for live video streaming of sports. In the following results a comparison of the energy efficiency of the CostVNE and EEVNE models, the best performing approaches in chapter 4, considering constraints on the virtual nodes location and link delay are analyzed. The two models with location and delay constraints are referred to as CostVNE-LD (Cost Virtual Network Embedding with Location and Delay) and EEVNE-LD (Energy Efficient Virtual Network Embedding with Location and Delay) models. In Fig. 5-2 an evaluation of the network power consumption, data centre power consumption and the overall power consumption, versus the increasing loads in Table 5-1 at $1 \leq \alpha \leq MAX$, where $MAX = 5$ is carried out.

Fig. 5-2(a) shows the network power consumption of both the CostVNE-LD model and the EEVNE-LD model. At $\alpha = 1$ each virtual node of a VNR is embedded in a different substrate node which increases network traffic thus allowing the CostVNE-LD model to achieve higher power savings in the network compared to the EEVNE-LD model by efficiently using the network wavelengths when embedding VNRs. With an increasing α however, the EEVNE-LD model starts to match the CostVNE-LD model as the network traffic is reduced by embedding more virtual nodes of a VNR in the same substrate node. The ability of the CostVNE-LD and EEVNE-LD to embed all the virtual machines of a VNR in one substrate node at $\alpha = 5$ allows them to minimise the network power consumption to zero at load 1. As the load increases the CPU resources become insufficient to embed all the virtual machines of each VNR in one substrate node thus virtual links have to be established between data centres thus increasing the network power consumption.

In Fig. 5-2(b) the analysis is extended to power savings in the data centres. The virtual node location constraints do not stop the EEVNE-LD model from efficiently consolidating CPU resources and maintaining the same power consumption in data centres as α increases. This is because the EEVNE-LD model manages to efficiently consolidate virtual nodes of different requests at various values of α.

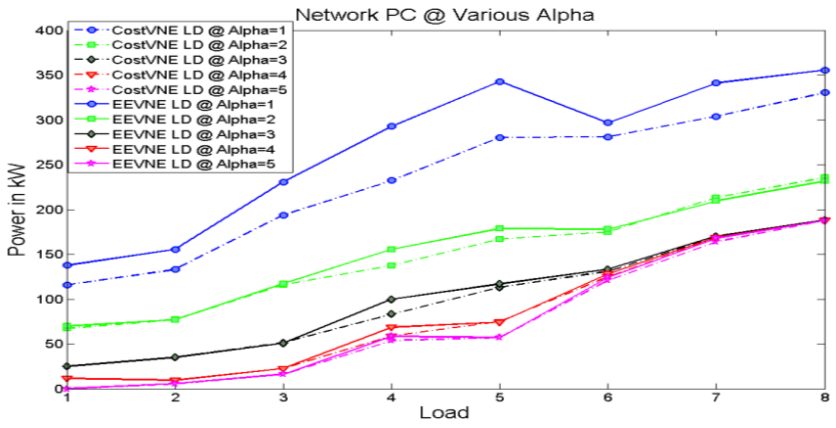

Fig. 5-2(a)

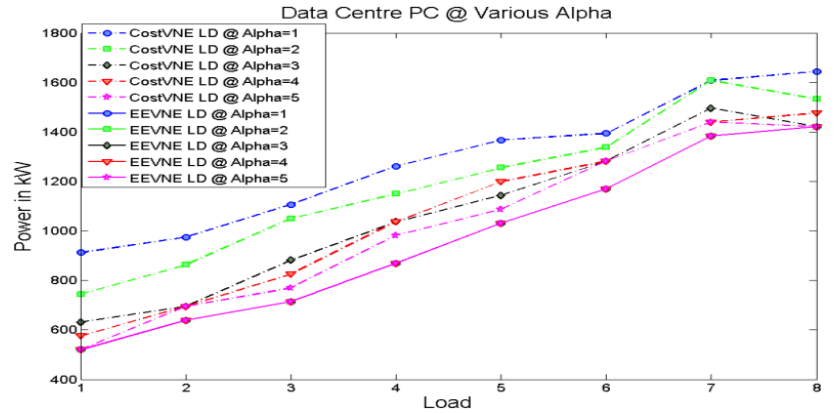

Fig. 5-2(b)

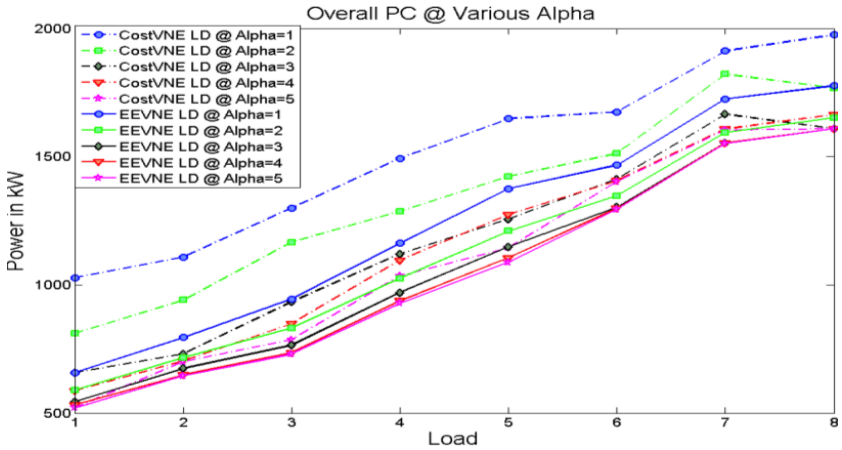

Fig. 5-2(c)

Figure 5-2: (a) Network Power Consumption at various values of **α**, (b) Data Centre Power Consumption at various values of **α**, (c) Overall Power Consumption at various values of **α**

Introducing further restrictions on the virtual node locations has, however, increased the power consumption in data centres for the CostVNE-LD model as more data centres will be activated to embed CPU resources while maintaining the minimum network power consumption. The EEVNE-LD model has saved 18% of the data centre power consumption at $\alpha = 1$ and 5% at $\alpha = 5$ over the CostVNE-LD model.

The impact of introducing restrictions on the virtual machine locations on the overall power consumption of the EEVNE-LD model (Fig. 5-2(c)) follows the same trends as the network power consumption, since the power consumption in data centres does not change as discussed above. The EEVNE-LD model outperforms the CostVNE-LD model in power consumption over all the values of α. Allowing more virtual machines to be embedded in the same substrate node has resulted in limited power savings. As far as the EEVNE-LD model is concerned, the highest savings in overall power consumption of 10% takes place during the transition from $\alpha = 1$ to $\alpha = 2$. The transition from $\alpha = 2$ to $\alpha = 3$ only gives a saving of 4% and the subsequent increases in α account only for very insignificant power savings. From these results it can therefore be deduced that for an infrastructure service provider offering a service such as the one presented here, the option of co-location of virtual machines belonging to the same enterprise customer will save power and subsequently cost less, but will not introduce any additional savings by increasing the number of embedded virtual nodes of a VNR to more than 2 in the same data centre. The power

savings acquired from relaxing the virtual nodes location constraints can guide service providers in cost reductions offered to enterprise customers.

5.3 Mathematical Model for Energy Efficient Virtual Network Embedding with Data Centre Location Optimisation

In order to solve the design problem of optimally locating data centres in cloud networks considering energy efficient virtual network embedding the model presented earlier in Chapter 4 has been adapted to include new constraints, variables and parameters. In addition to the sets, parameters and variables defined in Section 4.3 of Chapter 4 and Section 5.2 of Chapter 5, the following are defined:

Parameters:

NDC	The total number of data centres in the network
$C^{v,s}$	The number of CPU cores requested for virtual node s of VNR v
γ	The power consumption per CPU core embedded in a data centre

Variables:

DP_b	$DP_b = 1$ if substrate node b is a data centre,

	otherwise $DP_b = 0$
$\Delta_b^{v,s}$	$\Delta_b^{v,s} = 1$ if virtual node s of VNR v has been embedded at data centre node b otherwise $\Delta_b^{v,s} = 0$
C_b	The total capacity of CPU cores at data centre b
$\sigma_b^{v,s}$	$\sigma_b^{v,s}$ is the XOR of DP_b and $\delta_b^{v,s}$, i.e. $\sigma_b^{v,s} = DP_b \oplus \delta_b^{v,s}$, $\sigma_b^{v,s} = 1$ if either DP_b or $\delta_b^{v,s}$ is equal to 1, otherwise $\sigma_b^{v,s} = 0$.

The network power consumption is calculated in the same manner as Section 4.3 of Chapter 4. However, there is no minimisation of the power consumption of data centres. The location of data centres is however optimised in order to minimise the network power consumption. As a result, the objective function only has the network power consumption component and is devoid of the data centre power consumption component seen in the previous cases. The extended model is defined as follows:

Objective:

Minimise the network power consumption given as:

$$\sum_{m\in N}\sum_{n\in N_m} PR\cdot W_{m,n} + \sum_{m\in N}\sum_{n\in N_m} PT\cdot W_{m,n} + \sum_{m\in N}\sum_{n\in N_m} PE\cdot EA_{m,n}\cdot F_{m,n} + \sum_{m\in N} PO_m + \sum_{m\in N} PMD\cdot DM_m \tag{5-6}$$

In addition to constraints (4-3)-(4-15) defined in Section 4.3 of Chapter 4 and Constraint (5-1) in Section 5.2, the model is subject to the following new constrains:

$$C_b = \sum_{v\in V}\sum_{s\in R} C^{v,s}\cdot \Delta_b^{v,s} \qquad \forall b\in N \tag{5-7}$$

$$DP_b + \delta_b^{v,s} = 2\Delta_b^{v,s} + \sigma_b^{v,s} \quad \forall v\in V, \forall b\in N, \forall s\in R \tag{5-8}$$

$$\sum_{b\in N} \Delta_b^{v,s} = 1 \qquad \forall v\in V, \qquad \forall s\in R \tag{5-9}$$

$$\sum_{b\in N} DP_b = NDC \tag{5-10}$$

$$\sum_{s\in R} \Delta_b^{v,s} \le \alpha \qquad \forall v\in V, b\in N \tag{5-11}$$

Constraint (5-7) replaces Constraint (4-2) in Section 4.3 of Chapter 4. It calculates the capacity of each data centre in terms of the number of cores. Note that since the problem is now in design, the data centres and links are both un-capacitated. Constraint (5-8) ensures that virtual machines are embedded in nodes with data centres by implementing the AND operation of DP_b and $\delta_b^{v,s}$ $(DP_b + \delta_b^{v,s})$. Constraint (5-9) ensures that each virtual machine is only embedded in a data centre once. Constraint (5-10) gives the number of data centres. Constraint (5-11) determines how many virtual machines belonging to the same request can be embedded in the same data centre.

In order to extend the model to represent the bypass approach where all the lightpaths whose destination is not the intermediate node are directly bypassed via a cut-through, the power consumption in the router ports is modelled as follows:

$$\sum_{i \in N} \sum_{j \in N : j \neq N} PR \cdot C_{i,j} \qquad (5\text{-}12)$$

As such, the objective function for bypass becomes:

Minimise the network power consumption given as:

$$\sum_{i\in N}\sum_{j\in N:j\neq i} PR\cdot C_{i,j} + \sum_{m\in N}\sum_{n\in N_m} PT\cdot W_{m,n} + \sum_{m\in N}\sum_{n\in N_m} PE\cdot EA_{m,n}\cdot F_{m,n} + \sum_{m\in N} PO_m + \sum_{m\in N} PMD\cdot DM_m \quad (5\text{-}13)$$

5.3.1 Model Results and Analysis for Energy Efficient Virtual Network Embedding with Data Centre Location Optimisation

The NSFNET network in Fig. 5-1 is also used as the substrate network to evaluate the performance of the data centre locations optimisation model. A scenario where the client's entry point in the network is fixed but virtual nodes could be embedded anywhere is investigated. All the traffic demands should be routed through provisioned virtual links to and from the data centres. The concentration of enterprise clients at a substrate node is based on the population of the states where the cities (nodes) of the NSFNET network are located (see Fig. 5-1). In the case of California where we have two cities in one state (nodes 1 and 3), the population of the state has been evenly distributed between the two cities. An enterprise cloud service solution where enterprise clients request for virtual machines with a specific number of CPU cores has been depicted. The power consumption in the data centres is a function of the number of embedded CPU cores. A

total of 45 enterprise clients (VNRs) have been considered where the number of virtual machines per enterprise client is uniformly distributed between 1 and 5 and the number of CPU cores required by each machine is uniformly distributed between 1 and 10. The bandwidth requirement of virtual links is uniformly distributed between 10Gbps and 100Gbps.

The location of a single data centre in the NSFNET network under both non-bypass and bypass approaches is first investigated. The common practise in 2010 was to design the location of data centres with the goal of minimizing data centre cost, network infrastructure cost and the security cost. Considering the cost of the network, the optimal location of the single data centre is Node 6. This however also happens to be the optimal location of the data centre with the goal of minimizing power consumption in the network due to virtual network embedding. To verify the results, the model is evaluated while fixing the location of the data centre at the different NSFNET nodes to establish the network power consumption. Fig. 5-3 shows the results obtained in a single data centre design. The model picks a data centre such that the embedding of the virtual machines in the data centre will create virtual links that traverse routes with minimal hops.

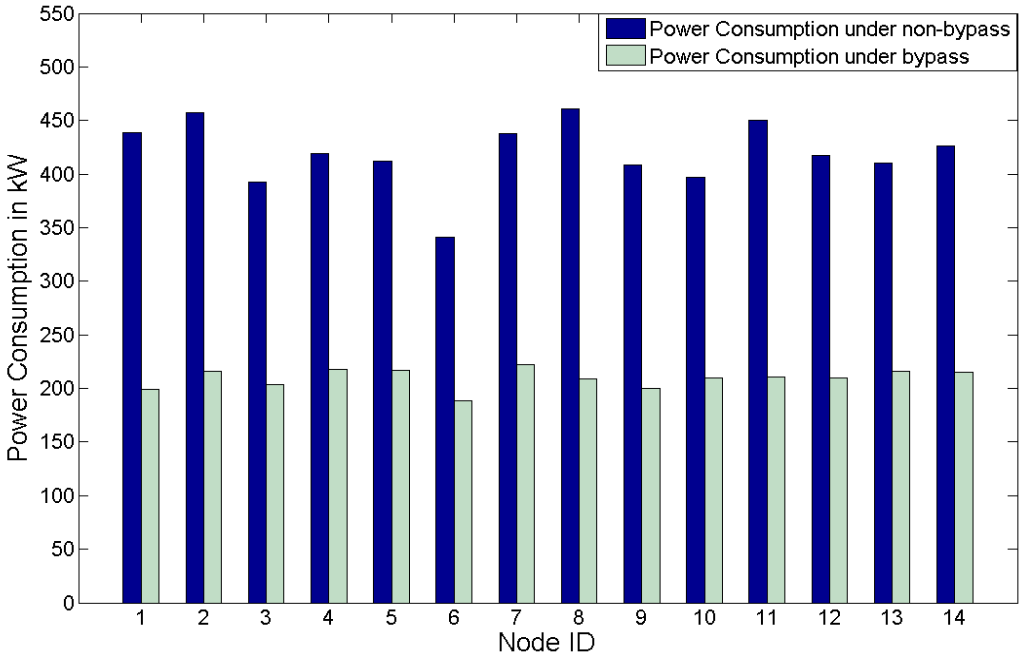

Figure 5-3: The Network Power Consumption of a Single Data Centre Scenario at Different Locations under Non-Bypass and Bypass Approaches

The hop count determines the number of router ports and transponders (the most energy consuming network devices) used under the non-bypass approach. Under the bypass approach, the IP layer is bypassed and therefore the hop count determines only the number of transponders used. Note that selecting a highly populated node and/or a node with highly populated neighbours to locate a data centre can significantly reduce the average hop count as more clients are served locally as a result or through a single hop. Therefore, the most populous and easily accessible (through minimum hop routes) Node 6 is selected to host the single data centre. The

optimal location has achieved power savings of 26% and 15% compared to the worst location for the non-bypass and bypass approaches, respectively.

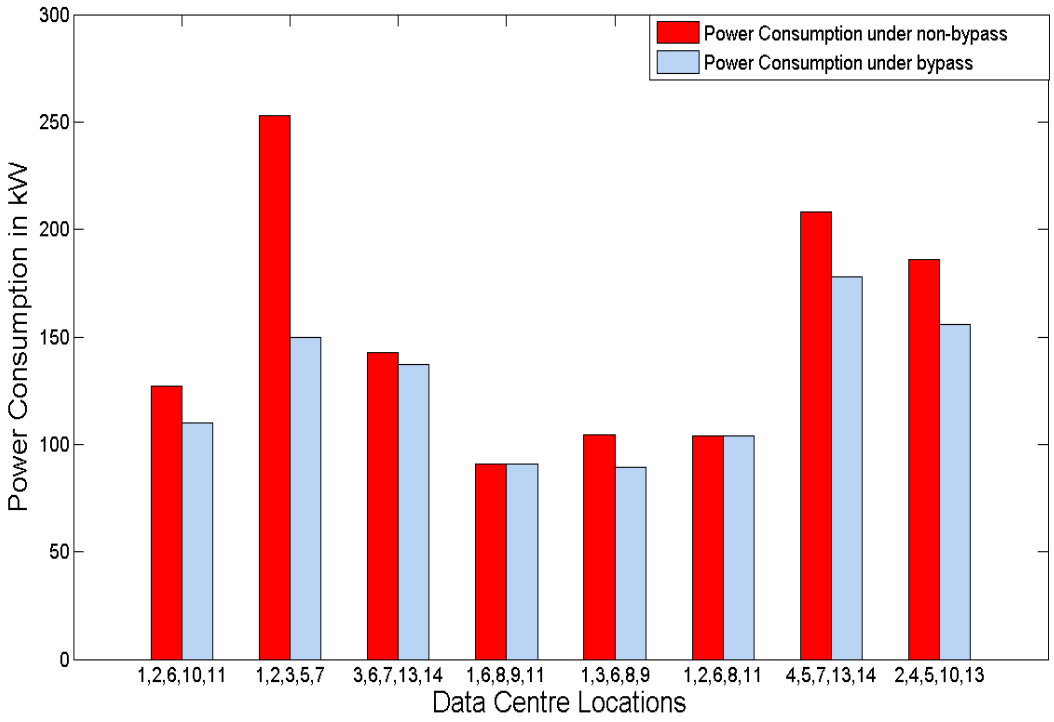

Figure 5-4: The Network Power Consumption of a 5 Data Centre Scenario under Non-Bypass and Bypass Approaches at $\boldsymbol{\alpha = 5}$

The current and future criterion for designing data centre infrastructure for cloud services is to distribute the content among a number of data centres to minimise the delay experienced by the users and to avoid the scenario of having a single hot node in the network. Therefore, a scenario where cloud services are supported by a total of 5 data centres in the network has been evaluated. The consolidation factor, alpha, for this

scenario has been set at $\alpha = 5$, i.e. co-location of virtual machines from the same VNR in the same data centre is allowed. The optimal locations of the data centres in this case are nodes (1, 6, 8, 9 and 11) for the non-bypass approach and nodes (1, 3, 6, 8 and 9) for the bypass approach as shown in Fig. 5-4. When minimizing the network power consumption, the model optimises two factors: the traffic requests served locally and the average hop count traversed by traffic demands. The optimal locations under the non-bypass approach are selected in such a way that all requests are either served locally or within a single hop. The bypass approach however can compromise on the number of hops traversed by low bandwidth demands in order to serve high demands locally. The power consumption of transponders used by the selection of routes with higher hop count is compensated for by the significant power savings obtained by embedding VNRs of higher bandwidth demands locally. Therefore Node 11 in the optimal data centres locations under the non-bypass approach is replaced with the highly populated Node 3 under the bypass approach. The optimal locations have achieved network power savings of 43% and 55% compared to the worst locations for the bypass and non-bypass approaches, respectively. Compared to the single data centre solution, distributing the virtual machines among multiple data centres has saved 53% and 73% of the network power consumption for bypass and non-bypass, respectively.

Fig. 5-5 shows the normalized size of optimally located data centres at $\alpha = 5$. Under non-bypass, the data centre located at Node 1 is used to

embed the highest number of virtual machines. This is because Node 1 has taken up all the virtual machines of its neighboring populous Node 3 due to the distance between Node 1 and Node 3 being much shorter than the distance between Node 3 and Node 6. Under the bypass approach, a data centre is created at Node 3 instead of Node 11.

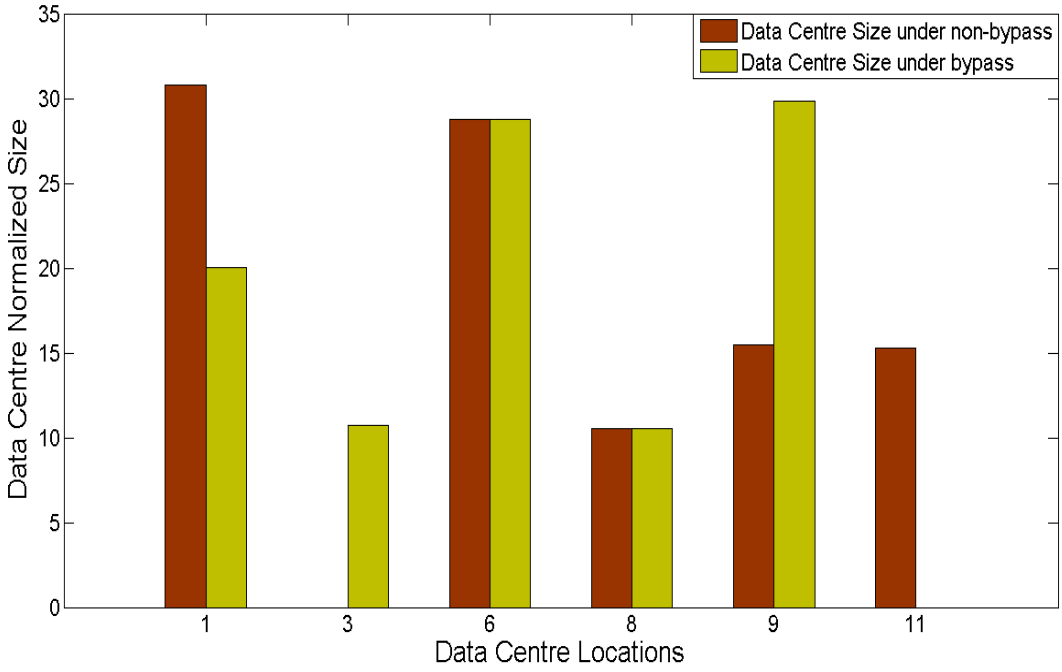

Figure 5-5: The Normalized Size of 5 Data Centres in Optimal Locations at $\boldsymbol{\alpha = 5}$

This has significantly reduced the number of virtual machines served by the data centre at Node 1 and increased the size of the data centre at Node 9 as it has taken up all the virtual machines served by the data centre at Node 11 under the non-bypass routing approach.

A scenario with geographical redundancy constraints where virtual machines that belong to the same client cannot be embedded in the same data centre ($\alpha = 1$), i.e. a client requesting five virtual machines will have one embedded in each of the five data centres has also been investigated. The optimal locations of the five data centres determined by the model are (3, 6, 7, 13, and 14) for both non-bypass and bypass approaches. As discussed earlier, the selection of a location to host a data centre is governed by two factors: the average hop count between the data centres and clients, and the client population of the candidate node and its neighbours. In this scenario where virtual machines of the same client cannot be collocated, the model will also try to minimise the hop count between data centres. Fig. 5-6 compares the network power consumption of embedding the VNRs under the optimal data centre locations to the other random data centre locations for both non-bypass and bypass approaches. The optimal locations have achieved power savings of 19% and 2% compared to the worst locations for the non-bypass and bypass approaches, respectively. It is clear that data centre location optimisation for alpha = 1 under the bypass approach does not offer significant savings.

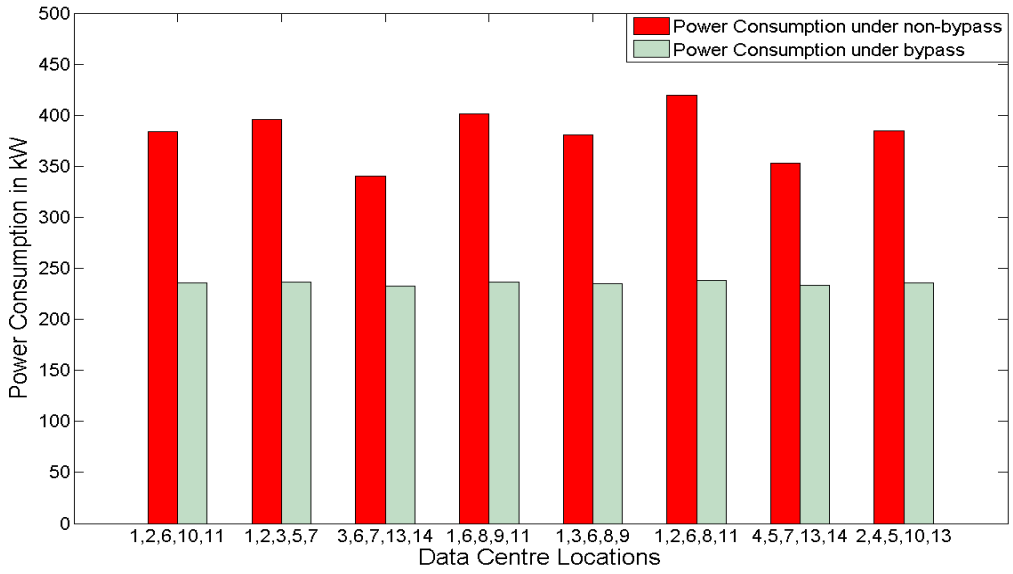

Figure 5-6: The Network Power Consumption of a 5 Data Centre Scenario under Non-Bypass and Bypass Approaches at alpha=1

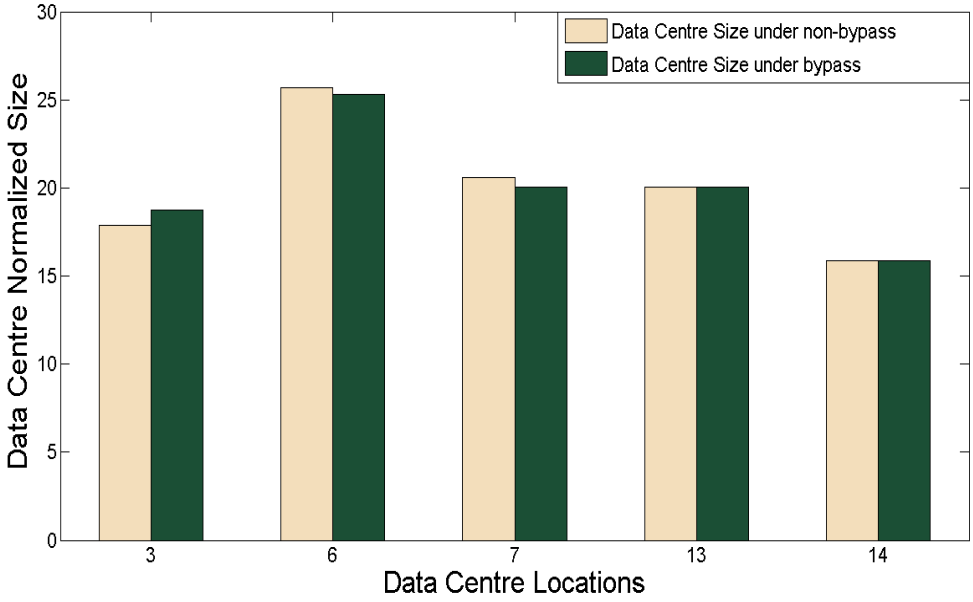

Figure 5-7: The Normalized Size of 5 Data Centres in Optimal Locations at alpha=1

Fig. 5-7 shows the normalized size of data centres in the optimal locations at $\alpha = 1$. The data centre located at Node 6 has the highest number of virtual machines embedded for both the non-bypass and bypass approaches. This is because Node 6, as mentioned above, is the most populous and easily accessible (through minimal hop routes) to other nodes as discussed above. The data centre sizes of Fig. 5-7 are much more balanced compared to those of Fig. 5-5. This is because the restriction to only put one virtual machine belonging to the same VNR in one data centre (Fig. 5-7) forces the distribution of virtual machines across the multiple data centres.

5.4 Summary

This chapter has investigated power consumption minimisation in virtual network embedding infrastructures subject to location and delay constraints. Data centre location optimisation for single and multiple data centre scenarios has also been investigated.

In the case of location and delay investigations, a single virtual node, referred to as the master node, has its location fixed while the other nodes belonging to the same virtual network request could be embedded in any location in the network providing redundancy or load balancing services. However, the load balancing or redundancy virtual nodes have to obey a maximum propagation delay threshold between them and the master node. A MILP model has been formulated to solve the location and delay virtual

network embedding power minimisation problem. The investigation has been carried out under different redundancy or load balancing formats defined by the node consolidation factor alpha (α). Alpha is a measure of the number of virtual nodes of a VNR that can be instantiated in the same substrate node such that if $\alpha = 1$, the model only allows one virtual node from the same request to be embedded in the same substrate node while $\alpha = 5$, allows all the five virtual nodes. The results show that for small values of alpha ($\alpha = 1$), the model that focusses on bandwidth minimisation (CostVNE-LD) achieves higher energy savings in the network compared to the EEVNE-LD model. However, as alpha increases, the EEVNE-LD model starts to match the performance of the CostVNE-LD model. As far as the power consumption in data centres is concerned, the EEVNE-LD model has superior power consumption performance over the CostVNE-LD model saving 18% of the power consumption at $\alpha = 1$ and 5% at $\alpha = 5$ due to high levels of node consolidation. When the power consumption in both cases is considered, it is observed that the EEVNE-LD model outperforms the CostVNE-LD model for all the values of alpha. The results also show that the savings accrued from increasing the value of alpha are only significant during the transition from $\alpha = 1$ to $\alpha = 2$, subsequent increases in the levels of consolidation have very little or no impact. It could therefore be inferred that for an infrastructure provider offering a service like this one, the option of co-location of virtual nodes belonging to the same enterprise customer will save power and

subsequently cost less, but will not introduce any significant additional savings beyond $\alpha = 2$.

In the single data centre location optimisation investigation, the most important factors influencing the selection of the location of the data centre by the model was that the embedding of virtual nodes in the data centre creates virtual links that traverse paths with minimal hopes. The results show that selecting a highly populated node and/or a node with highly populated neighbours with a high nodal degree to locate a data centre can significantly reduce the average hop count as more clients are served locally or through a single hop. The optimal location achieves power savings of 26% and 15% when compared to the worst locations under non-bypass and bypass approaches respectively. In the multiple data centre scenario where the optimal location of five data centres in the network is considered, complete co-location of virtual nodes from the same VNR was allowed. It was established that when minimizing the network power consumption, the model optimises two factors: the traffic requests served locally and the average hop count traversed by traffic demands. The optimal locations under the non-bypass approach are selected in such a way that all requests are either served locally or within a single hop. The bypass approach however could compromise on the number of hops traversed by low bandwidth demands in order to serve high demands locally. Compared to the single data centre solution, distributing the virtual nodes among

multiple data centres saves 53% and 73% of the network power consumption for bypass and non-bypass approaches respectively.

Chapter 6: Green Virtual Network Embedding in Optical OFDM Cloud Networks

6.1 Introduction

The ever increasing growth in the use of bandwidth intensive applications over the Internet means that the design of the underlying IP and optical infrastructure has become ever more significant. Wavelength division multiplexing (WDM) has been the preferred optical transport technology for core networks in the last decade. However, it's rigid nature and coarse granularity has created a bandwidth mismatch between WDM and the end user applications which have varying bandwidth requirements ranging from a few Gbps to hundreds of Gbps. The defined ITU fixed wavelength channels of WDM with data rates of 10Gbps, 40Gbps, 100Gbps and beyond, have resulted in inefficient utilization of network resources in terms of power and the optical spectrum. Elastic spectrum allocation, where connection requests are allocated the minimum spectral resources

required, has been proposed as a promising solution to support fine granularity [104]. Recently, orthogonal frequency-division multiplexing (OFDM) has been proposed as an enabling technique for elastic optical networks [105, 106]. In this chapter, an investigation of Virtual Network Embedding (VNE) in IP over Optical Orthogonal Frequency Division Multiplexing (O-OFDM) is carried out as a means of allocating resources in a cloud computing network environment. The energy and spectral efficiency of VNE in IP over O-OFDM based Cloud networks is studied and its performance compared to VNE in IP over WDM which has been used as the underlying physical layer in all the previous chapters.

6.2 IP over Optical-OFDM Network Architecture and Operation

OFDM has seen extensive use in present day high capacity wireless and wired networks because of its inherent effectiveness in minimizing inter-symbol interference (ISI) caused by a dispersive channel and the efficient use of the frequency spectrum [107]. Despite these advantages, OFDM has been hardly considered for optical communications. The consideration of O-OFDM for high capacity optical transport calls for significant changes in the overall optical infrastructure in core networks. The traditional fixed-grid allocation of optical spectrum as is the case for WDM will have to be broken down to allow for a much more flexible allocation of optical spectrum. This would then create what is often referred to as an elastic optical grid [108] - [110]. In Fig. 6-1, a comparison of spectrum utilization

between O-OFDM and WDM is shown. It can be seen that an O-OFDM based network has a much higher spectral efficiency through the use of tightly packed and overlapping orthogonal subcarriers.

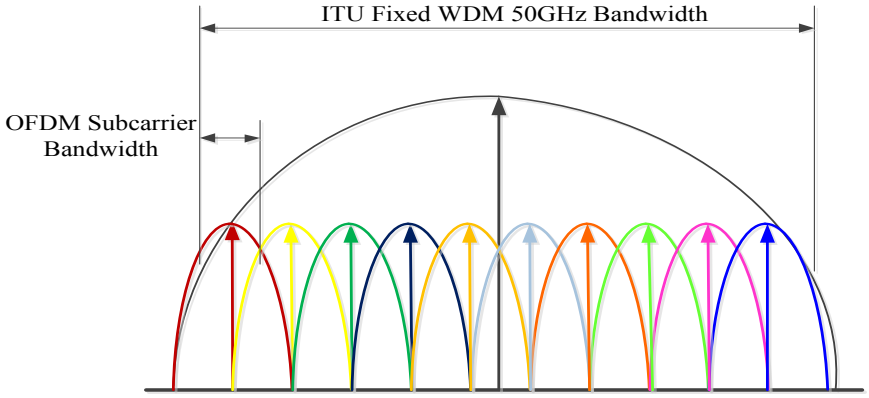

Figure 6-1: Spectrum Utilization of O-OFDM and WDM

An OFDM-based elastic optical network can support various data rates through the use of bandwidth variable transponders (BVTs) and bandwidth variable optical cross-connects (BV-OXCs) deployed at each node in the core network. BVTs can adjust their actual transmission rate in response to the actual traffic demand through expansion or contraction of the optical path by varying the number of subcarriers used or the modulation format of subcarriers. The virtual network embedding problem therefore extends all the way to the selection of the subcarrier and modulation format used during the link provisioning phase in the substrate network. In modelling the power consumption of the network, only the three most power consuming components in the network are considered; IP router ports, transponders and erbium doped fibre amplifiers (EDFAs). In

[105] a study on the power consumption of these components in an optical OFDM-based network was carried out and compared with the power consumption of similar components in IP over WDM networks. An adaptive line rate (ALR) power profile for the IP ports is assumed in the calculation of the power consumption of router ports supporting flexible wavelength rates. EDFAs can be used in O-OFDM-based optical networks as they can simultaneously amplify many data channels at different wavelengths within their gain region [111].

The power consumption of the O-OFDM transponder mainly depends on the electronic processing, modulation format used and the number of supported subcarriers. Therefore, a transponder using the highest modulation format with the maximum number of subcarriers, i.e. working at maximum rate, will have the highest power consumption. An O-OFDM signal, unlike in conventional WDM, is implemented at both the transmitter and receiver in the digital domain. Therefore, the signal properties of individual subcarriers can easily be changed by software through digital signal processing. The modulation format of individual subcarriers can then be modified according to the physical condition of the optical path [112]. The quality of transmission of an optical link is mostly associated with distance, therefore, O-OFDM presents an opportunity to adapt the modulation format of subcarriers according to the distance of the optical path giving rise to what is referred to as distance-adaptive

modulation. Distance adaptive modulation will increase the available capacity while at the same time preserve the quality of transmission.

6.3 MILP Model for VNE in O-OFDM Cloud Networks

Before the introduction of the model, the following sets, parameters and variables in addition to the ones from the previous chapters are defined.

Sets:

Q	Set of modulation formats of subcarriers

Parameters:

TP_{max}	Maximum power consumption of an O-OFDM transponder working at maximum line rate LR_{max}
NSC	Maximum number of subcarriers supported by an O-OFDM transponder
LR_{max}	Maximum Line Rate
M_q	The capacity of a single subcarrier with modulation format q
$F_{m,n}$	Number of fibres on physical link (m,n)
$d_q^{m,n}$	Distance adaptive modulation binary parameter which is

equal to 1 if the link (m, n) can support modulation format q and 0 otherwise

W Number of wavelengths per fibre

Variables:

$nsc_q^{b,e}$ Number of O-OFDM subcarriers using modulation format q to serve the traffic demand (b, e)

$SC_{m,n,q}^{b,e}$ Number of O-OFDM subcarriers using modulation format q to serve the demand (b, e) traversing a physical link (m, n)

$x_{m,n}^{b,e}$ $x_{m,n}^{b,e} = 1$, if O-OFDM subcarriers of traffic demand (b, e) traverse a physical link (m, n) otherwise $x_{m,n}^{b,e} = 0$

Therefore, the total power consumption of the O-OFDM substrate network under the bypass approach is composed of:

Power consumption of router ports:

$$\sum_{b \in N} \sum_{e \in N : b \neq e} PR \cdot L_{b,e}$$

Power Consumption of OFDM transponders:

$$\sum_{b \in N} \sum_{e \in N : b \neq e} \left(\sum_{m \in N} \sum_{n \in N_m} x_{m,n}^{b,e} \left(\xi \left(\frac{\sum_{q \in Q} SC_{m,n,q}^{b,e} \cdot M_q}{LR_{max}} \right) \cdot TP_{max} \right) \right)$$

where, $\xi()$ is the adaptive modulation rate power profile.

Power consumption of EDFAs:

$$\sum_{m\in N}\sum_{n\in N_m} PE \cdot EA_{m,n} \cdot F_{m,n}$$

The model objective is therefore as follows:

Objective: Minimise

$$\sum_{b\in N}\sum_{v\in V}\sum_{s\in R} C^{v,s}\cdot \Delta_b^{v,s}\cdot\gamma + \sum_{b\in N}\sum_{e\in N:b\neq e} PR\cdot L_{b,e} + \sum_{b\in N}\sum_{e\in N:b\neq e}\left(\sum_{m\in N}\sum_{n\in N_m} x_{m,n}^{b,e}\left(\xi\left(\frac{\sum_{q\in Q} SC_{m,n,q}^{b,e}\cdot M_q}{LR_{max}}\right)\cdot TP_{max}\right)\right) + \sum_{m\in N}\sum_{n\in N_m} PE\cdot EA_{m,n}\cdot F_{m,n} \quad (6\text{-}1)$$

In addition to constraints (4-12) to (4-15) in Chapter 4, constraint (5-1) and (5-8) to (5-10) in Chapter 5, the following new constraints are defined:

$$L_{b,e} \leq \sum_{q\in Q} nsc_q^{b,e}\cdot M_q \quad \forall b,e\in N: b\neq e \quad (6\text{-}2)$$

$$\sum_{n\in N_m} x_{m,n}^{b,e} - \sum_{n\in N_m} x_{n,m}^{b,e} = \begin{cases} 1, & m = b \\ -1, & m = e \\ 0, & otherwise \end{cases}$$

$$\forall m, b, e \in N: b \neq e \tag{6-3}$$

$$\sum_{n\in N_m} SC_{m,n,q}^{b,e} \cdot d_q^{m,n} - \sum_{n\in N_m} SC_{n,m,q}^{b,e} \cdot d_q^{m,n} = \begin{cases} nsc_q^{b,e}, & m = b \\ -nsc_q^{b,e}, & m = e \\ 0, & otherwise \end{cases}$$

$$\forall m, b, e \in N, q \in Q: b \neq e \tag{6-4}$$

$$\sum_{b\in N} \sum_{e\in N: b\neq e} \left(\sum_{q\in Q} SC_{n,m,q}^{b,e} / NSC \right) \leq W \cdot F_{m,n} \quad \forall m, n \in N: m \neq n \tag{6-5}$$

Constraint (6-2) ensures that the total capacity of the subcarriers allocated to a traffic demand is large enough to support it. Constraint (6-3) gives the flow conservation in the optical layer and ensures that traffic demands do not bifurcate. Constraint (6-4) ensures that for each traffic demand, the number of O-OFDM subcarriers using modulation format q entering node m is equal to the number of subcarriers using modulation format q leaving node m as long as node m is not the source or destination of the traffic demand. The constraint also ensures that the right modulation format is used for each link. Constraint (6-5) ensures that the number of O-OFDM

subcarriers allocated to a traffic demand does not exceed the number of wavelengths in an optical fibre.

Spectrum efficient VNE in IP over O-OFDM networks where the objective is to minimise the optical spectrum used to embed the VNRs has also been investigated. The objective function in this case is defined as:

Objective: Minimise

$$\sum_{b\in N}\sum_{e\in N:b\neq e}\sum_{q\in Q} SC_{n,m,q}^{b,e}/NSC \quad \forall m \in N, n \in N_m \tag{6-6}$$

6.4 MILP Model Results and Analysis

A similar scenario as the one in Section 5.2.1 of Chapter 5 where 45 VNRs of varying node and bandwidth requirements are embedded in the network is depicted. The power consumption and spectral efficiency of the network is determined as the load presented to the network changes due to the mapping of virtual networks. It has been assumed that the data centres considered for this model are energy efficient and as such their load is only dependent on the number of embedded CPU demands, therefore, the power consumption in data centres does not influence the optimisation. Consequently, only the network power consumption has been included in the objective (6-1). A total of 45 virtual networks are embedded at each load in ascending order with the highest load represented as load number 8.

The load distribution of CPU cores and bandwidth is shown in Table 6-1. All the links in the network have been capacitated to carry a maximum of 32 wavelength channels over a single fiber link. The network is comprised of a maximum of seven data centres whose optimal location is also determined by the model. The data centres in this scenario are not capacitated.

Similar to the work carried out by the authors in [106], a channel bandwidth of 50GHz as defined by the ITU has been used for both conventional WDM and O-OFDM networks. The maximum number of subcarriers for each O-OFDM channel is 10, each of 5GHz where two of the channels are used as guard bands. In conventional IP over WDM networks, the worst-case optical path limits the available capacity. A WDM line rate of 100Gbps per channel is used. The modulation format for O-OFDM subcarriers has been adapted according to the end to end physical conditions of the optical path which is measured by the distance dependent Optical Signal to Noise Ratio (OSNR) [111]. As discussed in [105], BPSK (1 bit/symbol) is used to modulate subcarriers over the largest transmission distance in NSFNET (2000 km). The subcarrier modulation format increases by 1 bit/symbol as the transmission distance decreases. Therefore, for the optical OFDM-based VNE network the modulation format will be intelligently selected to meet the required energy or spectral efficiency objective. 8QAM is the highest modulation format used giving the

maximum line rate for an O-OFDM transponder, LR_{max} of 5(GHz) ×3(Bits/Hz) ×8 = 120 Gb/s.

Table 6-1: Load Distribution

Load	CPU Cores Distribution	Link Bandwidth Distribution
1	1 - 5	10Gb/s – 40Gb/s
2	3 - 7	20Gb/s – 50Gb/s
3	5 - 9	30Gb/s – 60Gb/s
4	7 - 11	40Gb/s – 70Gb/s
5	9 - 13	50Gb/s – 80Gb/s
6	11 - 15	60Gb/s – 90Gb/s
7	13 - 17	70Gb/s – 100Gb/s
8	14 - 19	80Gb/s – 110Gb/s

The power consumption of an O-OFDM transponder working at the maximum line rate of 120Gbps was estimated in [105] as 204W. A cubic power profile at different modulation schemes as shown in Fig. 6-2 was used to estimate the power consumption of O-OFDM transponders. A linear power profile is considered to estimate the power consumption of router ports working at different rates given the power consumption of 25W per Gbps [105] and the rest of the power consumption values used in the model are shown in Table 6-2.

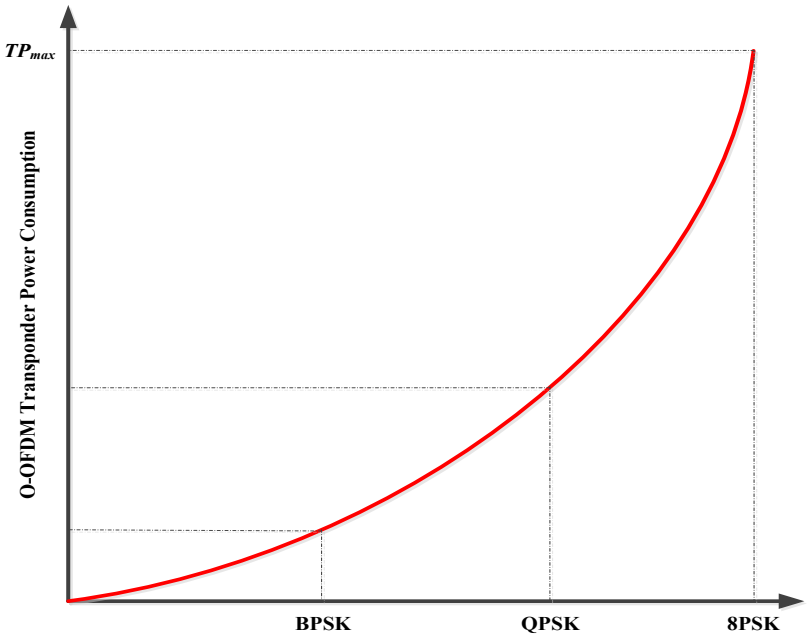

Figure 6-2: O-OFDM Transponder Cubic Power Profile

Table 6-2: Power Consumption of Network Devices

Power consumption of a 100Gb/s WDM transponder	135 (W)
Power Consumption of an OFDM transponder at Maximum Line Rate TP_{max}	200 (W)
Power consumption per Gb/s of an IP router port	25W/Gb/s
Power consumption of an EDFA	8 (W)

In the investigation, both power minimised and spectrum minimised VNE in IP over O-OFDM cloud networks were compared to VNE in conventional IP over WDM networks in terms of power consumption and spectral efficiency considering the lightpath bypass approach. In terms of data centre location, all the models have selected the most populous nodes (1, 3, 6, 8, 9, 11 and 12) as the optimal data centre locations in order to

serve as many demands as possible locally to minimise the use of network resources.

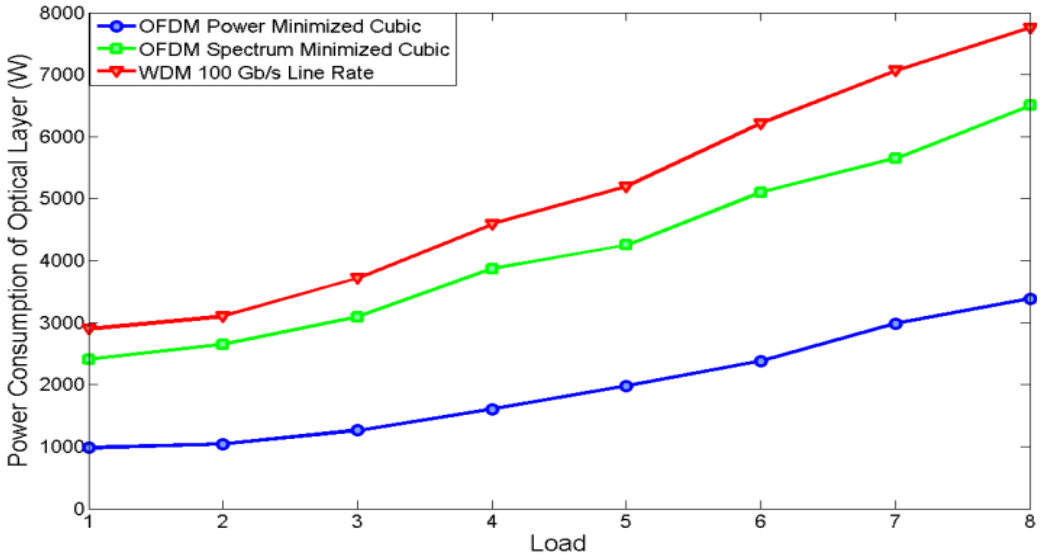

Figure 6-3: Optical Layer Power Consumption for all the Considered Models

Fig. 6-3 shows the power consumption in the optical layer. Virtual network embedding in power minimised IP over O-OFDM saves 63% of the optical layer power consumption compared to VNE in IP over WDM while the spectrum minimised virtual network embedding saves 17% of the optical layer power consumption compared to the WDM implementation. The power minimised O-OFDM network selects routes and modulation formats that result in minimum power consumption while the spectrum minimised O-OFDM selects routes that can support the highest modulation format to minimise the used spectrum. However, since the capacity of the links is limited, the two models might consume the same amount of power

to embed some of the VNRs at high loads under two scenarios. The first scenario is when the number of available subcarriers on the only available route is limited so the two models have to adopt the maximum modulation format to create enough capacity to embed the bandwidth requirement. The second scenario is when the bandwidth requirement has to be embedded over a longer route that can only support the lowest modulation format so the two models will have to adopt the lowest modulation format.

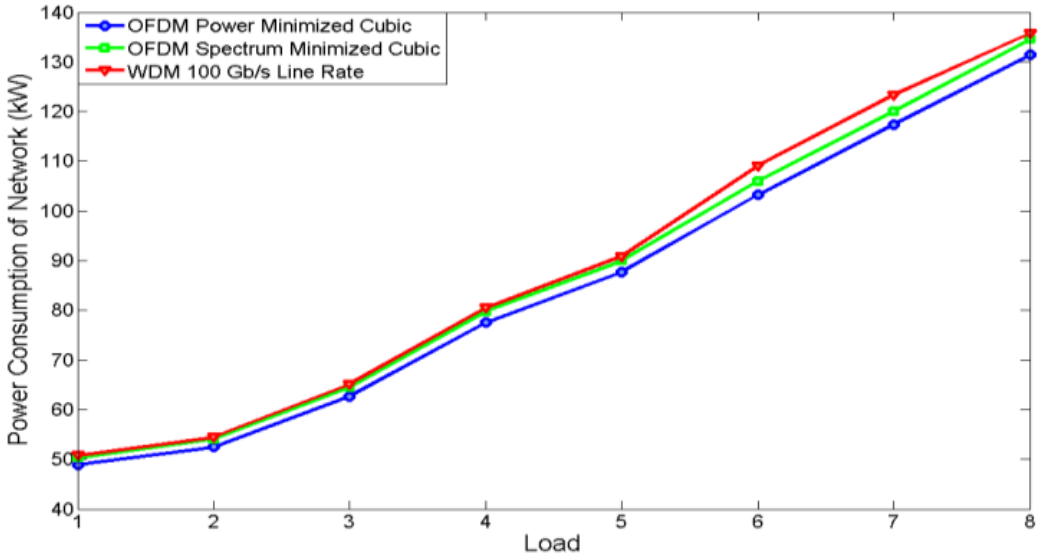

Figure 6-4: Network Power Consumption

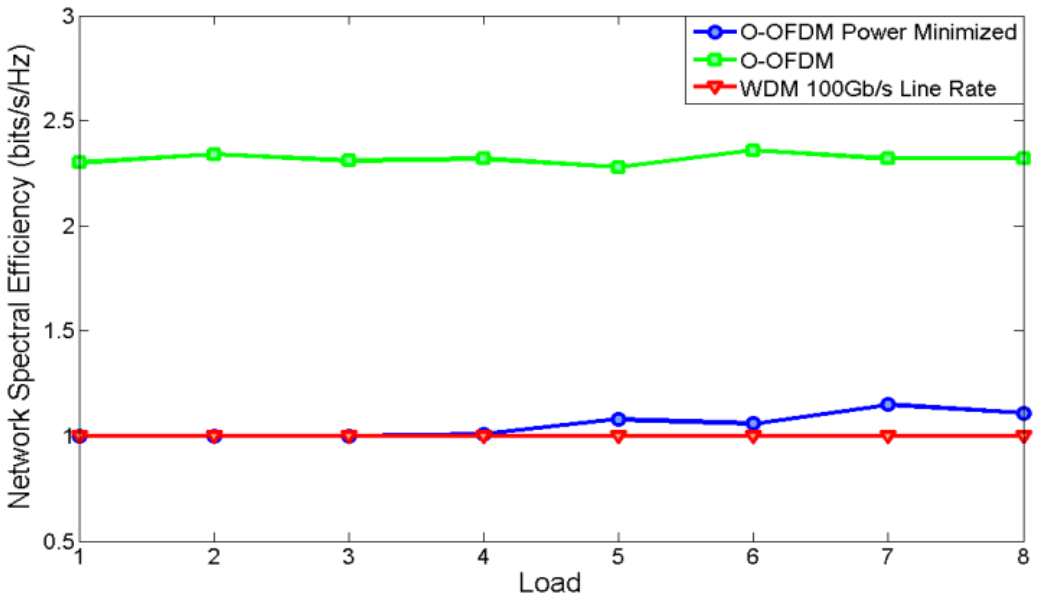

Figure 6-5: Network Spectral Efficiency

Fig. 6-4 shows the total network power consumption, which is the combination of the power consumed by the IP router ports and the power consumed in the optical layer. The power savings achieved by the power and spectrum minimised IP over O-OFDM considering the total network power consumption are 4% and 2%, respectively and they are all due to the savings in the optical layer.

Fig. 6-5 compares the spectral efficiency of the three models. As discussed above the power minimised O-OFDM network selects the modulation format that results in the minimum power consumption to embed virtual networks. Therefore the spectrum minimised O-OFDM network is 120% more efficient in spectrum utilization than the power minimised O-OFDM network. The results in Fig. 6-5 also show that the WDM network and the

power minimised O-OFDM network at low loads have similar spectral efficiency. This is because the O-OFDM network opts for the lowest modulation format (BPSK) to minimise power, which is the same modulation format, employed by WDM 100Gb/s OOK (On-Off Keying). However, as the load increases in the network, there is an improvement in spectral efficiency by the power minimised O-OFDM model due to its adaptation to higher modulation formats in order to efficiently accommodate the high load in the network. An assumption has been made that the 100Gbps WDM is implemented using OOK with vestigial sideband (VSB) filtering as found in [113]. The upside to this is that it makes the assumption of reach at 100Gbps much more realistic to cover the distances in the NSFNET network. However, the downside is that the channel spacing though improved by VSB filtering to 100GHz is still greater than the current ITU 50GHz channel spacing.

6.5 Summary

This chapter has investigated virtual network embedding (VNE) over Optical Orthogonal Frequency Division Multiplexing (O-OFDM) networks as a means of allocating resources in a cloud computing network environment for spectral and energy efficiency. Mixed Integer Linear Programming (MILP) models to investigate the energy and spectral efficiency of VNE in IP over O-OFDM have been developed and their performance compared to VNE in IP over Wavelength Division Multiplexing (WDM) networks. The environment under which the study

has been carried out is such that the model is also supposed to determine the optimal location of data centres to host the CPU demands of the virtual network requests. This has been done under the assumption that the data centres considered for this model are energy efficient and as such their load is only dependent on the number of embedded CPU demands. Therefore, the power consumption in data centres does not influence the optimisation. The results have shown that virtual network embedding in IP over O-OFDM based networks has superior performance both in terms of spectrum and power utilization compared to conventional IP over WDM networks. Power minimised and spectrum minimised virtual network embedding in IP over O-OFDM networks has average power savings of 63% and 17%, respectively compared to conventional IP over WDM. In terms of spectral efficiency, the spectrum minimised O-OFDM network is 120% more efficient in the utilization of the optical spectrum compared to the power minimised O-OFDM network. The difference stems from the fact that the power minimised model sacrifices the optical spectrum in order to achieve higher energy savings through the use of lower modulation formats that are more power efficient. Despite this scenario, the power minimised O-OFDM based network is still 16% more efficient in the use of the optical spectrum compared to conventional WDM based networks.

Chapter 7: Contributions to GreenTouch GreenMeter Research Study

7.1 Introduction

GreenTouch® is a consortium of leading Information and Communications Technology (ICT) research experts who include; academic, industry and non-governmental Organisations playing essential roles in technology breakthroughs in energy efficiency. The consortium was formed in 2010 to pursue the ambitious goal of bridging the gap between traffic growth and network energy efficiency. Members of GreenTouch include: Bell Labs, Huawei, Fujitsu, University of Leeds, University of Cambridge, China Mobile, Swisscom, Tokyo Institute of Technology and University of Surrey. The target was to achieve net energy efficiency improvement of 1000x in an end-to-end network in 2020 compared to 2010 levels while supporting a dramatic traffic increase from 2010 to 2020.

The GreenMeter is a comprehensive ICT research study conducted by the GreenTouch Consortium to assess the overall impact and overall energy efficiency benefits of various technologies, architectures, components, devices, algorithms and protocols investigated, developed and evaluated by GreenTouch. Since 2010, GreenTouch has conducted two comprehensive GreenMeter studies referred to as GreenMeter I and GreenMeter II. In GreenMeter I, energy efficiency improvements in core networks implementing various techniques have been presented. The techniques included the use of improved components of lower power consumption, use of mixed line rates (MLR), sleep and low energy state modes and topology optimisation. The results have been reported and published in [114]. In GreenMeter II, energy efficiency improvements in core networks extend the work presented in GreenMeter I by introducing new energy efficient concepts. These include; content distribution and virtual machine placement based on the work done in [115], energy efficient protection and energy efficient virtual network embedding techniques presented in the previous Chapters. In both studies, the 2020 equipment power consumption is based on two scenarios; a business as usual (BAU) scenario and a GreenTouch (GT) (i.e. BAU+GT) scenario. The BAU equipment power consumption scenario is obtained by only applying expected energy efficiency improvements due to advanced CMOS technologies in integrated circuit design. On the other hand, BAU+GT equipment power consumption includes new techniques developed by GreenTouch initiatives which include the use of optical interconnects, the use of dynamic voltage

and frequency scaling in transponder DSPs and adaptation of router processing capabilities to IP packet size. The outcomes of this research study have been published in the latest GreenTouch whitepaper [116] where a 98% overall reduction in energy consumption has been reported.

In this chapter, all the investigations that have been carried out and contributed to the GreenMeter study are presented. These investigations include; calculations and estimates for router port power consumption based on current and commercially available data sheets and the results of an integrated MILP model using GreenTouch initiatives as well as the virtualisation techniques that have been presented in Chapters four and five.

7.2 Router Ports Power Calculations and Network Equipment Power Consumption Improvements

The reference point for power consumption improvements in the GreenMeter study is the 2010 network. In the 2010 network, the best commercially deployed equipment in terms of both power consumption and capacity is used. The power consumption of the following network elements in the IP over WDM network were considered; (i) Routers (ii) Transponders (iii) Regenerators (iv) Erbium Doped Fibre Amplifiers (EDFAs) and (v) Optical Switches. The router port power consumption for 2010 is quoted at 40Gbps and it includes the share of the aggregate power (switching fabric, router processor, power module and other power

consuming elements including fans and their controllers) apportioned to the 40Gbps port. The power consumption for transponders and regenerators is also quoted at 40Gbps line rate and accounts for both the optical and electronic subsystems of the equipment.

7.2.1 Calculation of Router Port Power Consumption

In the previous chapters, the router port power consumption values that have been used in the MILP models and heuristics have all been obtained from the previous work that was done by the authors in [8]. Their estimates are based on the datasheets obtained from Cisco for the Cisco 8-Slot CRS-1 where they evaluate the average power consumption of the 40Gbps port. In this investigation, the router port power consumption calculations are based on the Cisco CRS-1 16-Slot Chassis [36] and the Cisco CRS-X 16-Slot Chassis [117]. Two methods of calculating the router port power consumption of a given line rate are considered. In method 1, a linear approximation method to determine the energy per bit, $\mathbb{Eb}$ in W/Gbps is used. In this method, the total chassis power consumption, $\mathcal{P}_{\text{chassis}}$, given in the Cisco CRS-1 datasheet, is simply divided by the total switching capacity of the router, $\mathbb{C}_{\text{rsw}}$ also obtained from the datasheet to determine $\mathbb{Eb}$. Therefore,

$$\mathbb{Eb} = \frac{\mathcal{P}_{\text{chassis}}}{\mathbb{C}_{\text{rsw}}} \tag{7-1}$$

$\mathbb{E}b$ is then used to calculate the power consumption of the router port at any given line rate. For example, a Cisco CRS-1 router port with a 40Gbps line rate would have a power consumption of $40 \cdot \mathbb{E}b$ Watts, where, $\mathbb{E}b$ is the energy per bit. The CRS-1 16-Slot chassis has a power rating of 13.2 kW and a Switching capacity of 1200 Gbps. This gives the power consumption of 440W for a single 40Gbps router port. This method does not consider the actual throughput of the CRS-1 16-Slot chassis, which is 40x16=640Gbps, but rather considers the switching capacity which is usually twice the equipment throughput and it is therefore not entirely accurate.

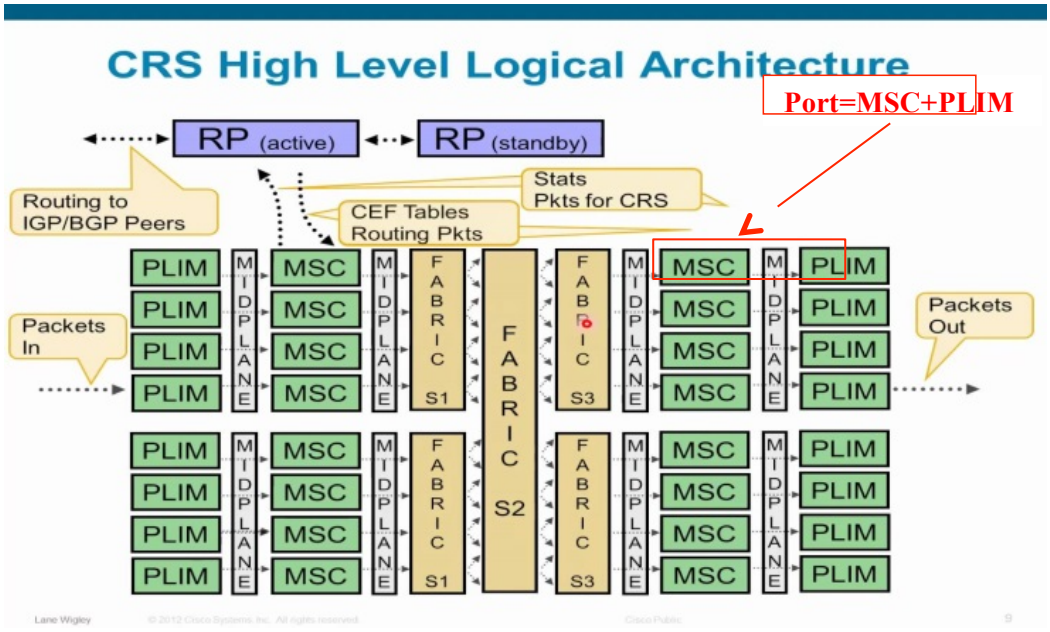

Figure 7-1: Cisco CRS High Level Logical Architecture [118]

Another much more accurate and representative calculation of the router port power consumption was considered. Method 2 took into account the

individual power consumption contributions of the various cards on the CRS-1 and CRS-X cisco router chassis. Fig. 7-1 shows the CRS high level logical architecture. The router port consists of an MSC (Modular Services Card) card and a PLIM (Physical Layer Interface Module) card. The PLIM card is the physical interface that receives the optical signal and converts it into electronic packets, which are sent to the MSC card. The MSC card performs ingress and egress packet forwarding operations. It segments packets into cells which are then presented to the router switching fabric. The port power consumption ($\mathcal{P}_{\mathrm{r}}^{(\mathrm{Rp})}$) at line rate r therefore consists of the MSC power consumption ($\mathcal{P}_{(\mathrm{MSC})}(\mathrm{r})$) at line rate r, the PLIM power consumption ($\mathcal{P}_{(\mathrm{PLIM})}(\mathrm{r})$) at line rate r and the idle power consumption per port ($\mathcal{P}_{\mathrm{o}}$) which includes the switching fabric, fans and the fan controller. This relationship can be written as:

$$\mathcal{P}_{\mathrm{r}}^{(\mathrm{Rp})} = \mathcal{P}_{(\mathrm{MSC})}(\mathrm{r}) + \mathcal{P}_{(\mathrm{PLIM})}(\mathrm{r}) + \mathcal{P}_{\mathrm{o}} \tag{7-2}$$

$\mathcal{P}_{(\mathrm{MSC})}(\mathrm{r})$ and $\mathcal{P}_{(\mathrm{PLIM})}(\mathrm{r})$ are given in the Cisco CRS datasheet. Therefore, only $\mathcal{P}_{\mathrm{o}}$ needs to be determined. Considering a port on the 16-Slot CRS chassis with a port speed r equal to the slot speed capacity of each of the 16 slots and letting $\mathcal{P}\mathrm{T}_{\mathrm{o}}$ be the total idle power of the router chassis, $\mathcal{P}_{\mathrm{o}}$ can be determined from the following expression:

$$\mathcal{P}_{\mathrm{o}} = \frac{\mathcal{P}\mathrm{T}_{\mathrm{o}}}{16} = \frac{\mathcal{P}_{\mathrm{chassis}}}{16} - \left(\mathcal{P}_{(\mathrm{MSC})}(\mathrm{r}) + \mathcal{P}_{(\mathrm{PLIM})}(\mathrm{r})\right). \tag{7-3}$$

Therefore,

$$\mathcal{P}_{\mathrm{r}}^{(\mathrm{Rp})} = \left(\mathcal{P}_{(\mathrm{MSC})}(\mathrm{r}) + \mathcal{P}_{(\mathrm{PLIM})}(\mathrm{r})\right) + \frac{\mathcal{P}_{\mathrm{chassis}}}{16} - \left(\mathcal{P}_{(\mathrm{MSC})}(\mathrm{r}) + \mathcal{P}_{(\mathrm{PLIM})}(\mathrm{r})\right) = \frac{\mathcal{P}_{\mathrm{chassis}}}{16} \quad (7\text{-}4)$$

Equation (7-4) shows that the port power consumption at a given line rate which is equal to the slot rate of the router is simply the total router power consumption divided by the total number of slots. If, however, the line rate of the port whose power consumption is to be determined is not equal to the slot rate of the router, the following criteria should be used:

$$\mathcal{P}_{\mathrm{r}}^{(\mathrm{Rp})} = \mathcal{P}_{(\mathrm{MSC})}(\mathrm{r}) + \mathcal{P}_{(\mathrm{PLIM})}(\mathrm{r}) + \mathcal{P}_{\mathrm{o}}(\text{at slot rate from eq. } (7-4)) \quad (7\text{-}5)$$

Equations (7-2) to (7-4) are used to determine the router port power consumption at different line rates and Table 7-1 shows the CRS chassis that have been used with their corresponding number of slots, slot rate and total chassis power consumption and Table 7-2 shows the specifications of modular cards found on the Cisco CRS chassis.

Table 7-1: Cisco CRS Chassis

Chassis Type	No. of Slots	Slot Rate	Total Power
Cisco CRS-1	16	40Gbps	13.2kW [36]
Cisco CRS-X	16	400Gbps	18kW [117]

Table 7-2: Cisco CRS Line Cards

Line Card	Chassis	Line Rate	Power Consumption
MSC_40	CRS-1 16-Slot	40Gbps	350W [34]
MSC_140	CRS-3 16-Slot	140Gbps	446W [34]
MSC_400	CRS-X 16-Slot	400Gbps	650W [34]
PLIM_40	CRS-1 16-Slot	40Gbps	150W [119]
PLIM_100	CRS-3 16-Slot	100Gbps	150W [120]
PLIM_400	CRS-1 16-Slot	4x100Gbps	125W [121]

It is expected that in 2020 line rates of 1000Gbps will be commercially available on most routers. In order to fully utilize the robustness of mixed line rate techniques in 2020, it is necessary to establish the power consumption of a 1000Gbps router port. Using the commercially available power consumption values determined using Method 2, it is possible to extrapolate the power consumption of a 1000Gbps port. First the power consumption of the 10Gbps port on the CRS-1 chassis is determined and then a curve (Fig. 7-2) is fitted on all the known power consumption points for each line rate calculated using the equations above and tabulated in Table 7-3 and then extrapolated to the 1000Gbps line rate.

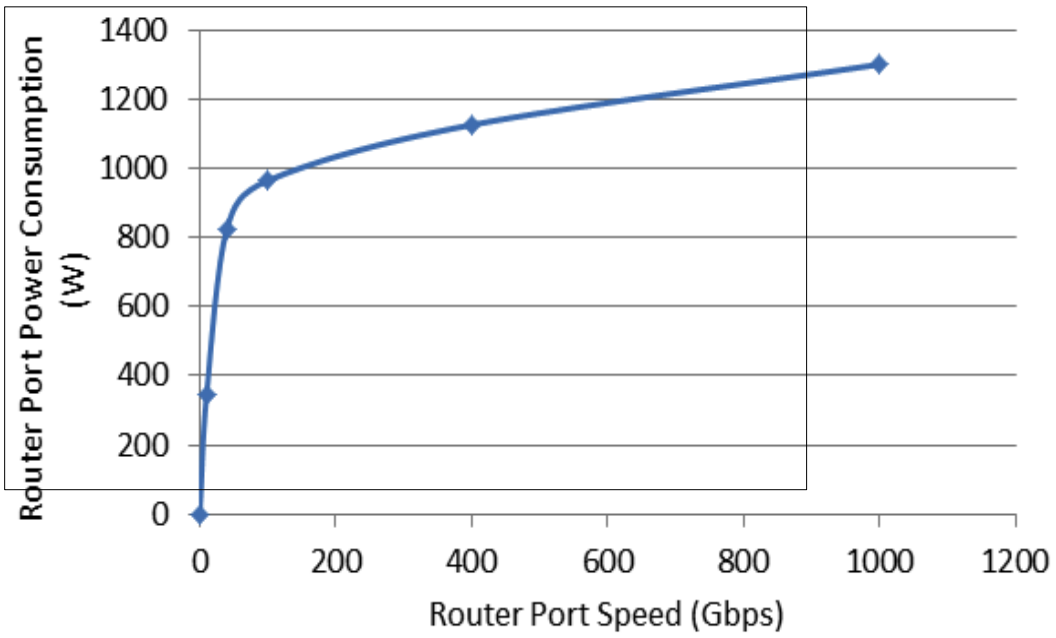

Figure 7-2: Port Power Consumption Curve

Table 7-3: Port Power Consumption at Different Line Rates

Port Speed (Gbps)	$\mathcal{P}_{(MSC)}(r) + \mathcal{P}_{(PLIM)}(r)$ (Watts)	$\mathcal{P}_r^{(Rp)}$ (Watts)	Note
0	0	0	extrapolated
10 CRS1	19.9	345	Method 2
40 CRS1	500	825	Method 2
100 CRSX	596	964	Method 2
400 CRX	775	1125	Method 2
1000 CR?	950 (=1300 – 350)	1300	Extrapolated

The router port power consumption values determined using Method 2 are the ones that have been adopted by GreenTouch and used in the GreenMeter study. For a 2010 network, the only high capacity

commercially available line rate on router interfaces and other optical transport equipment such as transponders and regenerators was 40Gbps and this is the value that was used to evaluate the power consumption performance. As for the 2020 network, new equipment power consumption values had to be projected. The 2020 equipment power consumption as evaluated by GreenTouch [116] is in two scenarios; a business as usual scenario (BAU) and a business as usual with GreenTouch improvements scenario (BAU+GT). The BAU equipment power consumption improvement factor has been evaluated by only applying expected energy efficiency improvements due to advanced CMOS technologies which is 0.22x for router ports and 0.21x for transponders and regenerators. For the BAU+GT case, GreenTouch initiatives which save power by implementing optical interconnects, matching and/or adapting router processor capabilities to packet size and employing dynamic voltage and frequency scaling in transponder DSPs [122], [123], are included. These initiatives improve the equipment power consumption in 2020 by a factor of 0.03x for routers and 0.17x for transponders. Applying the evaluated ratios by GreenTouch to the calculated power consumption values of routers and those of transponders and other optical transport equipment, yields the power consumption values shown in Table 7-4. These power consumption values are the ones that have been used for the entire GreenMeter study for core networks.

Table 7-4: Power Consumption Values

Device	*2010 Power Consumption*	*2020 Power Consumption*	
		BAU	*BAU+GT*
Router Port 40 Gb/s	*825 W*	*178.2 W*	*21.3 W*
Router Port 100 Gb/s	*Not widely deployed in the field*	*309.3 W*	*39.2 W*
Router Port 400 Gb/s	*Not widely deployed in the field*	*367.8 W*	*46.7 W*
Router Port 1 Tb/s	*Not widely deployed in the field*	*425.1 W*	*53.9 W*
Transponder 40 Gb/s	*167 W [124] Reach 2500 km*	*35.7 W Reach 2500 km*	*27.6 W Reach 2500 km*
Transponder 100 Gb/s	*Not widely deployed in the field*	*110.9 W Reach 1200 km*	*86 W Reach 1200 km*
Transponder 400 Gb/s	*Not widely deployed in the field*	*428 W Reach 400 km*	*332.6 W Reach 400 km*
Transponder 1 Tb/s	*Not widely deployed in the field*	*1032.6 W Reach 350 km*	*801.3 W Reach 350 km*
Regenerators 40 Gb/s	*334 W [124] Reach 2500 km*	*71.4 W Reach 2500 km*	*55.2 W Reach 2500 km*
Regenerators 100 Gb/s	*Not widely deployed in the field*	*221.8 W Reach 1200 km*	*172 W Reach 1200 km*
Regenerators 400 Gb/s	*Not widely deployed in the field*	*857.4 W Reach 400 km*	*665.2 W Reach 400 km*
Regenerators 1 Tb/s	*Not widely deployed in the field*	*2065.2 W Reach 350 km*	*1602.6 W Reach 350 km*
EDFA	*55 W [125]*	*15.3 W*	*15.3 W*
Optical Switch	*85 W [96]*	*85 W*	*8.5 W*

7.3 Network Virtualisation Contribution to GreenMeter Study

A MILP model that combines the cloud content delivery model [115] and virtual network embedding techniques that have been presented in Chapters four and five as well as all the GreenTouch techniques in [114] was developed to collectively optimise energy efficient cloud service provisioning in an IP over WDM core network. This model uses the power consumption parameters shown in Table 7-4 and the continental US AT&T topology network shown in Fig. 7-3 as the substrate network. In cloud content delivery, requests from clients are served by selecting the optimal number of clouds and their locations in the network so that the total power is minimised. A decision is also made on how to replicate content according to content popularity so that minimum power is consumed when delivering content. The virtual network embedding part of the model investigates the optimal way of embedding VNRs in the core network with clouds so that the power consumption in the network is minimised.

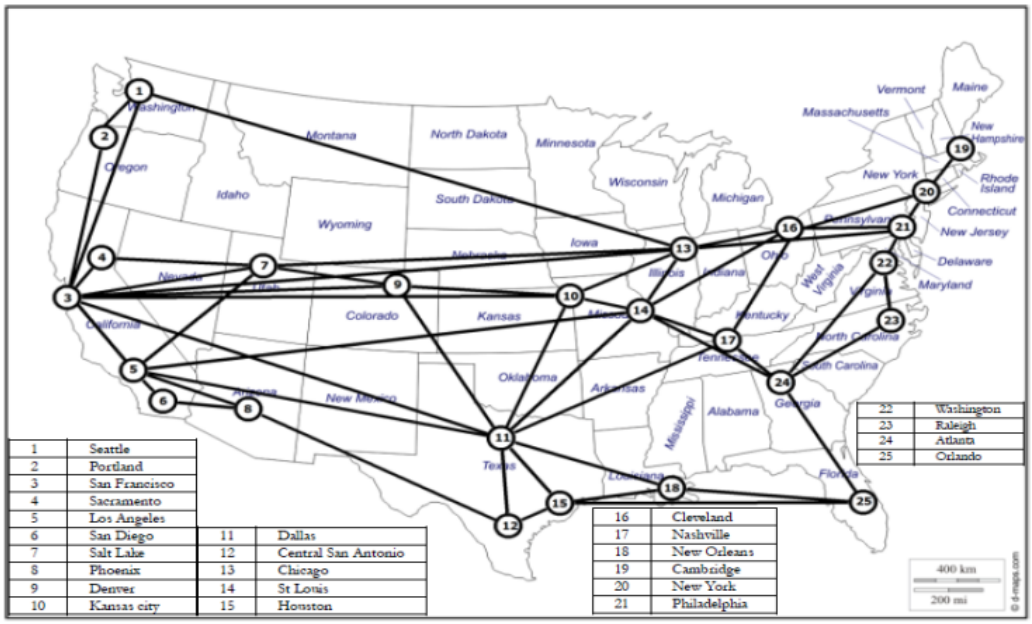

Figure 7-3: AT&T Network Topology used for the Combined MILP Model

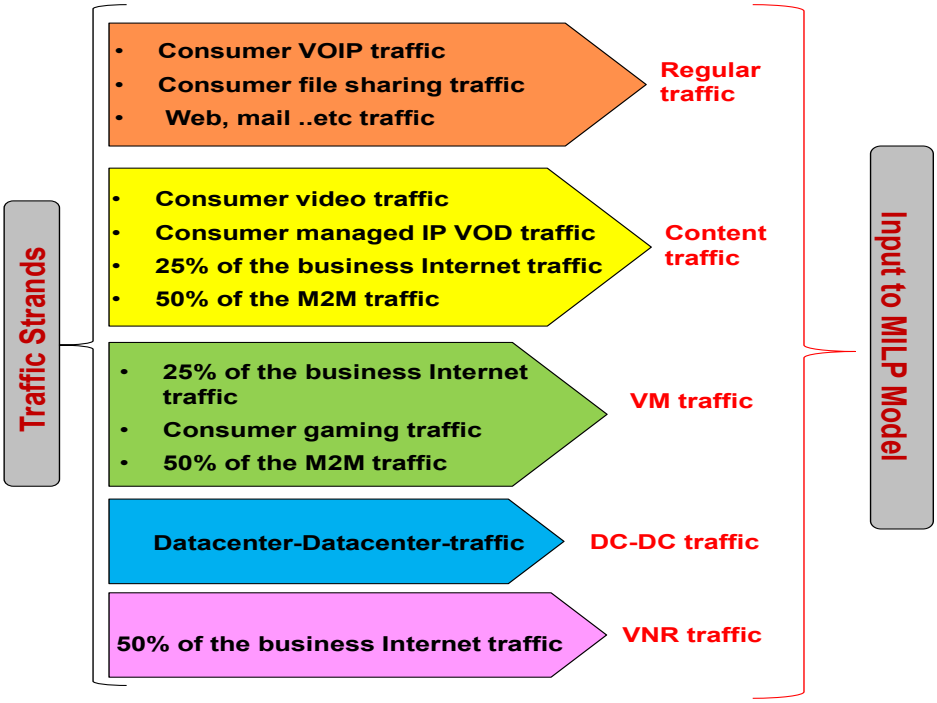

Figure 7-4: Traffic Strands For Distributed Cloud for Content Delivery and Network Virtualisation

In order to effectively carter for all the techniques described in the combined model, the 2020 traffic as projected by GreenTouch is broken down into various strands as shown in Fig. 7-4. For content distribution, users are uniformly distributed among all the nodes and the total number of users in the network fluctuates throughout the day between 200k and 1200k. For the virtual network embedding service, clients are distributed across the entire network. A total of 50 virtual network clients have been considered. The virtual network clients are considered to generate traffic in the network that is equivalent to 50% of the business internet traffic as shown in Fig. 7-4. The number of virtual nodes per virtual network request (VNR) from a client is uniformly distributed between 1 and 5. Each virtual node has a processing requirement in terms of virtual cores which are uniformly distributed between 500 and 3000 cores. In order to achieve load balancing, virtual nodes belonging to the same VNR are not allowed to be embedded in the same cloud data centre.

In the following results, the power consumption of individual components that make up the core network are shown. Fig. 7-5 shows the reference case which is the power consumption of the AT&T network under 2010 traffic, 2010 components and a 2010 network design where the network is dimensioned for maximum traffic and the non-bypass approach is implemented. Components in the network do not adapt their power usage as the traffic varies, hence the flat trend in Fig. 7-5. The major

contribution to the total power consumption in 2010 is due to the routers and then followed by transponders.

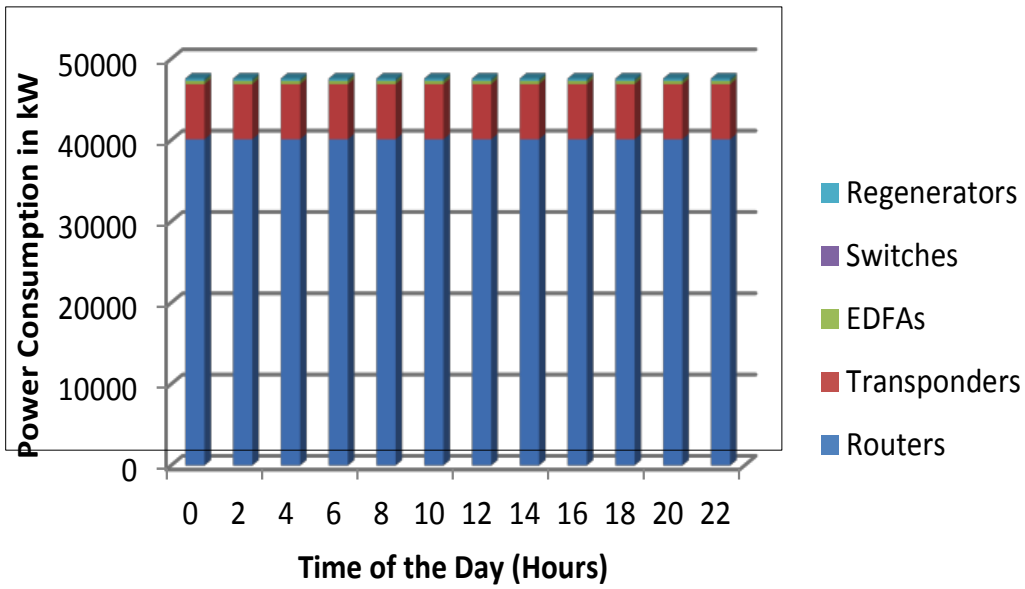

Figure 7-5: Power Consumption of a 2010 Core Network

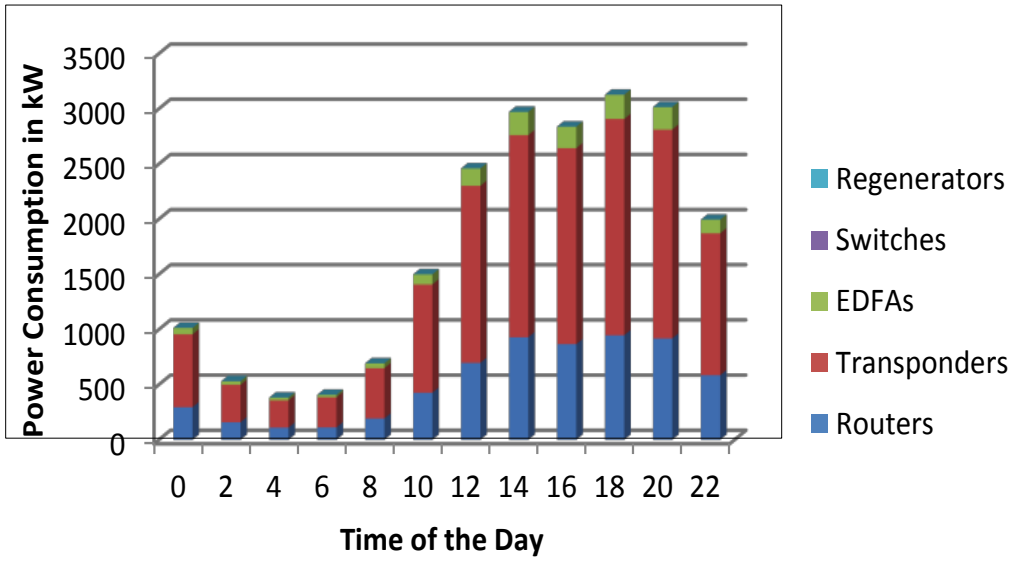

Figure 7-6: Power Consumption of a GreenTouch 2020 Core Network

Fig. 7-6 shows the power consumption of the 2020 AT&T network implementing GreenTouch techniques. Distributed clouds reduce the journeys up and down the network to access content and therefore reduce power consumption. The model establishes the optimal number of clouds to construct, where to locate them and which cloud should contain which object based on popularity. In network virtualisation, the use of resources is consolidated in the network by optimally embedding virtual network nodes and links such that they form minimal number of hops in the network. Virtual network requests from the same location but from different clients are co-located and the traffic they generate is groomed together to minimise network power consumption. When these approaches are implemented a power saving of 2.19x is achieved. The overall network saving considering all the GreenTouch approaches in 2020 (Fig. 7-6) compared to the 2010 network (Fig. 7-5) is 315x.

7.4 Summary

In this chapter, investigations that have been done as contributions to the GreenTouch GreenMeter research study have been presented. A very thorough investigation on the methods used to calculate the power consumption of router ports at various line rates based on the Cisco CRS router has been discussed. Two methods have been presented. The first method is a linear approximation method which first determines the energy per bit in Watts per Gbps by dividing the total chassis power consumption of the router given in the Cisco CRS-1 datasheet by the total switching

capacity of the router and then multiplying it by the line rate in Gbps to determine the port power consumption at that line rate. The method however does not consider the actual throughput of the router but rather considers the switching capacity which is usually twice the equipment throughput and it is therefore not entirely accurate. The second method, which is more accurate and representative of the router port power consumption, was considered. In this method, the individual power consumption contributions of the various cards on the cisco CRS router chassis were taken into account. The idle power consumption of the router was determined as well as the active power consumption of the router due to traffic. This method is the one that was adopted by GreenTouch and used in the GreenMeter study. The results of the combined MILP model that incorporates the virtual network embedding techniques of chapters four and five, cloud content delivery as well as the various energy optimisation techniques developed by the GreenTouch consortium for a 2020 network have been presented. The combined model improves energy savings in core networks by a factor of 2.19x while the incorporation of all the GreenTouch techniques into the combined model improves energy savings in core network by a factor of 315x when compared to a 2010 network.

Chapter 8: Profitable and Energy Efficient Virtual Network Embedding over Core Networks with Clouds

8.1 Introduction

In this chapter, a virtual network embedding framework for maximizing profit in cloud service provisioning of Infrastructure as a Service (IaaS) in non-bypass IP over WDM core networks is investigated. In the previous chapters, virtual network embedding has only been looked at from the perspective of energy minimisation without looking at the revenue and cost implications on the part of the infrastructure provider (InP). A mixed integer linear programming (MILP) model to study the impact of maximizing profit on the power consumption and acceptance of virtual network requests (VNRs) has been developed. Cloud data centres are mainly marketed as entities for outsourcing computational tasks. However,

the success of the cloud also depends on the network that connects clouds to the end users. Therefore, in the revenue and cost structure of an InP both bandwidth and computational resources should be considered. As clearly outlined in [126] bandwidth pricing among InPs significantly influences the choice of service provider selection among cloud service clients. Therefore, optimising both the bandwidth cost and the computational cost is an opportunity for InPs to make profit. The profit maximised VNE MILP model takes into account the relative difference in cost and pricing of computing resources and bandwidth in todays and future cloud networks. The results highlight the gulf that exists between maximizing profit and having high acceptance ratios as well as the impact that power optimisation has on profit. Using the insights from the models, a profit optimised and energy minimised heuristic, POEM, is developed with nearly the same power consumption, profit and VNR acceptance performance as the MILP model.

8.2 Considered Cloud Network Architecture and Operation

The considered cloud network infrastructure for profit maximised virtual network embedding is shown in Fig. 8-1. The figure shows the provisioning of VNRs denoted by different colours green, red and blue originating from nodes A, B and C respectively onto the physical network. Virtual nodes are instantiated in data centres at nodes B and D while their virtual links are also instantiated to route traffic from the data centres to the nodes where the clients are located.

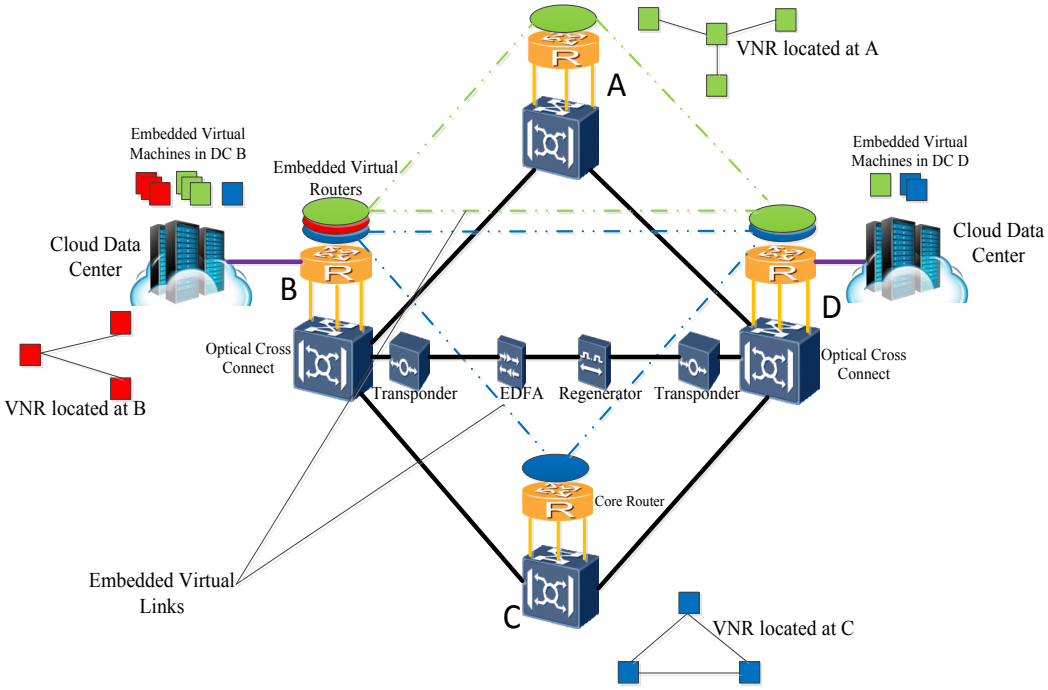

Figure 8-1: Virtual Network Embedding Cloud Infrastructure

The major difference in this architecture compared to those that have been considered in the previous chapters is the introduction of regenerators into the IP over WDM network. Regenerators have been introduced in the power consumption formulation to take care of propagation impairments stemming from the combined effects of fibre dispersion, noise accumulation and fibre non-linearities because the link distances considered in this case (Fig. 8-2) which are beyond 2000km which is the maximum reach of the considered Cisco ONS 15454 40Gbps transponder [127].

8.3 Mathematical Models for Profit Maximised VNE

New parameters, variables, objective functions and constraints have been developed to model the new profit maximised and power minimised approaches for virtual network embedding.

Parameters

$PPcore$ The price in US$ charged to the cloud client per single core

$CPcore$ The cost in US$ to the InP of hosting a single core in the cloud

$PPgbit$ The price in US$ per gigabit per second of network bandwidth charged to the cloud client

$CPgbit$ The cost in US$ to the InP of provisioning a gigabit per second of network bandwidth

$EG_{m,n}$ The number of regenerators on a physical link (m, n). Typically $\mathrm{EG_{m,n}} = \left\lfloor \left(\frac{\mathrm{D_{m,n}}}{\mathrm{RG}} \right) - 1 \right\rfloor$, where RG is the reach of the regenerator

PG Power consumption of a regenerator

Variables

$MxPrft$ Optimal profit evaluated from the profit maximised model

C_b The total number of Virtual cores at data centre b

The network power consumption under non-bypass now includes the power consumption of the regenerators in addition to the router ports, optical switches, transponders and EDFAs that were considered in the previous chapters. The power consumption of regenerators is given as:

$$\sum_{m \in N} \sum_{n \in N_m} PG \cdot W_{m,n} \cdot EG_{m,n}$$

The revenue generated by an InP over a given duration as a result of embedding a set of VNRs is given as:

$$\sum_{v \in V} \sum_{s \in R} C^{v,s} \cdot \Psi^v \cdot PPcore + \sum_{v \in V} \sum_{s \in R} \sum_{d \in R: s \neq d} H^{v,s,d} \cdot \Phi^v \cdot PPgbit$$

The cost associated with the embedding of VNRs by the InP is given as:

$$\sum_{v \in V} \sum_{b \in N} \sum_{s \in R} C^{v,s} \cdot \Delta_b^{v,s} \cdot CPcore + \sum_{m \in N} \sum_{n \in N_m} W_{m,n} \cdot B \cdot CPgbit$$

Note that the cost per virtual core ($CPcore$) and the cost per Gbps of bandwidth ($CPgbit$) include both the OPEX, and CAPEX to be recovered over the lifetime of the network.

The profit gained by the InP is given as the difference between the revenue generated and the cost. The profit maximised model is therefore defined as follows:

Objective 1 (Profit Maximised):

Maximise the overall profit given as:

$$\left(\sum_{v\in V}\sum_{s\in R} C^{v,s}\cdot \Psi^{v}\cdot PPcore + \sum_{v\in V}\sum_{s\in R}\sum_{d\in R:s\neq d} H^{v,s,d}\cdot \Phi^{v}\cdot PPgbit\right) - \left(\sum_{v\in V}\sum_{b\in N}\sum_{s\in R} C^{v,s}\cdot \Delta_{b}^{v,s}\cdot CPcore + \sum_{m\in N}\sum_{n\in N_m} W_{m,n}\cdot B \cdot CPgbit\right) \quad (8\text{-}1)$$

Subject to all the constraints given in chapters four and five. In order to achieve optimal power consumption for the optimal profit, a new objective of minimizing the power consumption in the network is needed. In addition, a constraint that achieves a profit that is equal to the optimal profit is included in the optimisation as shown in the following equations:

Objective 2 (Power Minimised):

Minimise network power consumption given as:

$$\sum_{m\in N}\sum_{n\in N_m} W_{m,n}\cdot PR + \sum_{m\in N}\sum_{n\in N_m} W_{m,n}\cdot PT + \sum_{m\in N}\sum_{n\in N_m} PG\cdot W_{m,n}\cdot RG_{m,n} + \sum_{m\in N}\sum_{n\in N_m} PE\cdot EA_{m,n}\cdot F_{m,n} + \sum_{m\in N} PO_m + \sum_{m\in N} PMD\cdot DM_m \tag{8-2}$$

Subject to all the constraints given in chapters four and five including:

$$\left(\sum_{v\in V}\sum_{s\in R} C^{v,s}\cdot \Psi^v\cdot PPcore + \sum_{v\in V}\sum_{s\in R}\sum_{d\in R:s\neq d} H^{v,s,d}\cdot \Phi^v\cdot PPgbit\right) - \left(\sum_{v\in V}\sum_{b\in N}\sum_{s\in R} C^{v,s}\cdot \Delta_b^{v,s}\cdot CPcore + \sum_{m\in N}\sum_{n\in N_m} W_{m,n}\cdot B\cdot CPgbit\right) = MxPrft \tag{8-3}$$

where $MxPrft$ is the optimal profit in the network evaluated from the profit maximised model.

8.4 Performance Evaluation of Profit Maximised VNE

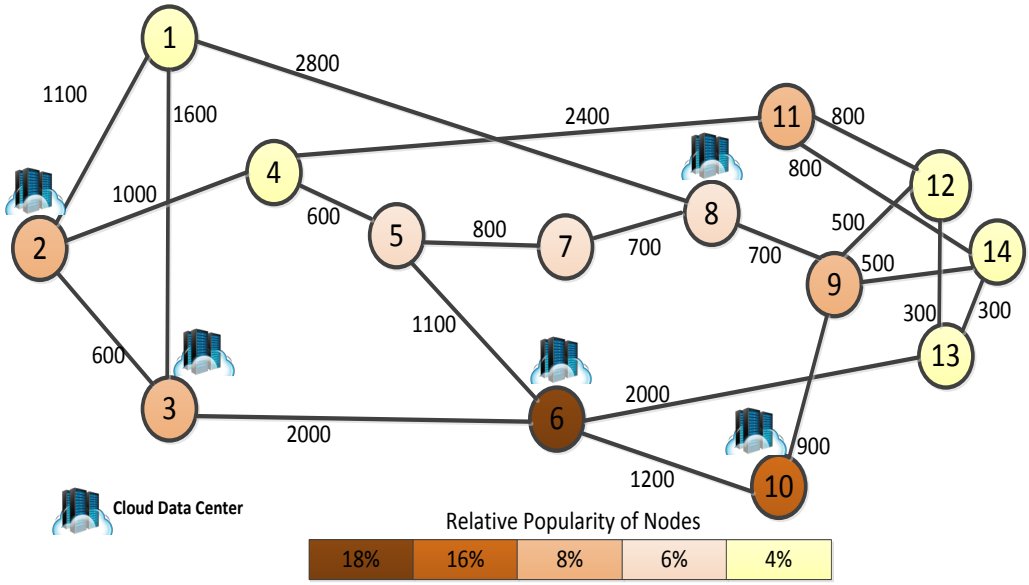

Figure 8-2: NSFNET Network with Updated Link Distances

The 14 node and 21 link NSFNET network, shown in Fig. 8-2, is used as the substrate network to evaluate the performance of the MILP models. Similar to the approaches taken in Chapters five and six, VNRs have been distributed in the substrate network such that their location is fixed. However, the requested virtual nodes could be embedded in any cloud data centre. The link distances have also been updated to reflect the realistic hop distances instead of the scaled distances that were used in the previous chapters. The concentration of VNRs at any substrate node is based on the population of the states where the node is located as was the case in chapter five.

Enterprise clients request virtual networks consisting of virtual machines with a specific number of virtual cores and virtual links of specific bandwidth. A total of 50 enterprise clients send VNRs to the InP over a 24 hour period at two hour time intervals. The traffic generated by the VNRs over a 24 hour period is modelled according to the 2020 business Internet traffic in the US as projected by the GreenTouch Consortium [114]. The daily traffic variation is as shown in Fig. 8-3. The requests once accepted stay in the network for the 2 hour slot after which they are torn down and adjusted according to the new arriving demands. The number of virtual nodes per VNR is random and uniformly distributed between 1 and 5 and the number of virtual cores per virtual node is random and uniformly distributed between 50 and 8000. The substrate network is un-capacitated in both node and link resources; i.e. node and link resources are not predetermined, which means that this is a network design problem where the link and node capacities are to be determined. This is in contrast to the capacitated problem to be considered later where the link and node capacities are pre-determined, i.e. the substrate network is already installed. The consolidation factors are set to $\alpha = \beta = 5$, i.e. all the virtual nodes and machines of a VNR can be co-located.

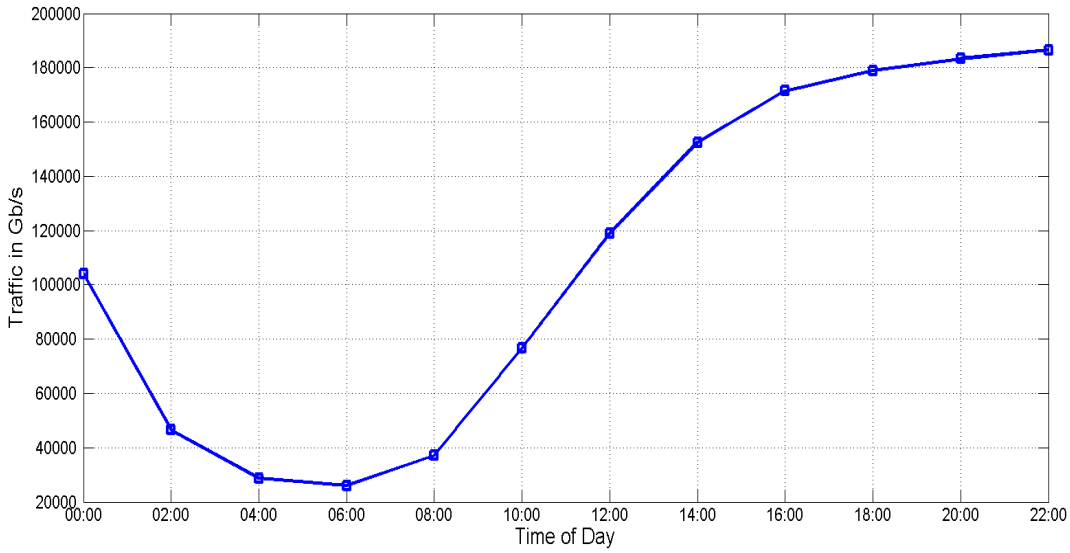

Figure 8-3: 2020 Average Business Internet 24 Hour Traffic Distribution [114]

In order to minimise the delay experienced by the users and to avoid the scenario of having a single hot node in the network, five data centres have been placed in the network at nodes (2, 3, 6, 8 and 10) as shown in Fig. 8-2, which are current locations of large data centres in the US as shown in [128]. Table 8-1 shows the values of the other parameters that have been used in the model. As was the case in Chapter 6, the power consumption in data centres is not optimised since an energy efficient data centre power profile is assumed. The actual cost of running a network is commercially sensitive and not publicly available. Therefore, to determine the values of $CPcore$ and $CPgbit$, Google "pay-as-you-use" cloud service pricing scheme in [129] and [130] was used with a typical profit margin for Internet providers of 20% [131].

Table 8-1: Evaluation Parameters

Distance between two neighboring EDFAs (S) [132]	80 (km)
Distance between two neighboring Regenerators (RG) [127]	2000 (km)
Bit rate of each wavelength (B)	40Gbps
Number of wavelengths in a fibre (W) [133]	32
Power consumption of a transponder (PT) [132]	167 (W)
Power consumption of a regenerator (RG) [124]	334 (W)
Power consumption of a 40Gb/s router port (PR)	850(W)
Power consumption of an EDFA (PE) [132]	55 (W)
Power consumption of an optical switch (PO)	85 (W)
Power consumption of a multi/demultiplexer (PMD)	16 (W)
Price of a virtual core in the cloud per 2 hour usage ($PPcore$) [129]	\$0.21
Price of 1Gbps of bandwidth in the cloud per 2 hour usage ($PPgbit$) [130]	\$0.30
Profit margin per core and per Gbps [131]	20%

The AMPL software with the CPLEX 12.5 solver is used as the platform for solving the MILP models on a server with a quad core 3.3 GHz Intel® Xeon CPU, with 64 Gigabytes of RAM. The running times for the models average 15 minutes for each solution (point on the curve).

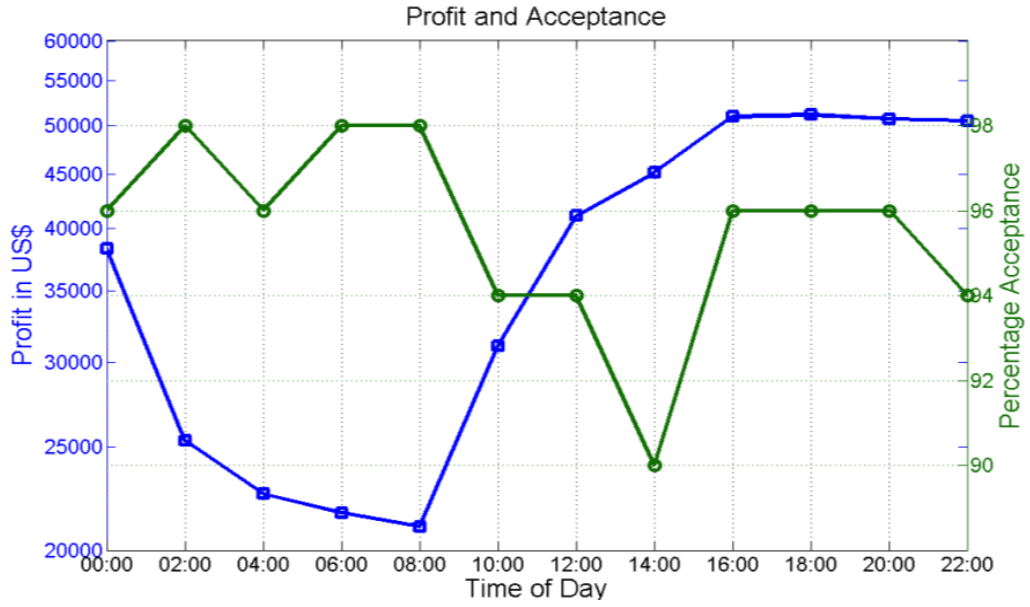

Fig. 8-4(a)

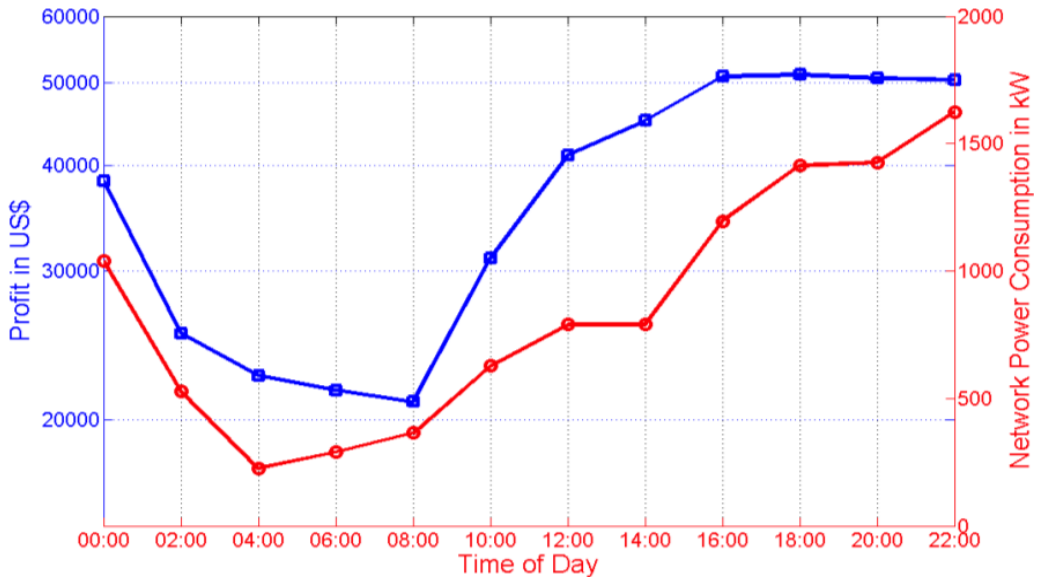

Fig. 8-4(b)

Figure 8-4: (a) Profit and Acceptance Performance of the Profit Maximised Model, (b) Profit and Power Consumption Performance of the Profit Maximised Model

Fig. 8-4(a) shows the optimal profit (left y-axis) and percentage acceptance (right y-axis) of VNRs over a 24-hour period for the profit maximised model. It shows that the profit achieved follows the traffic trend of Fig. 8-3. The profit is accrued from the minimal use of network resources (wavelengths) achieved through minimum hop routing, traffic grooming and the consolidation of data centre resources. VNRs are served locally as much as possible to save network resources. The model rejects VNRs that are very costly, in terms of use of network resources, in order to maximise the profit. It can be seen that despite the network having sufficient resources (since it's un-capacitated) to accommodate all the VNRs in the network, some of the requests are rejected. The average daily acceptance percentage is 96%. Hop count determines the number of router ports and transponders (the most energy consuming network devices) used under the non-bypass approach. Therefore, VNRs that can be served locally in a single data centre are more likely to be accepted as they lead to minimal power consumption and higher profits through node consolidation. On the other hand, VNRs that create multiple hops in the network are more likely to be rejected because of their high power consumption and high cost, i.e. low profit. It can therefore be concluded from these results that higher acceptance ratios are not necessarily representative of increased profit.

The power consumption performance of the profit maximised model is shown in Fig. 8-4(b) where it is plotted together with the profit. The power consumption also follows the traffic trend of Fig. 8-3. This is due to the

fact that a bigger load in the network would naturally cause higher power consumption in the network. This power consumption is however not optimal.

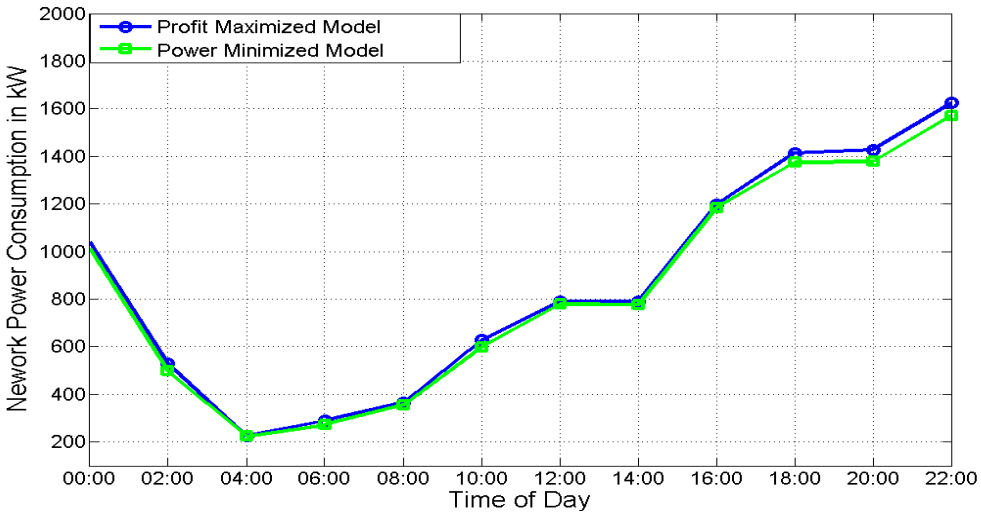

Figure 8-5: Network Power Consumption of the Power Minimised and Profit Maximised Models

Fig. 8-5 shows that optimal network power consumption can be achieved for the same optimal profit by running the model with the objective of minimizing power consumption and constraining the model to achieve the same optimal profit. In this scenario, 300kW of the network power is saved through power optimisation. The actual network components where these savings are made can be seen in Fig. 8-6 which shows the daily power consumption of individual components.

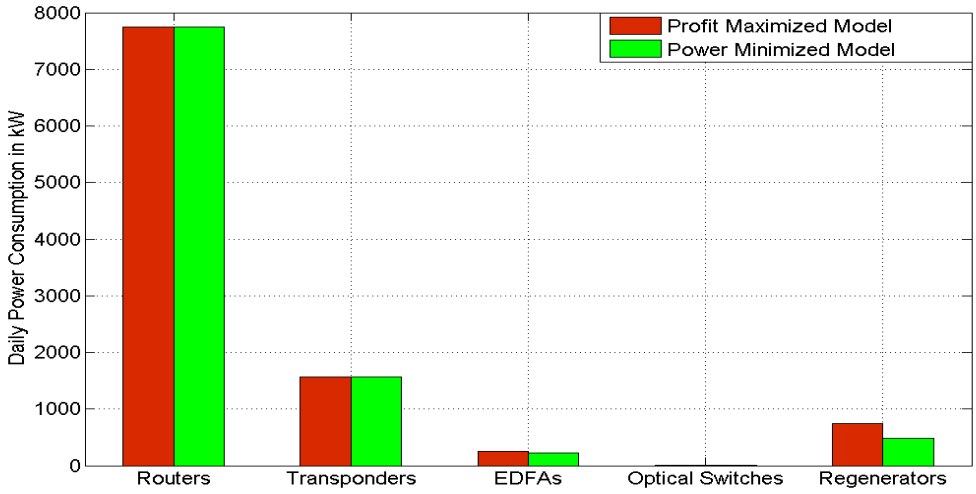

Figure 8-6: Device Network Power Consumption Comparison

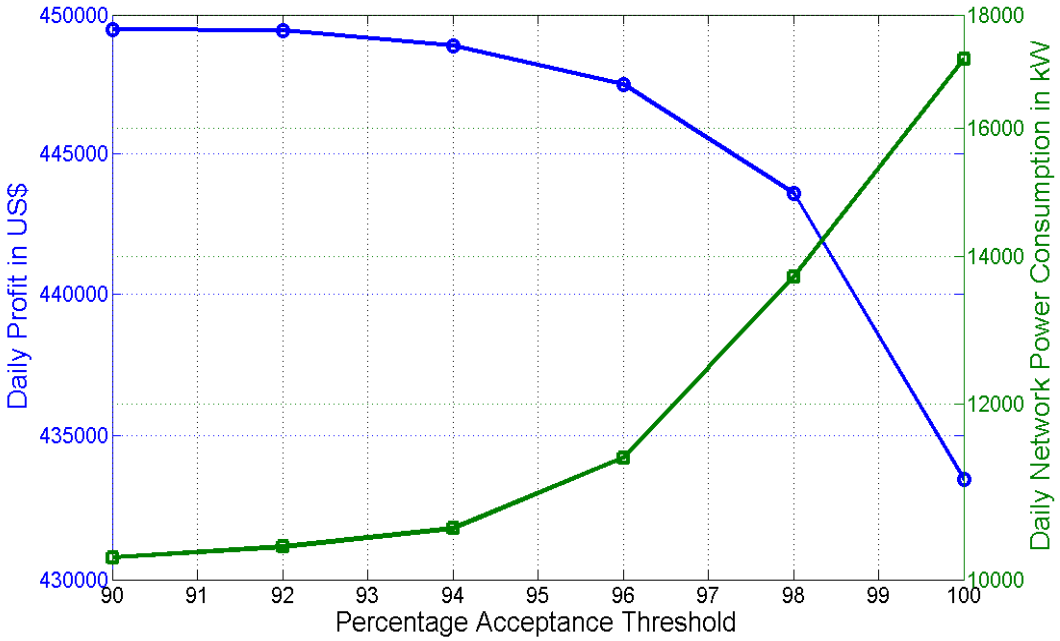

Figure 8-7: Profit and Power Consumption at Various Acceptance Thresholds

The routers and transponders in both cases consume the same amount of power because the approaches taken by the profit and power models to achieve their objectives are similar in that they reduce the use of network

wavelengths. However, the situation is different with regard to the EDFAs and Regenerators. The difference in this case is attributed to the selection of shorter links by the power minimised model for minimal usage of EDFAs and Regenerators. This is where all the savings are made.

Having established that higher acceptance ratios are not necessarily representative of increased profits, it is important to consider the fact that bad customer experience resulting from poor acceptance ratios could easily lead to high customer churn. It is therefore necessary to find an optimal percentage acceptance threshold that is high enough to give a good customer experience but also power efficient and profitable at the same time. To achieve this goal, the profit maximised and power minimised models were evaluated at varying percentage acceptance thresholds between 90% and 100% to determine the optimal threshold that would minimise churn. Fig. 8-7 shows the results. Typical cloud SLAs demand task acceptance exceeding 99% and this is predicted to provide good performance and customer experience [134]. At 99% acceptance, Fig. 8-7 shows that the profit is still within 97% of its peak value although the network power has increased by 1.67x compared to its minimum value; an attractive feature of the developed cloud network design.

8.5 Profit Optimised and Energy Minimised (POEM) Heuristic

Based on the insights from the results obtained from both the profit maximised and power minimised models, the POEM (Profit Optimised and Energy Minimised) heuristic has been developed. The heuristic combines both the benefits of the profit maximised model and the power minimised model. The algorithm in Fig. 8-8 shows the operation of the POEM heuristic.

Following the process outlined in Fig. 8-8, when a VNR arrives, POEM first checks if the VNR can be embedded locally by checking if the VNR originates from a node with a data centre. If it does, the VNR is accepted and embedded at the local cloud data centre. This option is selected because locally provisioned VNRs are the most profitable and consume the least amount of power in the network. The algorithm then calculates the profit earned as a result of embedding the VNR at a local data centre. If however the VNR is not located at a cloud data centre node, POEM selects the best possible data centre among the subset of data centres to embed the VNR by the use of both minimum hop and shortest path routing. The data centre which results in minimal cost and minimal power consumption after embedding the VNR is selected as the host for virtual cores of the VNR. The procedure in Fig. 8-9 shows how a cloud data centre is selected as the optimal location for embedding virtual cores of a VNR.

Algorithm : Profit Optimized and Energy Minimized (POEM) Heuristic

Input: $\forall N \in Set\ of\ Physical\ Nodes\ in\ Network,\ \forall v \in Set\ of\ VNRs$, $Loc(v) \in Location\ of\ VNR\ v, \forall dc \in set\ of\ data\ centre\ nodes\ in\ N$

Output:

$Network\ Power\ Consumption\ (v), Cost\ (v), Revenue(v), Profit\ (v), Total\ l$
$Total\ Profit$

1. $Total\ Power = 0$
2. $Total\ Profit = 0$
3. **for all** $v \in VNRs$ **do**
4. **if** $Loc(v) = dc$
5. **Accept** v
6. Calculate the $Profit\ (v)$ of Embedding v at dc
7. **else**
8. **for all** $dc \in N$
9. Determine the best dc to embed v using $Procedure\ One$
10. Determine the $Cost\ (v)$ and $Revenue(v)$ of embedding v
11. in selected dc
12. **if** $Revenue(v) - Cost\ (v) < 0$
13. **Reject** v
14. **else**
15. **Accept** v
16. Determine the $Profit\ (v)$ of Embedding v at dc
17. Determine the $Network\ Power\ Consumption\ (v)$ of
18. Embedding v at dc
19. **end if**
20. **end for**
21. **end if**
22. $Total\ Power = Total\ Power + Network\ Power\ Consumption\ (v)$
23. $Total\ Profit = Total\ Profit + Profit\ (v)$
24. **end for**

Figure 8-8: POEM Algorithm

Algorithm : Procedure One

Output: $Hops\ (dc)$

1. **for all** $dc \in N$ **do**
2. | $Hops\ (dc) = Number\ of\ hops\ from\ Loc(v) to\ dc$
3. **end for**
4. **Sort** $Hops\ (dc)$
5. Select $Hops\ (dc)$ with the least value
6. **if** there is more than one with least value
7. | Select $Hops\ (dc)$ with shortest path from $Loc(v)\ to\ dc$
8. **else if** there is more than one with shortest path
9. | Select $Hops\ (dc)$ at random among those with path shortest
10. **end if**
11. Return the dc value for the selected $Hops\ (dc)$

Figure 8-9: Cloud Data Centre Selection Procedure

The process starts with testing the entire subset of data centre nodes to establish which one of them has the least hop count between itself and the node where the VNR is located. Sorting all the hop counts and then selecting one with the least value achieve this. If there is more than one with the least value, then the one with the shortest combined distance between hops is selected. If there is a tie in distance as well, the algorithm randomly picks one between the two. If the revenue obtained from the embedding of a VNR is greater or equal to the cost incurred, the VNR is accepted and both the profit and power consumption are established. If however the revenue obtained is less than the cost incurred, the VNR is rejected. The process is repeated for the entire set of VNRs and the overall power consumption, profit and number of rejected requests are determined.

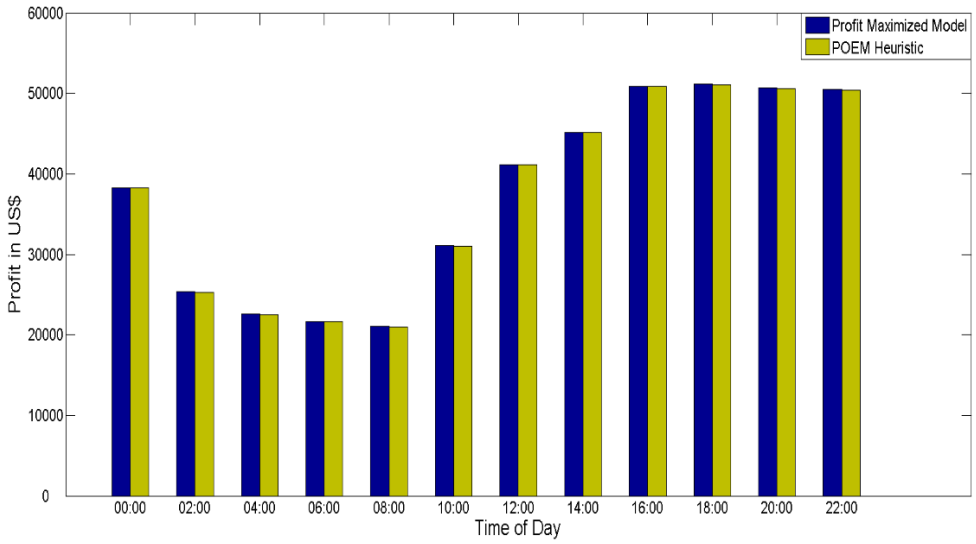

Figure 8-10: Profit Performance of the Profit Maximised Model and the POEM Heuristic

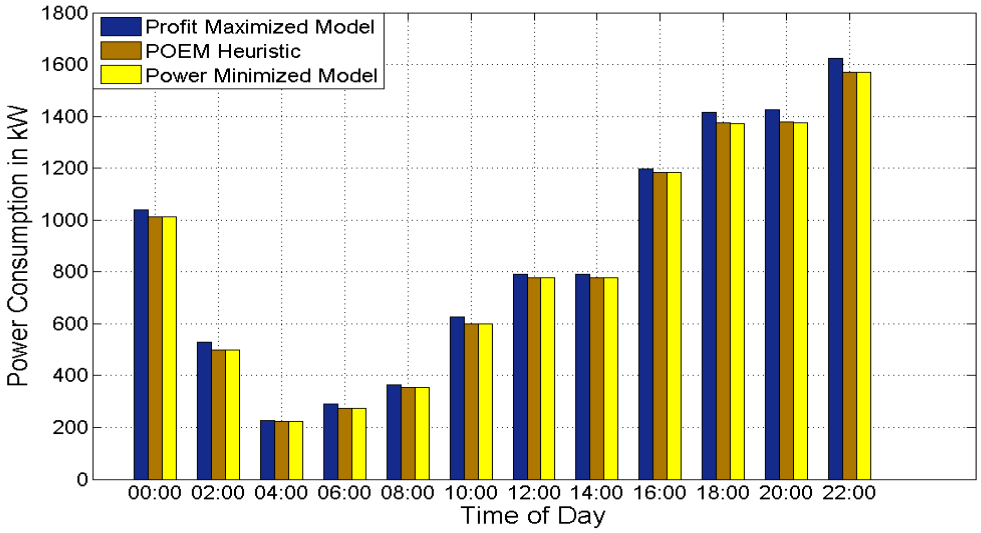

Figure 8-11: Profit Performance of the Profit Maximised Model and the POEM Heuristic

The POEM heuristic performs almost as good as the profit maximised MILP model in terms of profit as shown in Fig. 8-10. POEM optimises the

use of wavelengths, which are the largest contributors to the overall cost, in its selection of data centres that can accommodate virtual cores of VNRs and by doing so, its performance is nearly as good as that of the profit maximised model. Fig. 8-11 shows the power consumption of the POEM heuristic compared to the profit maximised and power minimised models. POEM performs better than the profit maximised model and performs nearly as good as the power minimised model. This is due to the fact that the ability to use less EDFAs and Regenerators is also built into the POEM heuristic during the selection of a data centre when embedding VNRs. POEM therefore adequately satisfies the objectives of both profit maximization and power minimisation. This is the desired outcome of every infrastructure provider who seeks to make a profit as well as consume less energy. However, customer perception in terms of VNR acceptance should also be put into consideration in addition to the goals of profit maximization and power minimisation.

8.6 Profit Maximised and Power Minimised Model with Capacitated Link and Data Centre Resources

Further investigations on the behaviour of both the profit maximised and power minimised models in a scenario where both link and cloud data centre resources in the network are capacitated have been done. This is the scenario that is more likely to be encountered in practice where the data centre locations are predetermined and fixed and the network resources are

predetermined as both the data centres and the network are already designed and deployed. Data centres have been limited to hosting a maximum of 300000 virtual cores. This is equivalent to having 75000 servers in a data centre assuming that each server has a quad core CPU and each virtual core takes all the resources of one physical CPU core. The links have been configured to have a maximum of two bi-directional fibres giving a link capacity of $2\times32\times40=2560$Gbps.

The limitation in both bandwidth and data centre resources forces both the profit maximised and power minimised models to traverse more hops in the network to find data centres that would lead to optimal profit and minimal power consumption. The increased hop count reduces the daily average acceptance percentage reported in Section 8.5 and also reduces the overall maximum daily profit. The impact on the difference in power consumption between the profit maximised and power minimised models is shown in Fig. 8-12. More significant energy savings by the power minimised model over the profit minimised model can be seen by comparing figures 8-5 and 8-12. In a capacitated network, the power minimised model saves 500kW per day compared to the profit maximised model.

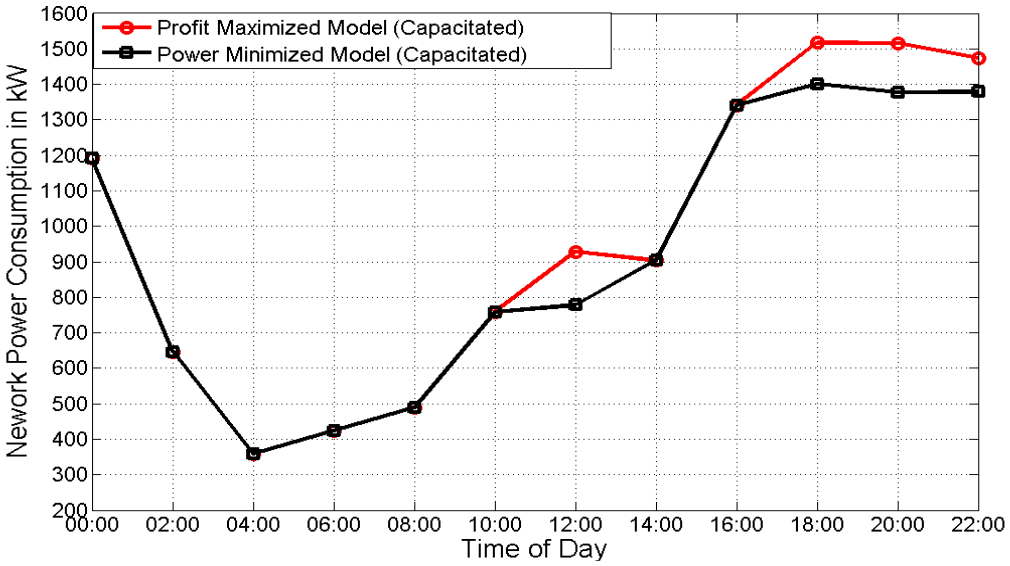

Figure 8-12: Network Power Consumption of the Power Minimised and Profit Maximised Models in a Capacitated Network.

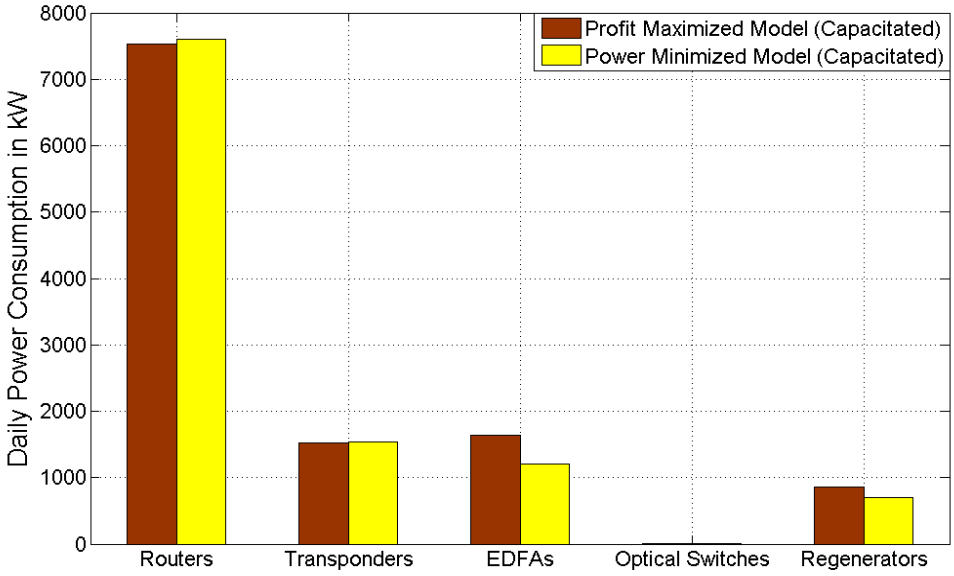

Figure 8-13: Device Network Power Consumption Comparison in Capacitated Network

Fig. 8-13 shows the individual network components' daily power consumption for both the profit maximised and power minimised models.

In order to save power in the network, it is interesting to observe that the power minimised model uses more router ports and transponders in order to achieve much higher energy savings in EDFAs and Regenerators. This can be explained by noting that the power minimised model embeds requests that lead to the selection of a path with more than one hop but with a much shorter combined distance instead of using a single hop path that has a much longer distance. The longer distance in this case leads to higher power consumption through the use of EDFAs and regenerators than what would otherwise be consumed in router ports and transponders due to the increased number of hops.

8.7 Summary

This chapter has investigated maximizing the profit achieved by Infrastructure providers (InPs) from embedding VNRs. A MILP model to study the impact of maximizing profit on the power consumption and acceptance of VNRs has been developed. The results of the profit maximised model show that higher acceptance ratios are not necessarily representative of increased profits. It has also been shown that the power consumption can be optimised without any compromise on the profit achieved as the approaches taken to maximise profit and minimise network power consumption are similar in that they both reduce the use of wavelengths. A jointly optimised heuristic algorithm, POEM (Power Optimised and Energy Minimised), which combines both profit maximization and power minimisation of virtual network embedding in

cloud networks has been developed using the insights from the MILP model results. POEM can be implemented in real time and the results obtained from the heuristic are nearly as good as those of the MILP models in both profit and power consumption performance. It has also been shown that when a network that is capacitated in both link and data centre resources is considered, the difference in power savings between the profit maximised model and the power minimised model increases significantly compared to the un-capacitated network.

Chapter 9: Green and Electricity Cost Minimised Virtual Network Embedding over Core Networks with Clouds

9.1 Introduction

Environmental sustainability in high capacity networks and cloud data centres has become one of the hottest research subjects. In this chapter, an investigation on the effective use of renewable energy in virtual resource allocation in IP/WDM core networks with clouds as a means of reducing the carbon footprint has been carried out. The authors in [86] have developed an energy aware hybrid VNE approach where VNs are assigned to nodes with the cleanest energy sources. The authors have used CO_2 emission factors of cities as the determinant of where nodes are embedded. The city with the least factor becomes the most attractive. Whereas this approach seems reasonable in mitigating CO_2 emissions, it falls short of making full use of renewable energy that may be available in a city because it is possible that a city with a comparatively high CO_2 emission factor

could also have a high availability of renewable energy. A Green Virtual Network Embedding (GVNE) framework for minimizing the use of non-renewable energy through intelligent provisioning of bandwidth and cloud data centre resources has been developed. The problem is modelled as a mixed integer linear program (MILP) and the results show that CO_2 emissions could be reduced by up to 48% and that it is better to instantiate virtual machines in cloud data centres that have access to abundant renewable energy even at the expense of traversing multiple links across the network.

While it is important for cloud infrastructure owners to address the problem of greenhouse gas (GHG) emissions, they are also equally concerned about the operational expenditure (OPEX) that is associated with electricity costs in the network. The work in [85] has addressed electricity cost minimisation in virtual network embedding infrastructures where virtual networks are embedded in geographically distributed substrate networks considering location-varying and time-varying electricity pricing. The work however does not consider the impact of the availability of renewable power and how it can help cloud infrastructure owners reduce their overall carbon footprint. In the investigation, it has been shown that completely focusing on reduction of non-renewable power consumption has the potential to significantly increase the overall OPEX associated with electricity consumption considering the geographical price discrimination of electricity. Therefore, a framework that addresses both concerns of reducing

electricity costs and GHG emissions has been developed. The results of the developed model show that while maintaining the electricity cost at the lowest optimal value, GHG emissions could be reduced by up to 16%. Through monetization of the GHG emissions resulting from the use of non-renewable energy due to the provisioned virtual network requests, the model results show that it would be prudent to prioritize energy costs instead of GHG emissions at the present market price of carbon credits.

9.2 Network Architecture and Operation

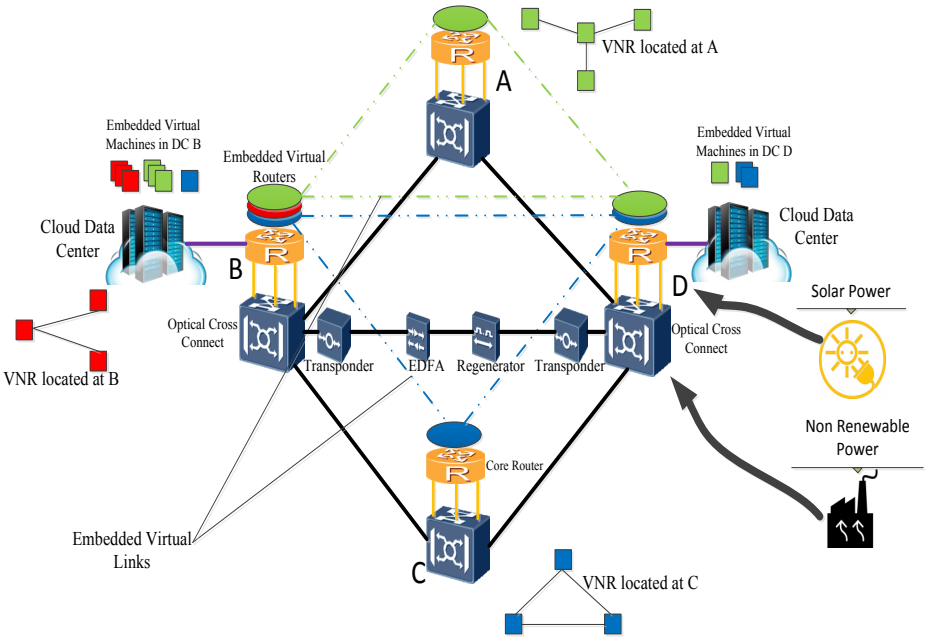

Figure 9-1: Considered Green Virtual Network Embedding Architecture

The virtual network embedding problem defines how virtualized resources should be realized onto the substrate network. In Fig. 9-1, the virtual

network requests (VNRs) denoted by the colours green, red and blue with node and link demands are to be embedded onto the substrate IP over WDM network with data centres whose operation and setup has been described in the previous chapters. Once embedded, the VNRs take up processing resources in data centres and bandwidth resources on physical links. This mapping process across multiple layers is as described in Chapter 4. The difference in this chapter is that the nodes of the substrate network, as shown in Fig. 9-1, have access to hybrid power supplies being composed of non-renewable energy and renewable energy sources. The renewable energy considered here is supplied by solar photovoltaics from the energy utility supplier. The renewable energy can be used to power the data centres and the IP over WDM equipment to reduce the overall greenhouse gas (GHG) emissions of the Infrastructure provider. The nodes with access to renewable energy also have access to non-renewable energy to guarantee quality of service in the absence of renewable energy.

9.3 MILP Model for Green Virtual Network Embedding

The energy efficient VNE MILP model developed in Chapter 4 is extended further in this chapter to incorporate the use of renewable energy sources in the optimisation. The problem becomes that associated with minimizing the non-renewable energy consumption of virtual network embedding in the hybrid-power IP over WDM network with cloud data centres. The model should be intelligent enough to decide whether to embed virtual network requests in a locally based data centre or to seek out

a distant data centre that has better access to renewable energy resources. This decision, takes into account the network power consumption that would be consumed if the virtual nodes were embedded in a distant data centre.

In addition to the variables, parameters and constraints defined in the previous chapters, the following new variables, parameters and constraints are defined for the Green Virtual Network Embedding (GVNE) model.

Parameters

SE_m	Solar power capacity at node m

Variables

$WN_{m,n}$	Number of wavelengths in physical link (m,n) powered by non-renewable energy
$WS_{m,n}$	Number of wavelengths in physical link (m,n) powered by renewable energy
$C_b^{(S)}$	Number of cores embedded at node b powered by renewable energy
$C_b^{(NR)}$	Number of cores embedded at node b powered by non-renewable energy

The objective of the optimisation is given as:

Minimise the overall non-renewable power consumption given as:

$$\sum_{m\in N}\sum_{n\in N_m} WN_{m,n}\cdot PR + \sum_{m\in N}\sum_{n\in N_m} WN_{m,n}\cdot PT + \sum_{m\in N}\sum_{n\in N_m} EG\cdot\lambda_{m,n}\cdot RG_{m,n} + \sum_{m\in N}\sum_{n\in N_m} PE\cdot EA_{m,n}\cdot F_{m,n} + \sum_{b\in N} C_b^{(NR)}\cdot\gamma \tag{9.1}$$

Subject to the following constraints including those presented in chapters four and five.

$$C_b = C_b^{(S)} + C_b^{(NR)} \quad \forall b \in N \tag{9.2}$$

Constraint (9.2) calculates the total number of cores in a data centre as the sum of the embedded cores powered by renewable energy and the embedded cores powered by non-renewable energy.

$$W_{m,n} = WN_{m,n} + WS_{m,n} \quad \forall m,n \in N \tag{9.3}$$

Constraint (9.3) calculates the total number of wavelength in fibre link as the sum of the wavelengths powered by renewable energy and the wavelengths powered by non-renewable energy.

$$\sum_{n\in N_m} WS_{m,n}\cdot PR + \sum_{n\in N_m} WS_{m,n}\cdot PT + C_m^{(S)} \le SE_m \quad \forall m \in N \tag{9.4}$$

Constraint (9.4) ensures that the total renewable energy consumption by router ports, transponders and data centres at each node does not exceed the maximum renewable power available for the node. Due to the location of EDFAs and regenerators in between nodes, it has been assumed that they only have access to non-renewable energy.

9.3.1 GVNE Performance and Evaluation

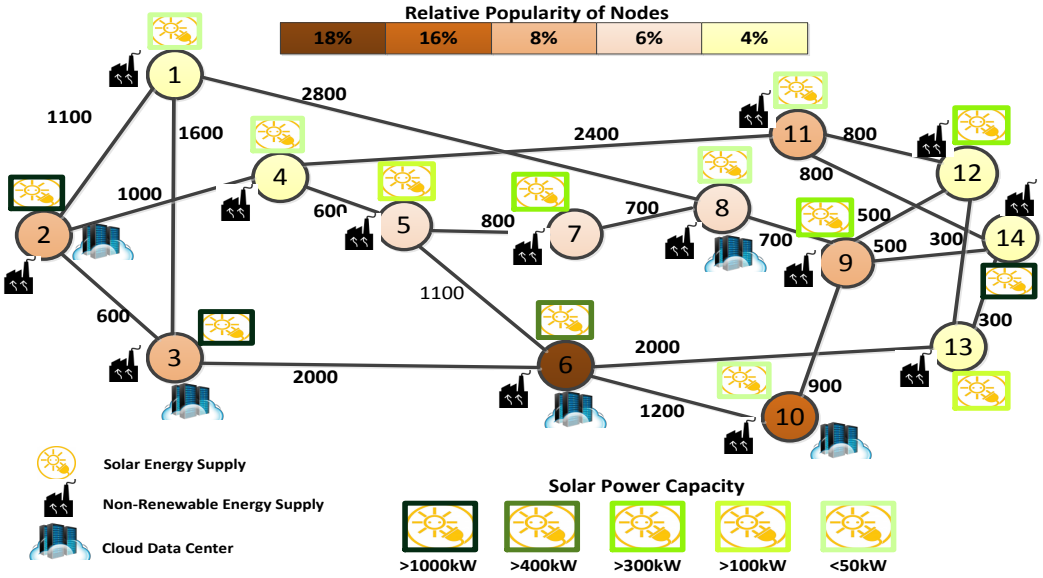

Figure 9-2: NSFNET Network with Popularity and Solar Capacity Information

The performance of the GVNE MILP model is examined using the same NSFNET reference network topology that was used in the previous chapters. In this case as shown in Fig. 9-2, the nodes are also equipped with solar energy sources with varying maximum installed capacities. VNRs come from enterprise clients from all the nodes in the network. The enterprise client's location is fixed but the requested virtual nodes could be

embedded in any data centre in the cloud data centres. The concentration of VNRs at any substrate node is based on the population of the states where the node is located.

Table 9-1: Solar Power Availability in Different Cities. SR: Sunrise, SS: Sunset Recorded in Individual Cities in June [39], [135]

City ID / Time	1	2	3	4	5	6	7	8	9	10	11	12	13	14
	SR: 05:14	SR: 05:43	SR: 05:16	SR: 05:54	SR: 05:27	SR: 05:55	SR: 05:51	SR: 05:39	SR: 05:17	SR: 05:53	SR: 05:18	SR: 05:41	SR: 06:27	SR: 05:30
	SS: 21:02	SS: 20:04	SS: 19:34	SS: 20:40	SS: 20:41	SS: 20:10	SS: 20:53	SS: 20:47	SS: 20:24	SS: 19:56	SS: 20:30	SS: 20:29	SS: 20:30	SS: 20:59
	Seattle	Palo Alto	San Diego	Salt Lake	Boulder	Houston	Lincoln	Champaign	Pittsburg	Atlanta	Ann Arbor	Ithaca	College Pk	Princeton
00:00	0.0kW	0.0kW	0.0kW	0.0kW	0.0kW	0.0kW	0.0kW	0.0kW	0.0kW	0.0kW	0.0kW	0.0kW	0.0kW	0.0kW
02:00	0.0kW	0.0kW	0.0kW	0.0kW	0.0kW	0.0kW	0.0kW	0.0kW	0.0kW	0.0kW	0.0kW	0.0kW	0.0kW	0.0kW
04:00	0.0kW	0.0kW	0.0kW	0.0kW	0.0kW	0.0kW	0.0kW	0.0kW	0.0kW	0.0kW	0.0kW	0.0kW	0.0kW	0.0kW
06:00	0.0kW	0.0kW	0.0kW	0.0kW	0.0kW	0.0kW	0.0kW	0.0kW	0.0kW	0.0kW	1.5kW	14.3kW	0.0kW	75.3kW
08:00	0.0kW	0.0kW	0.0kW	0.0kW	27.0kW	10.9kW	8.2kW	5.1kW	125.3kW	1.4kW	4.6kW	171.5kW	54.8kW	903.6kW
10:00	0.3kW	412.6kW	412.6kW	8.1kW	81.1kW	130.3kW	98.4kW	12.3kW	271.4kW	4.1kW	9.9kW	371.6kW	158.3kW	1957.8kW
12:00	2.3kW	2063.2kW	2063.2kW	15.1kW	175.7kW	282.4kW	213.1kW	36.9kW	375.8kW	12.2kW	15.2kW	571.6kW	243.5kW	3012.0kW
14:00	4.1kW	3713.8kW	3713.8kW	20.9kW	270.2kW	434.4kW	327.8kW	36.9kW	375.8kW	12.2kW	9.9kW	371.6kW	158.3kW	1957.8kW
16:00	4.1kW	3713.8kW	3713.8kW	20.9kW	243.2kW	391.0kW	295.1kW	26.7kW	271.4kW	8.8kW	5.7kW	214.4kW	91.3kW	1129.5kW
18:00	2.9kW	2682.2kW	2682.2kW	20.9kW	175.7kW	282.4kW	213.1kW	16.4kW	167.0kW	5.4kW	3.8kW	142.9kW	60.9kW	753.0kW
20:00	1.8kW	1650.6kW	1650.6kW	9.3kW	108.1kW	173.8kW	131.1kW	6.2kW	62.6kW	1.4kW	1.5kW	57.2kW	24.4kW	301.2kW
22:00	0.6kW	619.0kW	103.2kW	4.6kW	27.0kW	10.9kW	49.2kW	0.0kW	0.0kW	0.0kW	0.0kW	0.0kW	0.0kW	0.0kW

The same scenario regarding virtual network requests capacities and distribution that was used in chapter eight has also been used in this chapter. The consolidation factors are set to $\alpha = \beta = 5$, i.e. all the virtual nodes of a VNR can be co-located. The current and future criterion for designing cloud infrastructure is to distribute the content among a number of data centres to minimise the delay experienced by the users and to avoid the scenario of having a single hot node in the network. Data centre locations have been fixed at five locations at nodes (2, 3, 6, 8 and 10).

Solar energy has been considered as the source of renewable energy at each node. The solar power availability profile for nodes is shown in Table 9-1. The solar power data is obtained from the Open PV Project [136] of the National Renewable Energy Laboratory of the United States of America. It provides detailed data of the total installed photovoltaic capacity of each individual state in the United States. The data from the Open PV Project shows the total installed solar capacity for each state which has contributions from residential areas, private industries and utilities. The data obtained from the U.S. Energy Information Administration [135] shows that approximately 20% of the solar installed capacity is from utilities. We have assumed that the cloud InP has access to 1% of this solar power as well as non-renewable power (Fig. 9-2) through the utility at each node. Since the output power of solar energy sources varies at different times of the day, we use the sunrise and sunset data used by the authors in [39] to work out the available solar power at any given

two hour intervals as a fraction of the maximum installed capacity. Table 9-2 shows the values of the parameters that have been used in the model.

Table 9-2: Parameter Values For the GVNE Model

Distance between two neighbouring EDFAs (S)	80 (km)
Distance between two neighbouring Regenerators (RG)	2000 km)
Number of wavelengths in a fibre (W)	32
Wavelength Rate (B)	40Gbps
Power consumption of a transponder (PT)	167 (W)
Power consumption of a regenerator (RG)	334 (W)
Power consumption of a 40Gb/s router port (PR)	850(W)
Power consumption of an EDFA (PE)	55 (W)
Power consumption per CPU core (γ)	11.25(W)

AMPL software with the CPLEX 12.5 solver is used as the platform for solving the MILP models on a PC with an Intel® Xeon™ CPU, running at 3.5 GHz, with 64 GB of RAM. The running times for obtaining optimal solutions for the model averages 15 minutes for each time point in the NSFNET topology.

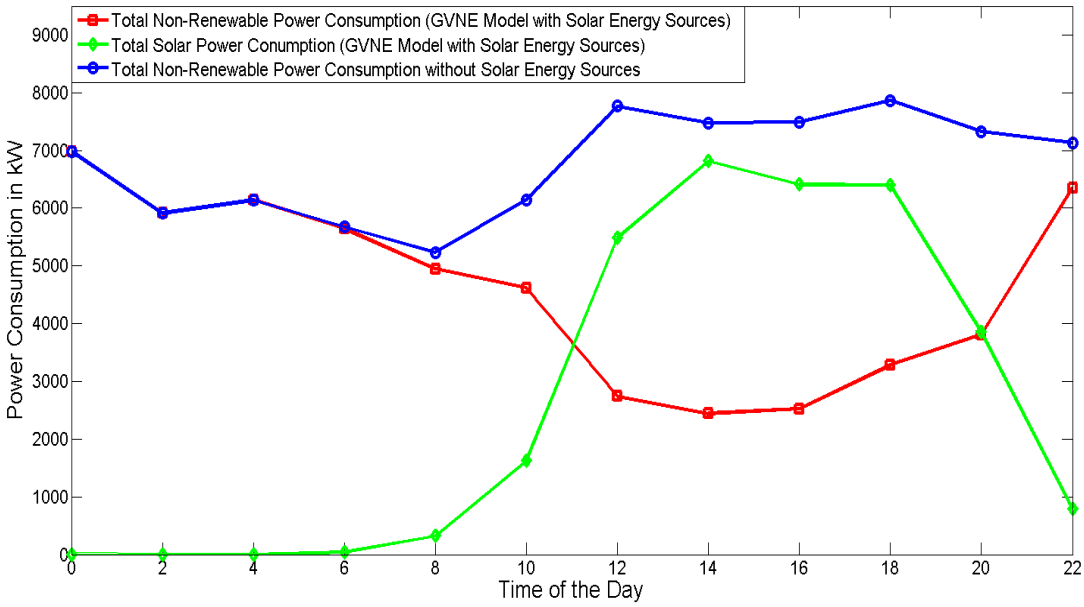

Figure 9-3: Total Solar and Non-Renewable Power Consumption

Fig. 9-3 shows the overall non-renewable power consumption and solar power consumption of the GVNE model at different times of the day. The non-renewable power consumption follows that of the traffic demand profile until about 06:00 hours when the solar energy starts to take up some of the load in the network. It can be observed that despite having an increase in the CPU cores workloads and bandwidth demand between 06:00 hours and 12:00 hours, the non-renewable power consumption continues to decrease as expected due to the increasing availability of solar power. In order to adequately serve the further increase in load from the VNRs, there is a subtle increase in non-renewable power consumption from 14:00 hours until 20:00 hours and thereafter; there is a sharp increase in non-renewable power consumption due to the dwindling solar energy supply during this period. The non-renewable power consumption curve without access to

solar energy follows the traffic profile throughout the day. The overall reduction in CO_2 emissions in this scenario achieved by GVNE is 32%.

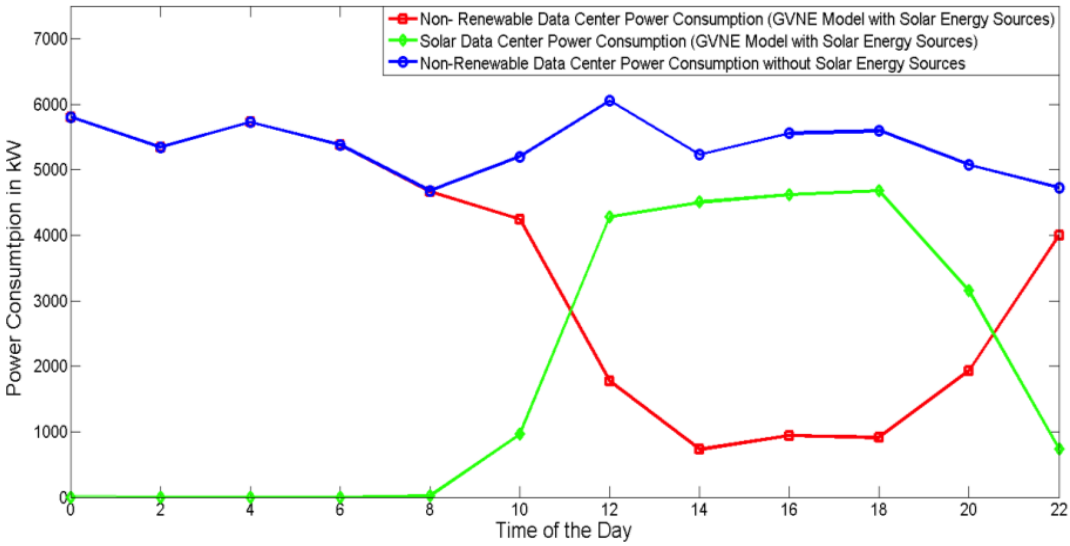

Fig. 9-4(a)

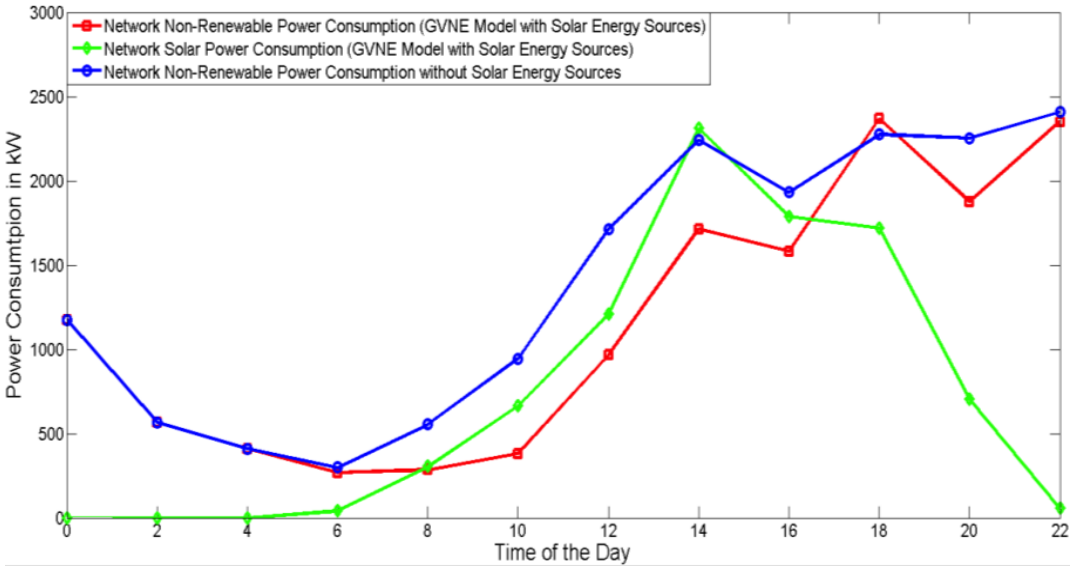

Fig. 9-4(b)

Figure 9-4: Non-Renewable and Solar Power Consumption in (a) Data Centres, (b) Networking Components

In Fig. 9-4 we examine the individual non-renewable and solar power consumption contributions for both data centres and the network. Fig. 9-4(a) shows that the power consumption in data centres has the most significant influence on how the embedding of VNRs is done in all the data centres. The model maximises the savings in the amount of consumed non-renewable power by consolidating the embeddings in data centres with abundant solar power even at the expense of using more non-renewable power in the network as can be seen in Fig. 9-4(b). Whereas the non-renewable power consumption in data centres drastically falls between 06:00 hours and 14:00 hours, the non-renewable power consumption in the network shows a steady increase. The CO_2 emissions of the data centre and network are reduced by an average of 35% and 15%, respectively compared to the scenario with no access to renewable energy. This picture is made much clearer by looking at how the embedded CPU cores for various VNRs are distributed across the five data centres in the network.

Fig. 9-5(a) show the embedding of virtual cores in the different data centres under the scenario with no access to renewable energy. The most popular destination for embedded virtual machine workloads is in the data centre at node 6 (Houston) due to its relatively high nodal degree and the high concentration of VNRs located at the node itself and those connected to it. The data centre in node 3 (San Diego) does not get a high utilization at any time of the day. The data centres in nodes 2 (Palo Alto) and 3 (San Diego), do not surpass the data centre in node 6 in utilization at any time

during of the day. This picture however changes when solar energy is introduced in the network.

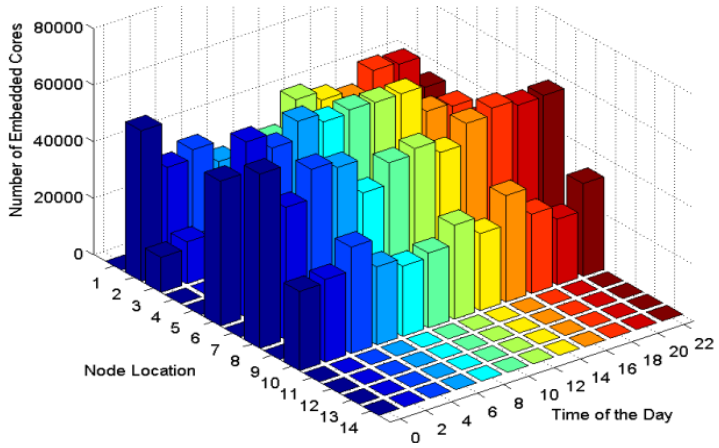

Fig. 9-5(a)

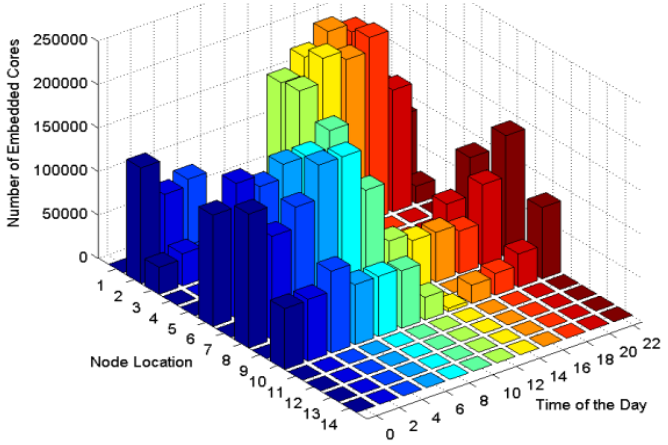

Fig. 9-5(b)

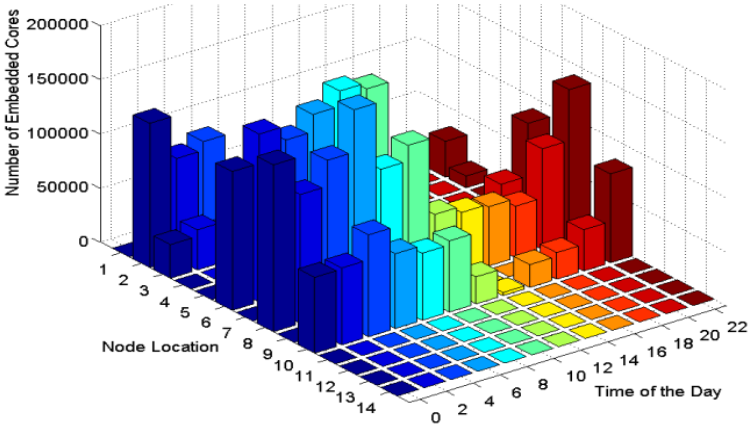

Fig. 9-5(c)

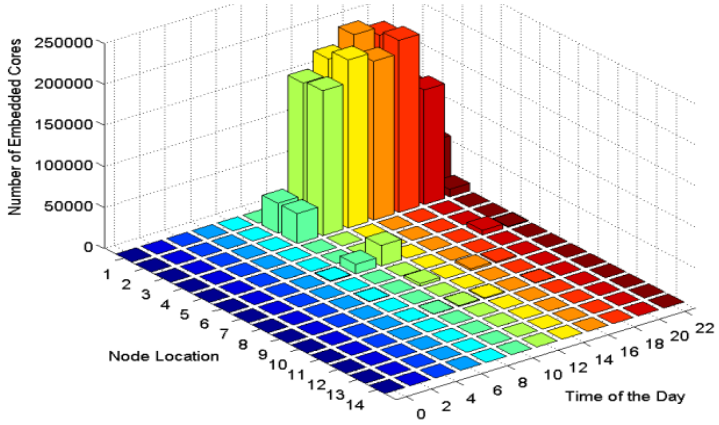

Fig. 9-5(d)

Figure 9-5: Embedded Cores Distribution in Data Centres, (a) Supplied Only by Non-Renewable Energy Sources (Reference Case), (b)GVNE Supplied by Both Non-Renewable and Solar Energy Sources, (c) Non-Renewable Energy Powered Cores Under GVNE (d) Solar Energy Powered Cores under GVNE

Fig. 9-5(b) shows that the GVNE model embeds a high proportion of virtual machines in nodes 2 and 3 which hosted only a minimal amount when solar energy sources are not considered. A large proportion of virtual cores which would normally be embedded in data centres located at nodes 6, 8 and 10 at periods between 12:00 hours and 20:00 hours are taken up by the data centres in nodes 2 and 3 which have abundant solar energy at these periods. Fig. 9-5(c) and Fig. 9-5(d) show the distribution of embedded cores in the five data centres powered by non-renewable energy and solar energy, respectively. The little or no use of solar energy at data centres in nodes 8 and 10 (Fig. 9-5(d) is due to the fact that these nodes have very minimal solar energy. It is therefore optimally used for routing traffic demands to data centres in nodes 2 and 3 where more savings can be accrued by tapping into the abundant renewable energy sources. These results raise a question on whether virtual machines from clients across the network should be migrated to data centres built in locations with abundant renewable energy or the renewable energy should be transmitted to central data centres built in popular locations taking into account transmission losses as well as performance trade-offs in delay sensitive applications.

9.4 GVNE with Data Centre Selection and Electricity Cost Optimisation

In the previous section, the GVNE model operates in a network that has fixed data centre locations at nodes 2, 3, 6, 8 and 10. The fixed locations of data centres offers very little flexibility in the movement of virtual machines belonging to different clients at different time of the day. If the model is however developed in such a way that it can select the best five optimal data centre locations at different times of the day according to the availability of solar energy, more savings in CO_2 emissions are possible. In this section, evaluation scenarios where at each two hour time interval, a set of data centres could be selected for embedding virtual network requests belonging to different clients are investigated. The location of each client is still fixed, as was the case in the previous section, but the model is at liberty to select one or more data centres at different times of the day where the virtual cores belonging to a client could be embedded.

The electricity cost that is borne by the infrastructure provider is very often not included in most energy efficient virtual network embedding designs. However, infrastructure providers are very much concerned about the cost of electricity in their networks as it significantly contributes to the overall operational expenditure (OPEX). It is therefore not realistic to only consider CO_2 footprint reduction as the main objective in the design but rather to consider a holistic approach that provides opportunities for OPEX reduction for infrastructure providers. This section therefore goes further to

provide a design that not only considers overall CO_2 reductions but also improves the OPEX that is accrued from electricity consumption in the cloud infrastructure network.

9.4.1 MILP Model for GVNE with Data Centre Selection and Electricity Cost Optimisation

The model in Section 9.3 is extended to investigate data centre selection optimisation and electricity cost optimisation. We first define the following new parameters and variables:

Parameters

EP_m The price of electricity in US$ per kWh at node m

$\emptyset$ Non-renewable energy conversion factor given as:
$\emptyset = (\text{Tonnes of } CO_2 \text{ per kWh})\text{x}(\text{Carbon Credit Price in US\$})$

Variables

$DLOC_b$ $DLOC_b = 1$ if substrate node b is selected as a data centre, otherwise $\mathrm{DP_b} = 0$

$EcNet_m$ Electricity cost in US$ at node m due to power consumed in networking components

$EcDC_m$ Electricity cost in US$ at node m due to power consumed in the data centre

The following new objectives are defined.

Objective 1:

Minimise the overall non-renewable energy power consumption given as:

$$\sum_{m\in N}\sum_{n\in N_m}\lambda_{m,n}^{(NR)}\cdot PR+\sum_{m\in N}\sum_{n\in N_m}\lambda_{m,n}^{(NR)}\cdot PT+\sum_{m\in N}\sum_{n\in N_m}EG\cdot\lambda_{m,n}\cdot RG_{m,n}$$
$$+\sum_{m\in N}\sum_{n\in N_m}PE\cdot EA_{m,n}\cdot F_{m,n}+\sum_{b\in N}C_b^{(NR)}\cdot\gamma$$

Objective 2:

Minimise Overall Electricity Cost given as:

$$\sum_{m\in N}EcNet_m+EcDC_m$$

Objective 3:

Minimise Overall Electricity Cost and Non-Renewable Energy cost gives as:

$$\sum_{m\in N}EcNet_m+EcDC_m$$
$$+\emptyset\left(\sum_{m\in N}\sum_{n\in N_m}\lambda_{m,n}^{(NR)}\cdot PR+\sum_{m\in N}\sum_{n\in N_m}\lambda_{m,n}^{(NR)}\cdot PT\right.$$
$$+\sum_{m\in N}\sum_{n\in N_m}EG\cdot\lambda_{m,n}\cdot RG_{m,n}+\sum_{m\in N}\sum_{n\in N_m}PE\cdot EA_{m,n}\cdot F_{m,n}$$
$$\left.+\sum_{b\in N}C_b^{(NR)}\cdot\gamma\right)$$

Objective 1 is the same objective as in Section 9.3 except in this case the model takes into account data centre selection optimisation in minimisation of non-renewable energy. Objective 2 simply focusses on the minimisation of the overall OPEX accrued due to electricity consumption in the network. Objective 3 combines both the electricity cost and the non-renewable power consumption in the optimisation. In addition to constraints (9.2)-(9.4) given in Section 9.4, the following new constraints are introduced:

$$DLOC_b \cdot \delta_b^{v,s} = \Delta_b^{v,s} \quad \forall v \in V, \forall b \in N, \forall s \in R \tag{9.5}$$

$$\sum_b DLOC_b = NDC \quad \forall b \in N \tag{9.6}$$

$$EcNet_m = \sum_{n \in N_m} \lambda_{m,n} \cdot PR \cdot EP_m + \sum_{n \in N_m} \lambda_{m,n} \cdot PT \cdot EP_m \quad \forall m \in N \tag{9.7}$$

$$EcDC_b = C_b \cdot \gamma \cdot EP_b \quad \forall b \in N \tag{9.8}$$

As was the case in Chapter 5, Constraints (9.5) and (9.6) define the location and number of data centres in the network respectively. Constraint (9.6) ensures that the number of selected data centres is always equal to the number of required data centres in the network. Constraint (9.7) calculates the electricity cost per node in the network due to the power consumed in router ports and transponders. Constraint (9.8) calculates the electricity cost per node due to the power consumed in data centres.

9.4.2 Electricity Cost Green VNE MILP Model Results and Analysis

The NSFNET network is also considered as the substrate network to evaluate the model. The network traffic and distribution of virtual network requests is kept the same as in Section 9.3 to ensure a fair and accurate comparison in performance. The commercial price of electricity per kWh is obtained from the United States Energy Information Administration (EIA) [137]. The price quoted for each node is the electricity price per state and not per city because that is the information that is made available by the EIA because electricity price discrimination in the US is mainly by state and not by city. The resulting information is as shown in Table 9-3.

Table 9-3: Commercial Electricity Prices in US Cities

Node ID	City	Electricity Price in US Cents per kWh
1	Seattle	8.47
2	Palo Alto	14.81
3	San Diego	14.81
4	Salt Lake City	8.2
5	Boulder	9.78
6	Houston	7.64
7	Lincoln	8.44
8	Champaign	8.83
9	Pittsburgh	9.53
10	Atlanta	9.05
11	Ann Arbor	10.55
12	Ithaca	15.33
13	College Park	10.63
14	Princeton	13.01

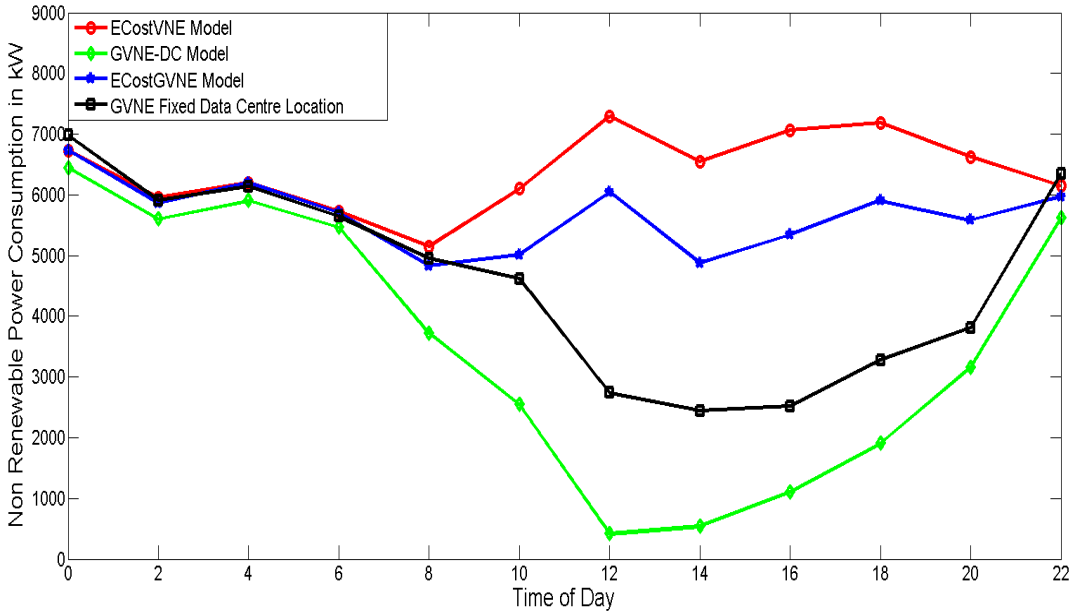

Figure 9-6: Non-Renewable Power Consumption Performance for Various Approaches

Fig. 9-6 shows the non-renewable power utilization for the electricity cost minimised model with data centre selection optimisation (ECostVNE), the green virtual network embedding model with data centre selection optimisation (GVNE-DC), the ECostGVNE model, which integrates the objectives of both ECostVNE and GVNE-DC and finally the GVNE model with fixed data centre locations as presented in Section 9.3. The GVNE-DC model as expected uses the least amount of non-renewable energy over the 24 hour time period. Its enhanced performance comes from the added ability to choose any five suitable locations out of fourteen to embed virtual cores so as to minimise the overall use of non-renewable power. Locations that have abundant solar energy and are highly populated become the most favoured locations for embedding virtual cores. The GVNE-DC model has

non-renewable energy savings of 23% and 48% when compared to the GVNE model with fixed data centre locations and the VNE solution without renewable energy sources respectively.

Infrastructure providers are very much concerned about energy costs in their networks. The ECostVNE model is developed so as to minimise the overall cost due to electricity utilization in the network. The model in this case picks the best locations to embed virtual cores so as to minimise the overall electricity cost. Cities that are located in states with the lowest energy cost and are highly populous will be the ideal candidates for embedding virtual cores. As a result, the performance in terms of non-renewable power consumption is compromised. Infrastructure providers in this case will have to decide which one of the two (CO_2 emissions or electricity costs) is important. Since both CO_2 emissions and electricity costs are of concern to infrastructure providers, the ECostGVNE model that combines both objectives during the optimisation process is developed. The optimisation seeks an optimal solution that satisfies both requirements. As shown in Fig. 9.6, in terms of non-renewable power consumption, the ECostGVNE model does not perform as well as the GVNE-DC model but it does perform better than the ECostVNE model.

Fig. 9-7 shows the electricity cost incurred by the infrastructure provider for each one of the approaches. The interesting part of the results is that the ECostGVNE model performs just as good as the ECostVNE model despite having used much less non-renewable energy.

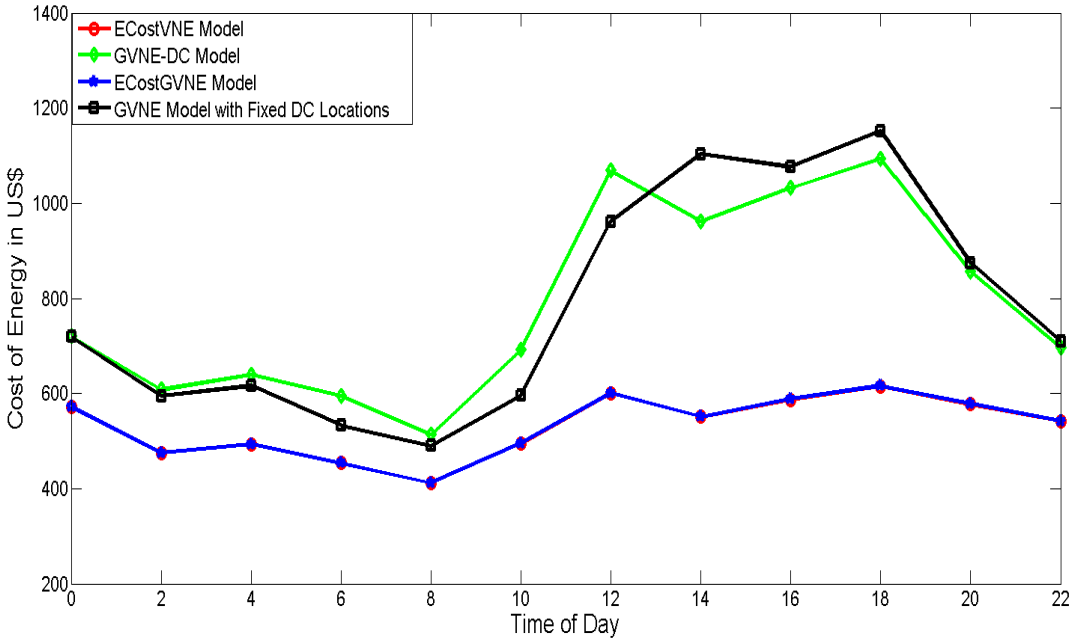

Figure 9-7: Energy Cost Performance for Various Approaches

During the data centre selection process, the ECostGVNE model will have scenarios where a candidate node for a data centre will have a low electricity price and abundant solar energy at certain times of the day. In this case, the decision to select such a node as a data centre will be complementary for the two model objectives. However, there will also be situations where the node will have a high solar power availability and a very high energy price or a low energy price and very high solar availability. In these cases, the objectives of the model will act against each other and one among the two with the highest weighting will get the decision. In order to put this in context and make a fair and reasonable comparison, the non-renewable power consumption also has to be expressed in monetary terms.

The authors in [138] define a carbon credit as the amount of money paid to someone to absorb or avoid to release a metric tonne of CO_2 emissions into the atmosphere. The system of carbon credits was introduced to offer business incentives to slow down the overall growth in greenhouse gas (GHG) emissions to avert global warming. This system provides a platform at which the saved non-renewable energy could be converted into equivalent carbon credits and then monetarized. Carbonfund.org [139] estimate that on average, from the emission factors of the United States Environmental Agency based on the 2009 and 2012 data, electricity sources emit 0.0005925 tonnes of CO_2 per kWh. From the results, the ECostGVNE model saves US$3095 per day in electricity costs when compared to the GVNE-DC model. However, the GVNE-DC model saves a total of 25644kWh of non-renewable energy per day compared to the ECostGVNE model. If the UK's carbon floor price of US$26 per tonne of CO_2 [140] is used, which is considerably higher than what the open market would sell a carbon credit for in the US, the saved non-renewable energy is equivalent to 25644x0.0005925x26 = US$395. This amount is almost 10 times smaller than the US$3095 that the Infrastructure provider would save from the ECostGVNE model. At this carbon credit price therefore, the electricity cost objective in the ECostGVNE model will always carry more weight than the non-renewable energy objective. If however, the price of the carbon credits increased significantly, the weighting of the overall objective in the ECostGVNE model will shift towards minimisation of non-renewable energy. In implementation therefore, the developed algorithm that

combines both objectives of energy cost and non-renewable energy minimisation should be able to take the carbon credit price as an input in order to achieve the desired results. The ECostGVNE model has an overall CO_2 saving of 16% and electricity cost saving of 22% when compared to a VNE solution that does not incorporate renewable energy sources in the design.

Fig. 9.8 shows the frequency at which each node is selected as a data centre location by the various approaches at different loads during the day. The fixed data centre locations have been included to provide perspective. From the results, it is clear that some locations have not been selected at all by all the models while at the same time, there are locations that have been frequently selected by all the models. In a design scenario where only five locations are required, from the results, the popular locations for both the ECostVNE and ECostGVNE models are nodes 3, 6, 8, 9 and 12. These locations would offer the best electricity cost and renewable power utilization for the infrastructure provider. If only renewable energy is considered, the popular data centre locations would be at nodes 3, 6, 8, 12 and 14.

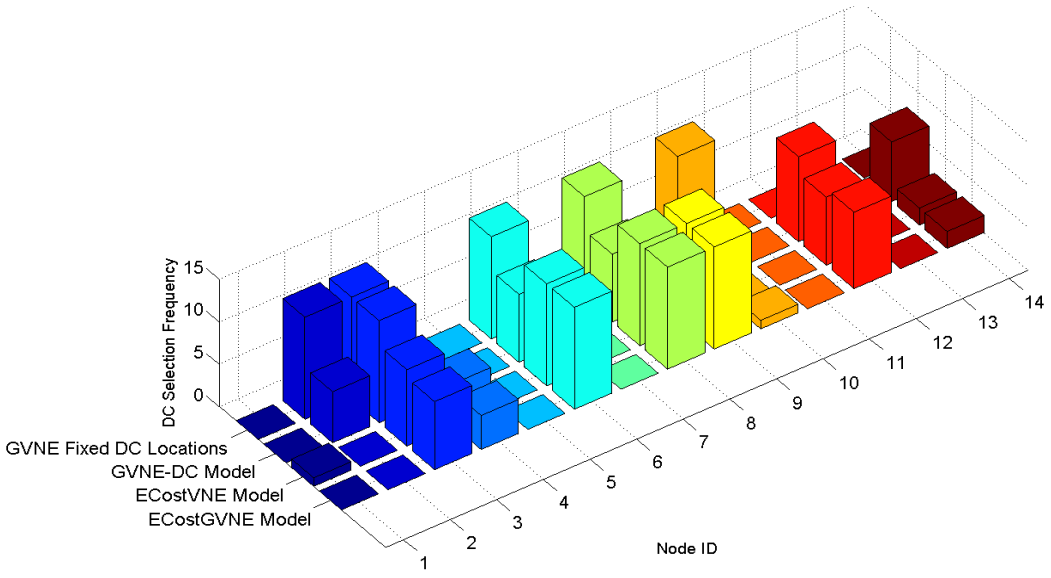

Figure 9-8: Data Centre Selection Frequency for Various Approaches

9.5 GVNE-DC and ECostGVNE Models Scalability and Performance Trade-offs

As described in the previous chapters, virtual network embedding problems with satisfy both node and link constraints are usually NP-Hard. While it is not practical to implement the developed models in real time, it is however expected that the optimal solutions obtained from the models offer a benchmark for determining the performance of developed heuristics and algorithms. Therefore, the versatility of the developed models have been tested by implementing them in different networks, with different traffic profiles to check their scalability and consistency in results. The computational complexity of the models has also been evaluated in different scenarios.

The AT&T network topology in Fig. 7.3 of Chapter 7 and the USNET topology shown in Fig. 9-9 have been used to test the scalability, versatility and computational complexity of the MILP models. The AT&T network has 25 nodes and 54 bidirectional links while the USNET topology has 24 nodes and 43 bidirectional links. The generation of the virtual network requests at each node is again proportional to the population of each city for both topologies.

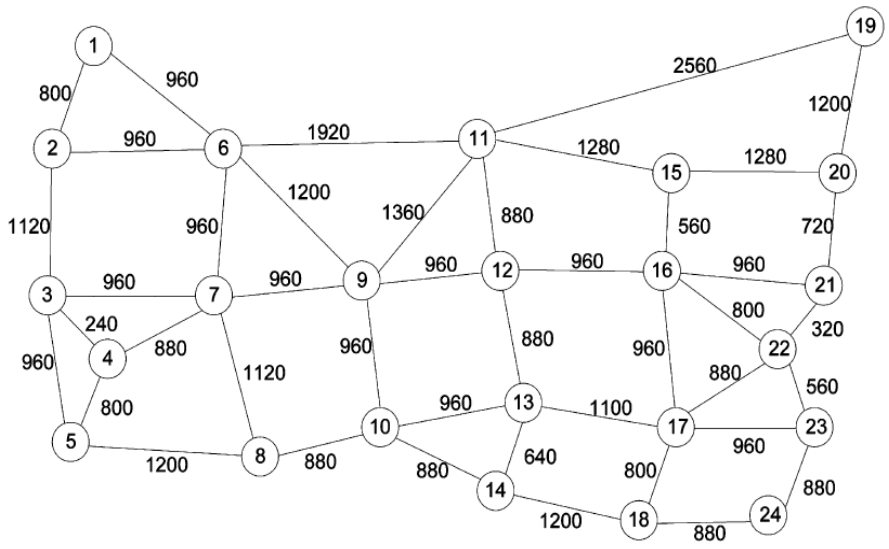

Figure 9-9: USNET Network

A total of 50 VNRs are generated at each two hour time interval. The solar power capacities and electricity price for each node were computed in the same way as was done for the NSFNET network.

9.5.1 Scalability of the Models

The model results from the use of larger topologies consistently produce desired results. Having increased the number of nodes and links as well as the traffic and node demands of the VNRs, the models' performance in terms of the GHG emissions savings and the electricity cost are quite consistent. Table 9-4 shows the performance in terms of equivalent GHG emissions savings and electricity cost savings of the GVNE-DC model and the ECostGVNE models compared to a VNE design that does not use renewable energy sources for all the three network topologies. All the topologies consistently report savings in electricity cost and GHG emissions for the ECostGVNE model. This shows that the models can scale and produce consistent results. As expected, the GVNE-DC model reports higher electricity costs for all the topologies. This is the reason why attention in designs should not only focus on reducing GHG emissions but should also focus on reducing the overall electricity cost.

Table 9-4: Savings in Different Topologies

	GVNE-DC Model		**ECostGVNE**	
Topology	*GHG Emissions Savings*	*Electricity Cost Savings*	*GHG Emissions Savings*	*Electricity Cost Savings*
NSFNET	48%	-15%	16%	22%
USNET	48%	-28%	10%	10.40%
AT&T	36%	-17%	12%	20%

9.5.2 Computational Complexity

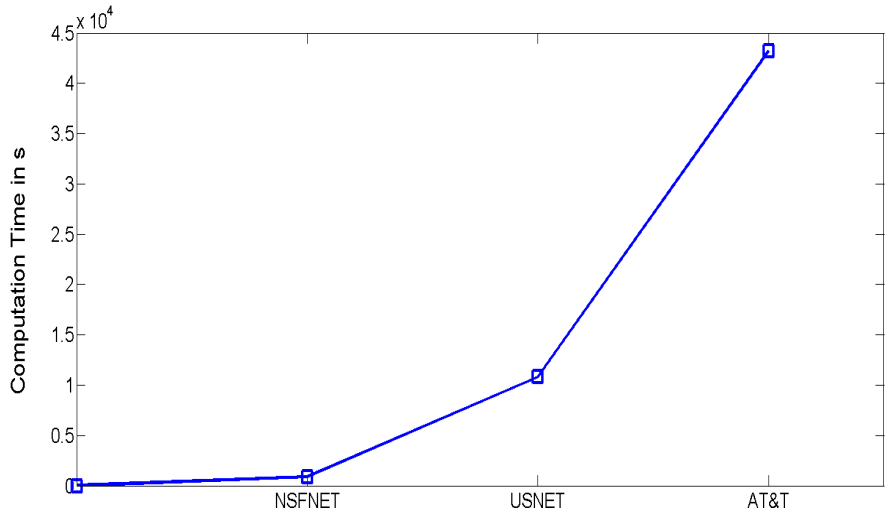

Figure 9-10: Computation Times for ECostGVNE Model in Various Topologies

The computation time for both the GVNE-DC and ECostGVNE models increases almost exponentially as the number of nodes and links in the substrate network increases. Fig. 9-10 shows the computation time for running the ECostGVNE model considering the NSFNET, USNET and AT&T networks. These times confirm that these models cannot be implemented in real time applications. They should therefore be used as benchmarks for developing heuristic algorithms that can perform nearly as good but also in real time.

9.5.3 Performance Trade-Offs Considerations

The goals of optimising the use of non-renewable energy and electricity cost utilization for a cloud infrastructure provider would definitely have some performance trade-offs. Enterprise clients requesting for infrastructure

services from the InP would use the provisioned virtual networks for various applications. In the case of delay sensitive applications, such as live video streaming, embedding a virtual node running such an application in a distant data centre that has abundant renewable energy or a very low electricity price, would cause serious quality of service problems. It is therefore expected that each enterprise client would send a request to the InP with specific delay requirements. This would therefore entail that the InP would consider the maximum tolerable delay during the provisioning stage. Investigations dealing with delay requirements in virtual network provisioning were adequately covered in Chapter five and the same techniques and constraints discussed would apply also in this case. It should also be mentioned that the models are not designed in such a way that the solution to select a data centre to embed a virtual node is simply based on solar energy availability and the price of electricity. It is a complex optimisation problem that takes into account many factors such as the concentration of requests from a particular location as well as the relative concentration of requests of the neighbouring nodes and the overall energy consumption due to bandwidth provisioning. It is therefore expected that, in a network with a high concentration of links like the USNET and the AT&T network, the average hop count from a selected data centre to the location of an enterprise client will most of the time be minimal to cause significant propagation and packet processing delay and subsequently quality of service problems.

9.6 Summary

This chapter has investigated the effective use of renewable energy sources to reduce the GHG emissions and electricity costs due to cloud service provisioning of virtual network requests by infrastructure providers. A Green Virtual Network Embedding (GVNE) framework for minimizing the use of non-renewable energy through intelligent provisioning of bandwidth and cloud data centre resources has been developed. The results of the GVNE MILP model show that it is better to instantiate virtual nodes in cloud data centres that have access to abundant renewable energy even at the expense of traversing multiple links across the network. An overall reduction in CO_2 emissions of up to 48% has been achieved. In order to address the high OPEX costs accrued from electricity use which might result from focusing on GHG emissions reduction, another MILP model, ECostGVNE which addresses both electricity cost and GHG emissions reduction in the optimisation has been developed. The results have shown that significant electricity cost savings of up to 22% could be achieved while at the same time reducing the GHG emissions by 16%. The MILP model results are a benchmark for heuristics and algorithms that would be developed and implemented in the control plane of an SDN based core network architecture with clouds. Further, the scalability and computation time complexity of the developed models has also been investigated and it has been shown that the models are scalable but the computation time increases almost exponentially as the number of substrate nodes and links

increases. As far as performance trade-offs are concerned, introduction of delay requirements in virtual network requests would completely guarantee very high quality of service.

Chapter 10: Summary of Contributions and Future Work

This chapter is a summary of the main contributions that have been presented in this thesis. It also suggests the possible future research directions in the area of energy efficiency in core networks with clouds leveraging the use of network virtualisation.

10.1 Summary of Contributions

This thesis addresses the problem overprovisioning and hence high energy utilization in core networks with clouds. Geographically distributed data centres required to serve the ever increasing number of users demanding cloud based applications require flexible traffic management, energy efficiency and bandwidth on demand capabilities.

In order to address these challenges, the first contribution in this thesis was to develop a new core network architecture with clouds that exploits the benefits of network virtualisation to bring about energy efficiency.

Energy efficient virtual network embedding in IP over WDM networks with clouds was proposed in Chapter 4 and a MILP optimisation model was developed with the objective of minimizing power consumption in the core network and the data centres. It is the first approach to energy efficient virtual network embedding that incorporates both the IP and Optical layers during the link embedding stage. Resource consolidation in the network and the data centres brought about by intelligent virtual resource provisioning ensured minimal use of idle power in data centre servers as well as minimal link activation. For real time implementation, the Real Time Energy Optimised Virtual Network Embedding (REOViNE) heuristic algorithm has been developed whose results are nearly as good as the MILP model. Maximum energy savings of 60% have been achieved by the developed MILP model when compared to an approach that purely focusses on bandwidth cost reduction in the network. The investigation was taken further to show the energy efficiency of virtual network embedding considering an energy efficient data centre power profile. The results show that the optimal virtual network embedding approach with the minimum power consumption is the one that only minimises the use of network bandwidth. This however is only valid when it is assumed that the network is not reconfigured when embedding new requests.

Energy efficient virtual network embedding in core networks with clouds has also been investigates in Chapter 5 with location and delay considerations. A MILP model was developed to investigate the impact on

power consumption performance of introducing virtual network requests' location and delay constraints. Under delay and location constraints, the study also covered the power savings achieved by removing geographical redundancy constraints when embedding protection and load balancing virtual nodes and it was observed that the power savings obtained could guide service providers in determining cost reductions offered to enterprise customers not requiring full geographical redundancy. The investigation also showed how virtual network embedding could impact the optimal locations of data centres for minimal network power consumption in cloud networks. The results have shown that the selection of a location to host a data centre is governed by two factors: the average hop count to other nodes and the client population (which determines how many requests originate from that node) of the candidate node and its neighbours.

In Chapter 6, a new network architecture for virtual network embedding in core networks with clouds that uses optical orthogonal frequency division multiplexing (O-OFDM) as the underlying technology has been developed. The new architecture has been investigated for both spectral and energy efficiency benefits. The results have shown that virtual network embedding in IP over O-OFDM based networks has superior performance both in terms of spectrum and power utilization compared to conventional IP over WDM networks. Power minimised and spectrum minimised virtual network embedding in IP over O-OFDM networks has average power savings of 63% and 17%, respectively compared to conventional IP over WDM. In terms of

spectral efficiency, the spectrum minimised O-OFDM network is 120% more efficient in the utilization of the optical spectrum compared to the power minimised O-OFDM network. The difference stems from the fact that the power minimised model sacrifices the optical spectrum in order to achieve higher energy savings through the use of lower modulation formats that are more power efficient. Despite this scenario, the power minimised O-OFDM based network is still 16% more efficient in the use of the optical spectrum compared to conventional WDM based networks.

GreenTouch is a consortium of leading Information and Communications Technology (ICT) research experts who include; academic, industry and non-governmental Organisations playing essential roles in technology breakthroughs in energy efficiency. The consortium was formed in 2010 to pursue the ambitious goal of bridging the gap between traffic growth and network energy efficiency. Chapter 7 presents the original contributions that have been made to the GreenTouch GreenMeter research study. It presents the detailed equations and assumptions made in the new estimates for router port power consumption at various line rates. The adopted method took into account the individual power consumption contributions of the various cards on the Cisco CRS-1 and CRS-X router chassis. Considering the modular nature of the router, it was realistically estimated that the power consumption of a router port is therefore a combination the power consumption of the individual modules that make up the port and the idle power consumption due to the router power supply, fan module

and the switching fabric. The resulting estimates in port power consumption have been adopted by GreenTouch and used in the GreenMeter study for energy efficiency improvements in core networks. Further, results of an integrated MILP model using GreenTouch initiatives as well as the virtualisation techniques developed in this thesis have been presented.

In Chapter 8 an energy efficient virtual network embedding framework for maximizing profit in cloud service provisioning of Infrastructure as a Service (IaaS) in non-bypass IP over WDM core networks was introduced. A mixed integer linear programming (MILP) model to study the impact of maximizing profit on the power consumption and acceptance of virtual network requests was developed. The results of the investigation show that higher acceptance rates do not necessarily lead to higher profit due to the high cost associated with accepting some of the requests. In order to obtain optimal power consumption in the network, another model was developed with the objective of minimizing power consumption for the same optimal profit and the results indicate that more power consumption savings are achievable for the same profit. Using the insights from the models, a profit optimised and energy minimised (POEM) heuristic was developed, with nearly the same power consumption, profit and virtual network request acceptance performance as the MILP models.

Chapter 9 is an investigation into the effective use of renewable energy in virtual resource allocation in IP over WDM core networks with clouds as a

means of reducing the carbon footprint. The investigation also addresses the concern that completely focusing on reduction of non-renewable power consumption in cloud infrastructure networks has the potential to significantly increase the overall operational expenditure (OPEX) associated with electricity consumption considering the geographical price discrimination of electricity. A Green Virtual Network Embedding (GVNE) framework for minimizing the use of non-renewable energy through intelligent provisioning of bandwidth and cloud data centre resources has been developed. The problem is modelled as a mixed integer linear program (MILP) and the results show that greenhouse gas (GHG) emissions could be reduced by up to 48% and that it is better to provision virtual machines in cloud data centres that have access to abundant renewable energy even at the expense of traversing multiple links across the network. In addressing OPEX associated with electricity costs, a framework that addresses both concerns of reducing electricity costs and GHG emissions has been developed and the results of the model show that while maintaining the electricity cost at the lowest optimal value, GHG emissions could be reduced by up to 16%. Through monetarization of the GHG emissions resulting from the use of non-renewable energy due to the provisioned virtual network requests, the model results show that it would be prudent to prioritize energy costs instead of GHG emissions at the present market price of carbon credits.

10.2 Future Directions

This thesis has investigated various virtual network embedding approaches that could be used to improve energy efficiency in core networks with clouds. Various models and heuristic based algorithms have been proposed and shown to significantly improve energy performance in core networks with clouds. These investigations have yielded the following future research directions that could be explored:

10.2.1 Software Defined Networking Implementation of Proposed Algorithms

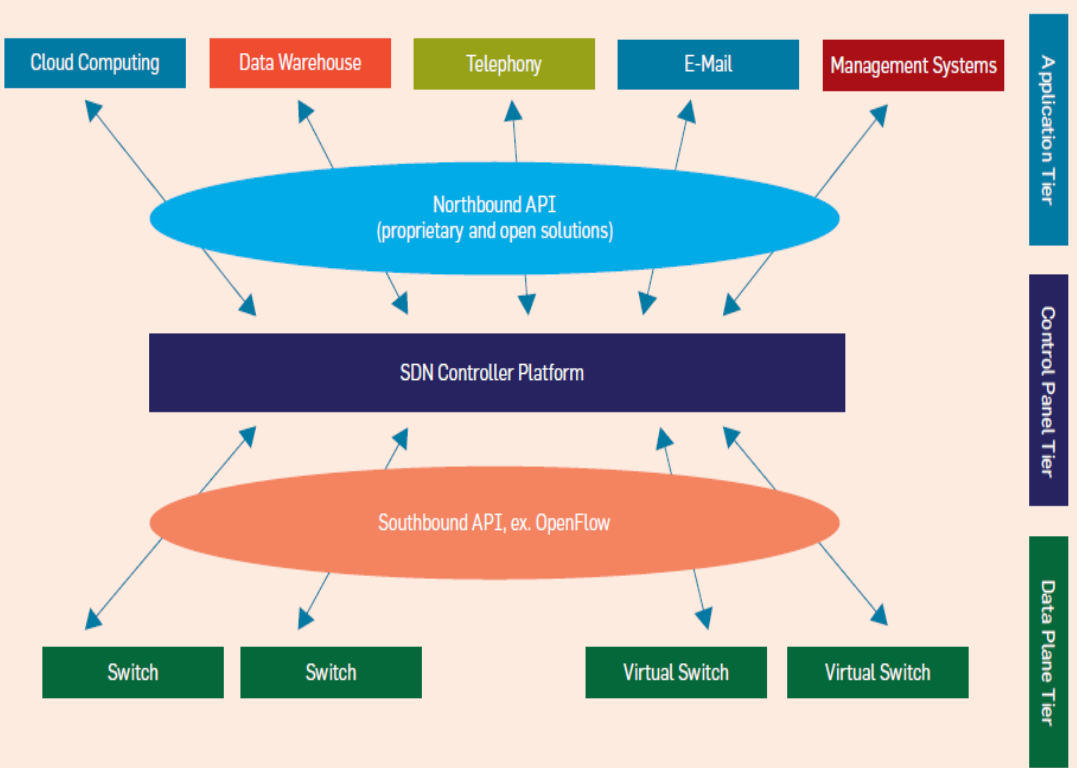

Figure 10-1: SDN three Tier Architecture [141]

Software-Defined Networking is a new networking architecture that is designed to use standard application programming interfaces (APIs) to respond quickly to changing business requirements via a centralized control plane [141]. The use of APIs allows dynamic reconfiguration of the network and its components such as optical switches, routers, servers, virtual machines and others in response to specific requirements at different times. The algorithms developed in this work can be implemented as applications in the application tier of the SDN three-tiered stack architecture shown in Fig. 10.1. These applications through the northbound API could then link with the SDN controller such as ONOS or OpenDaylight that would pass on the instructions to the physical devices via a southbound API such as OpenFlow. Such an implementation would be a clear litmus test of the developed algorithms on how they would operate in a real network. Different traffic conditions and resource availability would be created and then the response of the algorithms in terms of power consumption, provisioned resources, renewable energy used, cost, profit and other performance metrics measured.

10.2.2 Virtual Network Embedding in Multi Operator Networks

The work that has been done in this thesis has only focussed on virtual network embedding solutions in single operator networks. It has been assumed that one operator purely owns the entire cloud infrastructure. While this assumption is valid, in most cases, multiple operators who are interconnected with each other usually own the cloud infrastructure. In this

case, all the operators would want to maximise the number of customers that are service by their networks. However, the fact that operators have limited resources means that there are opportunities for cooperation among operators in service provisioning. Models could be developed in these scenarios to investigate how operators can cooperate with each other to bring about profit maximization, energy efficiency, improved quality of service and various other benefits in cloud service provisioning.

References

1. Bio Intelligence Service, E.C. Impacts of Information and Communications Technologies on Energy Efficiency. 2008; Available from: http://www.epractice.eu/files/media/media2311.pdf.

2. United States Environmental Protection Agency. Report to Congress on Server and Data Centre Energy Efficiency Public Law 109-431. 2007; Available from: http://www.energystar.gov/ia/partners/prod_development/downloads/EPA_Datacenter_Report_Congress_Final1.pdf.

3. Leisching, P. and M. Pickavet. Energy footprint of ICT: Forecasts and network solutions. in Ofc/nfoec. 2009.

4. Administration, E.I. Primary Energy Cinsumption by Source and Sector 2011. 2011; Available from: https://www.eia.gov/totalenergy/data/annual/pecss_diagram.cfm.

5. Gupta, M. and S. Singh. Greening of the Internet. in Proceedings of the 2003 conference on Applications, technologies, architectures, and protocols for computer communications. 2003. ACM.

6. Power, E.N. Energy Logic Reducing Data Center Energy Consumption. 2009 [cited 2013; Available from: http://www.cisco.com/web/partners/downloads/765/other/Energy_Logic_Reducing_Data_Center_Energy_Consumption.pdf.

7. The Green Grid. Available from: http://www.thegreengrid.org/.

8. Gangxiang, S. and R.S. Tucker, Energy-Minimized Design for IP Over WDM Networks. Optical Communications and Networking, IEEE/OSA Journal of, 2009. 1(1): p. 176-186.

9. Jain, R. and S. Paul, Network virtualization and software defined networking for cloud computing: a survey. Communications Magazine, IEEE, 2013. 51(11): p. 24-31.

10. Chaparadza, R., et al. SDN enablers in the ETSI AFI GANA Reference Model for Autonomic Management & Control (emerging standard), and Virtualization impact. in Globecom Workshops (GC Wkshps), 2013 IEEE. 2013.

11. Bin, W., et al. Reducing power consumption in embedding virtual infrastructures. in Globecom Workshops (GC Wkshps), 2012 IEEE. 2012.

12. Botero, J.F., et al., Energy Efficient Virtual Network Embedding. Communications Letters, IEEE, 2012. 16(5): p. 756-759.

13. Sen, S., et al. Energy-aware virtual network embedding through consolidation. in Computer Communications Workshops (INFOCOM WKSHPS), 2012 IEEE Conference on. 2012.

14. Botero, J.F. and X. Hesselbach, Greener networking in a network virtualization environment. Computer Networks, 2013. 57(9): p. 2021-2039.

15. Su, S., et al., Energy-Aware Virtual Network Embedding. Networking, IEEE/ACM Transactions on, 2014. PP(99): p. 1-1.

16. Lee, K.J. and T.J. Aprille. SONET evolution: the challenges ahead. in Global Telecommunications Conference, 1991. GLOBECOM'91.'Countdown to the New Millennium. Featuring a Mini-Theme on: Personal Communications Services. 1991. IEEE.

17. Ghani, N., S. Dixit, and T.S. Wang, On IP-over-WDM integration. Communications Magazine, IEEE, 2000. 38(3): p. 72-84.

18. Ramaswami, R., K.N. Sivarajan, and G.H. Sasaki, Optical networks: a practical perspective. 2009: Morgan Kaufmann.

19. Cisco White Paper. Converge IP and DWDM Layers in the Core Network. 2007; Available from: http://www.cisco.com/en/US/prod/collateral/routers/ps5763/prod_white_paper0900aecd80395e03.pdf

20. Dixit, S., IP over WDM: building the next-generation optical internet. 2004: John Wiley & Sons.

21. Rajagopalan, B., et al., IP over optical networks: architectural aspects. Communications Magazine, IEEE, 2000. 38(9): p. 94-102.

22. Cisco. Cisco Visual Networking Index: Global Mobile Data Traffic Forecast Update, 2015-2020. White Paper 2016 2016; Available from: http://www.cisco.com/c/en/us/solutions/collateral/service-provider/visual-networking-index-vni/mobile-white-paper-c11-520862.html.

23. Fettweis, G. and E. Zimmermann. ICT energy consumption-trends and challenges. in Proceedings of the 11th International Symposium on Wireless Personal Multimedia Communications. 2008.

24. Chiaraviglio, L., M. Mellia, and F. Neri. Energy-aware networks: Reducing power consumption by switching off network elements. in FEDERICA-Phosphorus tutorial and workshop (TNC2008) Bruges (Belgium). 2008.

25. Christensen, K.J., et al., The next frontier for communications networks: power management. Computer Communications, 2004. 27(18): p. 1758-1770.

26. Chiaraviglio, L., M. Mellia, and F. Neri. Energy-Aware Backbone Networks: A Case Study. in Communications Workshops, 2009. ICC Workshops 2009. IEEE International Conference on. 2009.

27. Muhammad, A., et al. Energy-Efficient WDM Network Planning with Dedicated Protection Resources in Sleep Mode. in Global Telecommunications Conference (GLOBECOM 2010), 2010 IEEE. 2010.

28. Idzikowski, F., et al. Saving energy in IP-over-WDM networks by switching off line cards in low-demand scenarios. in Optical Network Design and Modeling (ONDM), 2010 14th Conference on. 2010.

29. Zhang, Y., et al. Time-aware energy conservation in IP-over-WDM networks. in Photonics in Switching. 2010. Optical Society of America.

30. Zhang, Y., et al., Energy optimization in IP-over-WDM networks. Optical Switching and Networking, 2011. 8(3): p. 171-180.

31. Caria, M., M. Chamania, and A. Jukan, A comparative performance study of load adaptive energy saving schemes for IP-over-WDM networks. Optical Communications and Networking, IEEE/OSA Journal of, 2012. 4(3): p. 152-164.

32. Chowdhury, P., M. Tornatore, and B. Mukherjee. On the energy efficiency of mixed-line-rate networks. in Optical Fiber Communication (OFC), collocated National Fiber Optic Engineers Conference, 2010 Conference on (OFC/NFOEC). 2010.

33. Ciena. 6500 Packet-Optical Platform Data Sheet. 2012 [cited 2012 10/12/2012]; Available from: http://media.ciena.com/documents/6500_Packet_Optical_Platform_DS.pdf.

34. Cisco. Cisco CRS Modular Services Cards. 2014 [cited 2015 March 2015]; Available from: http://www.cisco.com/c/en/us/products/collateral/routers/carrier-routing-system/datasheet-c78-730791.pdf.

35. Lui, Y., G. Shen, and W. Shao. Energy-minimized design for IP over WDM networks under modular router line cards. in Communications in China (ICCC), 2012 1st IEEE International Conference on. 2012.

36. Cisco. Data sheet of CRS-1 16 slots chassis power systems. 2014; Available from: http://www.cisco.com/c/en/us/products/collateral/routers/crs-1-16-slot-single-shelf-system/product_data_sheet09186a008022d5f3.pdf.

37. Saunders, H.D., The Khazzoom-Brookes Postulate and Neoclassical Growth. The Energy Journal, 1992. 13(4): p. 131-148.

38. Figuerola, S., et al., Converged Optical Network Infrastructures in Support of Future Internet and Grid Services Using IaaS to Reduce GHG Emissions. Lightwave Technology, Journal of, 2009. 27(12): p. 1941-1946.

39. Xiaowen, D., T. El-Gorashi, and J.M.H. Elmirghani, IP Over WDM Networks Employing Renewable Energy Sources. Lightwave Technology, Journal of, 2011. 29(1): p. 3-14.

40. Google. Efficiency: How we do it. 2012 [cited 2012 17/11/2012]; Available from: http://www.google.com/about/datacenters/efficiency/internal/.

41. Cisco. Energy Efficient Cooling Solutions for Data Centers. 2007 [cited 2012 15/11/2012]; Available from: http://www.cisco.com/web/partners/downloads/765/other/Energy_Efficient_Cooling_Solutions_for_Data_Centers.pdf.

42. Xiaowen, D., T. El-Gorashi, and J.M.H. Elmirghani, Green IP Over WDM Networks With Data Centers. Lightwave Technology, Journal of, 2011. 29(12): p. 1861-1880.

43. Xiaowen, D., T.E.H. El-Gorashi, and J.M.H. Elmirghani, On the Energy Efficiency of Physical Topology Design for IP Over WDM Networks. Lightwave Technology, Journal of, 2012. 30(12): p. 1931-1942.

44. Musumeci, F., et al. The role of network topology on the energy efficiency of IP-over-WDM architectures. in Optical Network Design and Modeling (ONDM), 2012 16th International Conference on. 2012.

45. Musumeci, F., M. Tornatore, and A. Pattavina, A Power Consumption Analysis for IP-Over-WDM Core Network Architectures. Optical Communications and Networking, IEEE/OSA Journal of, 2012. 4(2): p. 108-117.

46. Chabarek, J., et al. Power Awareness in Network Design and Routing. in INFOCOM 2008. The 27th Conference on Computer Communications. IEEE. 2008.

47. Cianfrani, A., et al. An Energy Saving Routing Algorithm for a Green OSPF Protocol. in INFOCOM IEEE Conference on Computer Communications Workshops , 2010. 2010.

48. Tucker, R.S., et al., Evolution of WDM Optical IP Networks: A Cost and Energy Perspective. Lightwave Technology, Journal of, 2009. 27(3): p. 243-252.

49. Roberts, L.G., A radical new router. Spectrum, IEEE, 2009. 46(7): p. 34-39.

50. Baldi, M. and Y. Ofek. Time for a "Greener" Internet. in Communications Workshops, 2009. ICC Workshops 2009. IEEE International Conference on. 2009.

51. Dutta, R. and G.N. Rouskas, Traffic grooming in WDM networks: Past and future. Network, IEEE, 2002. 16(6): p. 46-56.

52. Yetginer, E. and G.N. Rouskas. Power Efficient Traffic Grooming in Optical WDM Networks. in Global Telecommunications Conference, 2009. GLOBECOM 2009. IEEE. 2009.

53. Shu, H., D. Seshadri, and R. Dutta. Traffic Grooming: A Changing Role in Green Optical Networks. in Global Telecommunications Conference, 2009. GLOBECOM 2009. IEEE. 2009.

54. Shuqiang, Z., S. Dong, and C. Chun-Kit. Energy Efficient Time-Aware Traffic Grooming in Wavelength Routing Networks. in Global Telecommunications Conference (GLOBECOM 2010), 2010 IEEE. 2010.

55. Ming, X., et al., Green Provisioning for Optical WDM Networks. Selected Topics in Quantum Electronics, IEEE Journal of, 2011. 17(2): p. 437-445.

56. Song, Y. and F. Kuipers. Energy-aware path selection for scheduled lightpaths in IP-over-WDM networks. in Communications and Vehicular Technology in the Benelux (SCVT), 2011 18th IEEE Symposium on. 2011.

57. Weigang, H., G. Lei, and W. Xuetao, Robust and Integrated Grooming for Power- and Port-Cost-Efficient Design in IP Over WDM Networks. Lightwave Technology, Journal of, 2011. 29(20): p. 3035-3047.

58. Musumeci, F., et al. On the Energy Efficiency of Optical Transport with Time Driven Switching. in Communications (ICC), 2011 IEEE International Conference on. 2011.

59. Ceuppens, L., A. Sardella, and D. Kharitonov. Power Saving Strategies and Technologies in Network Equipment Opportunities and Challenges, Risk and Rewards. in Applications and the Internet, 2008. SAINT 2008. International Symposium on. 2008.

60. Aleksic, x, and S., Energy Efficiency of Electronic and Optical Network Elements. Selected Topics in Quantum Electronics, IEEE Journal of, 2011. 17(2): p. 296-308.

61. Cisco. Cisco Carrier Routing System. 2008 [cited 2012 11/11/2012]; Available from: http://www.cisco.com/en/US/prod/collateral/routers/ps5763/prod_brochure0900aecd800f8118.pdf.

62. Aleksic, S., Analysis of Power Consumption in Future High-Capacity Network Nodes. Optical Communications and Networking, IEEE/OSA Journal of, 2009. 1(3): p. 245-258.

63. Li, S., P. Li-Shiuan, and N.K. Jha. Dynamic voltage scaling with links for power optimization of interconnection networks. in High-Performance Computer Architecture, 2003. HPCA-9 2003. Proceedings. The Ninth International Symposium on. 2003.

64. Chen, X., G.Y. Wei, and L.S. Peh. Design of low-power short-distance opto-electronic transceiver front-ends with scalable supply voltages and frequencies. in Proceedings of the 13th international symposium on Low power electronics and design. 2008. ACM.

65. Chowdhury, N.M.M.K. and R. Boutaba, Network virtualization: state of the art and research challenges. Communications Magazine, IEEE, 2009. 47(7): p. 20-26.

66. VMware The VMware NSX Network Virtualization Platform. 2013.

67. Khan, A., et al., Network virtualization: a hypervisor for the Internet? Communications Magazine, IEEE, 2012. 50(1): p. 136-143.

68. Drutskoy, D., E. Keller, and J. Rexford, Scalable Network Virtualization in Software-Defined Networks. Internet Computing, IEEE, 2013. 17(2): p. 20-27.

69. Carapinha, J., et al., Network virtualization: a view from the bottom, in Proceedings of the 1st ACM workshop on Virtualized infrastructure systems and architectures2009, ACM: Barcelona, Spain. p. 73-80.

70. Qiang, D., Y. Yuhong, and A.V. Vasilakos, A Survey on Service-Oriented Network Virtualization Toward Convergence of Networking and Cloud Computing. Network and Service Management, IEEE Transactions on, 2012. 9(4): p. 373-392.

71. Kasse, F.B., B. Gueye, and H. Elbiaze. Leveraging network virtualization for energy-efficient cloud: Future directions. in Local Computer Networks (LCN), 2014 IEEE 39th Conference on. 2014.

72. Nejabati, R., et al. Optical network virtualization. in Optical Network Design and Modeling (ONDM), 2011 15th International Conference on. 2011.

73. Fischer, A., et al., Virtual Network Embedding: A Survey. Communications Surveys & Tutorials, IEEE, 2013. 15(4): p. 1888-1906.

74. Yu, M., et al., Rethinking virtual network embedding: substrate support for path splitting and migration. SIGCOMM Comput. Commun. Rev., 2008. 38(2): p. 17-29.

75. Anderson, D.G. Theoretical Approaches to Node Assignement. 2002 [cited 2013 11/03/2013]; Available from: http://repository.cmu.edu/cgi/viewcontent.cgi?article=1079&context=compsci.

76. Long, G., et al. Revenue-driven virtual network embedding based on global resource information. in Global Communications Conference (GLOBECOM), 2013 IEEE. 2013.

77. Cheng, X., et al., Virtual network embedding through topology-aware node ranking. SIGCOMM Comput. Commun. Rev., 2011. 41(2): p. 38-47.

78. Chowdhury, M., M.R. Rahman, and R. Boutaba, ViNEYard: Virtual Network Embedding Algorithms With Coordinated Node and Link Mapping. Networking, IEEE/ACM Transactions on, 2012. 20(1): p. 206-219.

79. Long, G., et al. Toward profit-seeking virtual network embedding algorithm via global resource capacity. in INFOCOM, 2014 Proceedings IEEE. 2014.

80. Rahman, M.R. and R. Boutaba, SVNE: Survivable Virtual Network Embedding Algorithms for Network Virtualization. Network and Service Management, IEEE Transactions on, 2013. 10(2): p. 105-118.

81. Jarray, A., S. Yihong, and A. Karmouch. Resilient virtual network embedding. in Communications (ICC), 2013 IEEE International Conference on. 2013.

82. Zhu, Q., et al. Heuristic survivable virtual network embedding based on node migration and link remapping. in Information Technology and Artificial Intelligence Conference (ITAIC), 2014 IEEE 7th Joint International. 2014.

83. Lu, B., et al., Dynamic recovery for survivable virtual network embedding. The Journal of China Universities of Posts and Telecommunications, 2014. 21(3): p. 77-84.

84. Guan, X., B.-Y. Choi, and S. Song, Energy efficient virtual network embedding for green data centers using data center topology and future migration. Computer Communications, 2015. 69: p. 50-59.

85. Zhongbao, Z., et al. Minimizing electricity cost in geographical virtual network embedding. in Global Communications Conference (GLOBECOM), 2012 IEEE. 2012.

86. Triki, N., et al., A green energy-aware hybrid virtual network embedding approach. Computer Networks, 2015. 91: p. 712-737.

87. Fan, X., W.-D. Weber, and L.A. Barroso, Power provisioning for a warehouse-sized computer. ACM SIGARCH Computer Architecture News, 2007. 35(2): p. 13-23.

88. Greenberg, A., et al., The cost of a cloud: research problems in data center networks. ACM SIGCOMM Computer Communication Review, 2008. 39(1): p. 68-73.

89. Google. Efficiency: How do we do it. 2014 [cited 2014 22/10/2014]; Available from: http://www.google.co.uk/about/datacenters/efficiency/internal/.

90. Microsoft. Microsoft's Cloud Infrastructure – By the Numbers. 2013 [cited 2014 22/10/2014]; Available from: http://www.microsoft.com/eu/PRESSRELEASE_Microsoft_cloud_services_growth_drives_Expansion.aspx?path=10-1.

91. Technologies, P. Advanced Power Management with Dell Open Manage Power Centre. 2012 [cited 2013 14/04/2013]; Available from: http://www.principledtechnologies.com/Dell/R720_power_0312.pdf.

92. Cisco, Data sheet of CRS-1 16 slots chassis power systems.

93. Cisco, Data sheet of Cisco ONS 15454 10-Gbps multi-rate transponder card

94. Cisco, Data sheet of Cisco ONS 15501 EDFA.

95. Cisco, Data sheet of Cisco ONS 15454 100-GHz 4-CH Multi/Demultiplexer.

96. Glimmerglass. Data sheet of Glimmerglass Intelligent Optical System 500. 2014 [cited 2014; Available from: http://www.glimmerglass.com/products/intelligent-optical-system-500/.

97. Houidi, I., et al., Virtual network provisioning across multiple substrate networks. Computer Networks, 2011. 55(4): p. 1011-1023.

98. Hammadi, A. and L. Mhamdi, A survey on architectures and energy efficiency in Data Center Networks. Computer Communications, 2014. 40(0): p. 1-21.

99. Cisco. Cisco Catalyst 4900M Switch. [cited 2014; Available from: http://www.cisco.com/c/en/us/products/collateral/switches/catalyst-4900-series-switches/Data_Sheet_Cat_4900M.html.

100. Cisco. Cisco 7613 Router Data Sheet. [cited 2014; Available from: http://www.cisco.com/c/en/us/products/collateral/routers/7613-router/product_data_sheet09186a008015cfeb.html.

101. Lawey, A.Q., T.E.H. El-Gorashi, and J.M.H. Elmirghani, BitTorrent Content Distribution in Optical Networks. Lightwave Technology, Journal of, 2014. 32(21): p. 3607-3623.

102. Valancius, V., et al., Greening the internet with nano data centers, in Proceedings of the 5th international conference on Emerging networking experiments and technologies2009, ACM: Rome, Italy. p. 37-48.

103. Broaband_Forum. Triple-play Services Quality of Experience (QoE) Requirements. Technical Report TR-126 2006 [cited 2014; Available from: http://www.broadband-forum.org/technical/download/TR-126.pdf.

104. Gerstel, O., et al., Elastic optical networking: a new dawn for the optical layer? Communications Magazine, IEEE, 2012. 50(2): p. s12-s20.

105. El-Gorashi, T.E.H., X. Dong, and J.M.H. Elmirghani Green optical orthogonal frequency-division multiplexing networks. IET Optoelectronics, 2014. 8, 137-148.

106. Xiaowen, D., T.E.H. El-Gorashi, and J.M.H. Elmirghani. Energy efficiency of optical OFDM-based networks. in Communications (ICC), 2013 IEEE International Conference on. 2013.

107. Guoying, Z., M. De Leenheer, and B. Mukherjee, Optical traffic grooming in OFDM-based elastic optical networks [Invited]. Optical Communications and Networking, IEEE/OSA Journal of, 2012. 4(11): p. B17-B25.

108. Gerstel, O.A. Flexible use of spectrum and photonic grooming. in Photonics in Switching. 2010. Optical Society of America.

109. Takagi, T., et al. Algorithms for maximizing spectrum efficiency in elastic optical path networks that adopt distance adaptive modulation. in 36th European Conference and Exhibition on Optical Communication. 2010.

110. Armstrong, J. OFDM: From Copper and Wireless to Optical. in Optical Fiber Communication Conference/National Fiber Optic Engineers Conference. 2008. San Diego, California: Optical Society of America.

111. Mahad, F.D., M. Supa'at, and A. Sahmah, EDFA gain optimization for WDM system. Elektrika, 2009. 11(1): p. 34-37.

112. Bocoi, A., et al., Reach-dependent capacity in optical networks enabled by OFDM. OFC (OMQ4), 2009.

113. Lach, E. and W. Idler, Modulation formats for 100G and beyond. Optical Fiber Technology, 2011. 17(5): p. 377-386.

114. Elmirghani, J.M.H., et al. GreenTouch GreenMeter core network power consumption models and results. in Green Communications (OnlineGreencomm), 2014 IEEE Online Conference on. 2014.

115. Lawey, A.Q., T.E.H. El-Gorashi, and J.M.H. Elmirghani, Distributed Energy Efficient Clouds Over Core Networks. Lightwave Technology, Journal of, 2014. 32(7): p. 1261-1281.

116. GreenTouch, GreenTouch Final Results from Green Meter Research Study: Reducing the Net Power Consumption in Communication Networks by upto 98% by 2020. A GreenTouch White Paper 2015. 2.0.

117. Cisco. Cisco CRS 16-Slot Single-Shelf System. 2013 April 2015]; Available from: http://www.cisco.com/c/en/us/products/collateral/routers/carrier-routing-system/CRS-3_16-Slot_DS.pdf.

118. Cisco, CRS Platform Introduction, 2012.

119. Cisco. Cisco CRS 1-Port OC-768C/STM-256C DPSK+ Tunable WDMPOS

Interface Module. 2010 [cited 2015 March 2015]; Available from: http://www.cisco.com/c/en/us/products/collateral/routers/carrier-routing-system/data_sheet_c78-478689.pdf.

120. Cisco. Cisco CRS 100 Gigabit Ethernet Interface Modules. 2014 March 2015]; Available from: http://www.cisco.com/c/en/us/products/collateral/routers/carrier-routing-system/datasheet-c78-730788.pdf.

121. Cisco. Cisco CRS-X 4-Port 100GE LAN/OTN Interface Module. 2013 March 2015]; Available from: https://www.cisco.com/en/US/prod/collateral/routers/ps5763/data_sheet_c78-728888.pdf.

122. Dorize, C., P. Layec, and G. Charlet. DSP power balancing for multi-format WDM receiver. in Optical Communication (ECOC), 2014 European Conference on. 2014.

123. Dorize, C., et al. Adaptive power efficiency for chromatic dispersion compensation. in Optical Communication (ECOC 2013), 39th European Conference and Exhibition on. 2013.

124. Van Heddeghem, W., et al., A power consumption sensitivity analysis of circuit-switched versus packet-switched backbone networks. Computer Networks, 2015. 78(0): p. 42-56.

125. Van Heddeghem, W., et al., Power consumption modeling in optical multilayer networks. Photonic Network Communications, 2012. 24(2): p. 86-102.

126. Sharkh, M.A., et al., Resource allocation in a network-based cloud computing environment: design challenges. Communications Magazine, IEEE, 2013. 51(11): p. 46-52.

127. Cisco. Cisco ONS 15454 40 Gbps CP-DQPSK Full C-Band Tuneable Transponder Card. 2012 [cited 2015; Available from: http://www.cisco.com/c/en/us/products/collateral/optical-networking/ons-15454-series-multiservice-provisioning-platforms/data_sheet_c78-643796.pdf.

128. AT&T. AT&T's 38 Global Internet Data Centers. 2007 [cited 2015 01/04/2015]; Available from: http://www.business.att.com/content/productbrochures/eb_idcmap.pdf.

129. Google. 2014; Available from: https://cloud.google.com/compute/.

130. Google. Google Fiber. 2014; Available from: https://support.google.com/fiber/answer/2657118?hl=en.

131. Yahoo_Business. 2014; Available from: https://biz.yahoo.com/p/8qpmu.html.

132. Nguyen Huu, T., et al., Modeling and experimenting combined smart sleep and power scaling algorithms in energy-aware data center networks. Simulation Modelling Practice and Theory, 2013. 39(0): p. 20-40.

133. Ciena. DWDM vs. CWDM. 2015 [cited 2015; Available from: http://www.ciena.com/technology/dwdm-vs-cwdm/.

134. Buyya, R., et al., Cloud computing and emerging IT platforms: Vision, hype, and reality for delivering computing as the 5th utility. Future Gener. Comput. Syst., 2009. 25(6): p. 599-616.

135. EIA. 2015 [cited 2015 20/10/2015]; Available from: http://www.eia.gov/renewable/.

136. Project, O.P. Open PV Sate Rankings. 2015; Available from: https://openpv.nrel.gov/rankings.

137. EIA. Average Price of Electricity to Ultimate Customers by End-Use Sector. 2015 [cited 2016 23/01/2016]; Available from: https://www.eia.gov/electricity/monthly/epm_table_grapher.cfm?t=epmt_5_6_a.

138. Kollmuss, A., H. Zink, and C. Polycarp, Making sense of the voluntary carbon market: A comparison of carbon offset standards. WWF Germany, Stockholm Environment Institute/Tricorona, 2008.

139. Carbonfund.org. Carbon Calculator. 2015 [cited 2015; Available from: https://www.carbonfund.org/how-we-calculate.

140. HM_Revenue_&_Customs. Carbon Price Floor: Reform. 2015 [cited 2016; Available from: https://www.gov.uk/government/publications/carbon-price-floor-reform.

141. Kirkpatrick, K., Software-defined networking. Commun. ACM, 2013. 56(9): p. 16-19.